Transgenic Nematodes as a model for Parkinson's disease

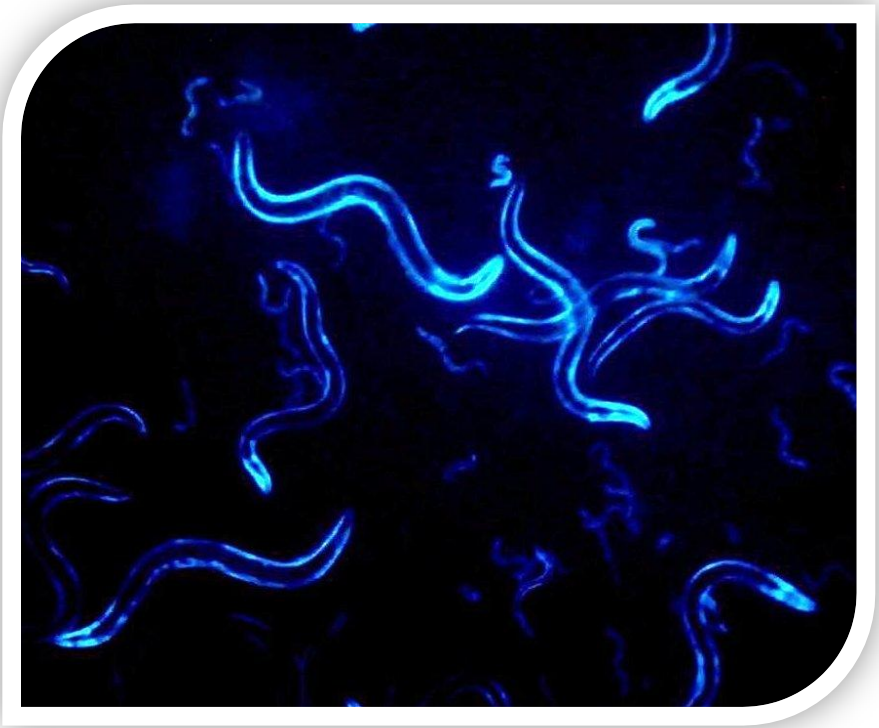

Bodhicharla Rakesh Kumar, MRes.

Thesis submitted to the University of Nottingham

for the degree of Doctor of Philosophy

December 2011

Abstract

Aggregation of the abundant neural protein α-synuclein contributes to cellular toxicity in Parkinson's disease. We have created transgenic nematodes carrying fusion constructs encoding human α-synuclein (S) tagged with YFP (V) and/or CFP (C) as a fluorescent marker. Using the *unc-54* myosin promoter, a synuclein-YFP (*unc*-54::SV (NI)) fusion construct was abundantly expressed in the body wall muscles of *Caenorhabditis elegans*. Permanent integrated lines were successfully generated for *unc*-54::V (NI), *unc*-54::S+V (I), *unc*-54::SC+SV (I), *unc*-54::C+V (I), and *unc*-54::CV (I) using gamma irradiation. The outcrossed transgenic synuclein strains were radiation sensitive and have shorter life span and lower pharyngeal pumping compared to wild type N2 and *unc*-54::V (I) worms. Fluorescence Resonance Energy Transfer (FRET) was measured for all the transgenic strains. The *unc*-54::SC+SV (I) worms showed FRET signals intermediate between the negative (*unc*-54::C+V (I)) and positive (*unc*-54::CV (I)) control strains. Confocal images were taken to confirm the presence of FRET. FRET signals increase markedly during early adult life in *unc*-54::SC+SV (I) worms. RNA interference by feeding was performed in *unc*-54::SC+SV (I) worms to knock out the Hip-1 co-chaperone function, thereby increasing the FRET signal. *unc*-

54::SC+SV (I) fusion worms were also exposed to pesticides such as chlorpyrifos and rotenone, and we observed an increase in the size and intensity of fluorescent aggregates thereby increasing the FRET signal. Finally we have quantified reactive oxygen species (ROS) for *unc*-54::SC+SV (I) fusion worms and NL5901 strains by using the H2DCF-DA assay, showing that ROS levels were increased by pesticide exposure.

Acknowledgements

I wish to acknowledge the guidance and encouragement of my supervisor, Dr David de Pomerai, who has been a constant source of support and direction throughout my PhD. I especially appreciate that he has shown me the importance of having critical views in science in many ways. This has been and will be extremely influential in all my scientific work. I would like to thank Dr. Ian Duce, who has been supportive and helpful during my PhD. I would also like to thank Declan Brady, Charumathi Anbalagan, Richard Wall, Himanshu Kharkwal, Archana Nagarajan, Kelly Vere and Kevin Webb for their help and advice.

I am very grateful to my parents who have given me the opportunity to study for my PhD in the U.K.

Dedicated to my Family

B.Malleswara Rao

B.Devika Rani

B.Bhargavi

B.Kunal Kumar

B.Jyotshna

Abbreviations

4-HNE	4- hydroxynonenol
AChE	Acetylcholinesterase
AD	Alzheimer's disease
ADP	Adenosine diphosphate
APP	Amyloid precursor protein
APS	Ammonium persulphate
ARJP	Autosomal Recessive Juvenile Parkinson disease
ATP	Adenosine triphosphate
bp	Base pair(s)
C	Cerulean (CFP) protein
C.elegans	*Caenorhabditis elegans*
C+V	Cerulean + Venus (separate proteins)
cDNA	Complementary DNA
CFP	Cerulean fluorescent protein
CGC	*Caenorhabditis* Genetics Centre
CI	Confidence interval
CNS	Central nervous system
CV	Cerulean-Venus fusion protein
DAQ	dopamine quinone
DAT	Dopamine transporter
DCF	2', 7'-dichlorofluorescein
DES	Diethyl sulphate
DN	Dopaminergic neurons

DNA	Deoxyribonucleic acid
DRPLA	Dentatorubral pallidoluysian atrophy
dsRNA	Double-stranded RNA
E.coli	Escherichia coli
ECL	Enhanced Chemiluminescence
EDTA acid	Ethylene diamine tetra-acetic
EGFP	Enhanced green fluorescent protein
EMS	Ethylmethanesulfonate
ENU	N-nitroso-N-ethylurea
ES	Embryonic stem
F1,F2,F3	1^{st} , 2^{nd}, 3^{rd} generation of P0
FRET	Forster Resonance Energy Transfer
FV	Feeding vector
GCIs	Glial cytoplasmic inclusions
GFP	Green fluorescent protein
GSH	Glutathione
GSSG	Glutathione disulfide
Gy	Gray
H_2DCF	2', 7'-dihydrodichlorofluorescein
H_2DCF-DA	2', 7'-dihydrodichlorofluorescin-diacetate
HD	Huntington's Disease
Hsp	Heat shock protein
Htt	Huntingtin
I	Integrated
IPTG	Isopropyl-β-D-thio-galactoside

kDa	Kilodalton(s)
L1-L4	*C.elegans* larval stages
LB	Lewy bodies
LN	Lewy neurites
mfn	mitofusin
MJD	Machado–Joseph disease gene
MPTP	N-methyl-4-phenyl-1,2,3,6-tetrahydropyridine
mRNA	Messenger RNA
NGM	Nematode Growth Medium
NI	Non-Integrated
NO	nitric oxide
ONOO-	peroxynitrite
P0	Parental generation
PAGE	Polyacrylamide Gel Electrophoresis
PD	Parkinson Disease
ppm	Parts per million
PVDF	Polyvinylidene difluoride
rde	RNAi deficient
RISC	RNA-induced silencing complex
RNA	Ribonucleic acid
RNAi	RNA Interference
ROS	Reactive oxygen species
rpm	Revolutions per minute
S	Human α-Synuclein protein
S+V	Synuclein + Venus (separate proteins)

SBMA	Spinobulbar muscular atrophy
SC+SV	Synuclein-Cerulean + Synuclein-Venus (two separate fusion proteins)
SCA3	Spinocerebellar ataxia type 3
SDS	Sodium Dodecyl Sulphate
siRNA	Small interfering RNAs
SOD	Superoxide dismutase
SV	Synuclein-Venus fusion protein
TBS	Tris Buffered Saline
TEMED	N, N, N', N'-Tetramethylethylenediamine
TTBS	Tween Tris Buffered Saline
UV	Ultraviolet
V	Venus (a variant form of YFP) protein
VMAT2	Vesicular monoamine transporter
WT	Wild type
YFP	Yellow fluorescent protein

Table of Contents

List of Figures

List of Tables

Chapter 1. Introduction

1.1 Neurological disorders in Humans

Neurodegenerative diseases are increasingly common as average lifespan increases (Marsh and Thompson 2004). Although the majority of such disorders are spontaneous (showing no evidence of heritability), a minority are inherited. Genetically, such familial neurodegenerative diseases leading to neuropathology are often caused by dominant mutations in a single gene (e.g. Huntingtin; Zeitlin et al. 1995), though some recessive mutations are also known (e.g. DJ-1; Bonifati et al. 2003). Although the wild-type gene and the disease causing mutation(s) may be known, the mechanisms that lead to pathology are not. For example, various genes which become mutated in CAG repeat (polyglutamine or polyQ) diseases are known but the basis of pathology remains complex and not well understood (e.g. Huntington's Disease [HD]; Marsh and Thompson 2004). In most neurodegenerative diseases, degeneration of specific neuronal regions takes place, where cellular proteins accumulate abnormally and often form aggregates that are visible at the light microscope level, correlated with the progression of disease (Carrell and Lomas 1997; Kopito and Ron 2000). Such protein aggregates can range

in size from submicroscopic to large (Yang et al. 2002; Kayed et al. 2003) the large visible aggregates being referred to as inclusions in polyQ diseases, amyloid plaques in Alzheimer's disease or Lewy bodies in Parkinson's disease. Inclusions are shown to be highly stable protein aggregates because they are insoluble in SDS solution. Examples of neurodegenerative diseases include:

i. Huntington's disease and at least 8 other CAG repeat diseases that are caused by polyglutamine expansions in the mutant protein (Zoghbi and Orr 2000; Ross 2002).
ii. Alzheimer's disease (AD) and other tauopathies which are characterized by the accumulation of amyloid plaques and neurofibrillary tangles that contain both β-amyloid and tau protein.
iii. Parkinson's disease which is caused by the accumulation of α-synuclein in Lewy Bodies (Thompson and Barrow 2002; Temussi et al. 2003).

A significant feature of all these diseases is that their diagnosis is usually not clear until late in life. These diseases are usually related to intellectual dysfunction such as memory loss, cognitive deficits and often movement disorders. Once symptoms appear, there is a slow progression over the next 10–

20 years as neuronal functions become more and more impaired, ultimately resulting in death.

1.2 Invertebrate models of neurodegenerative diseases

Both the nematode *Caenorhabditis elegans* (Baumeister and Ge 2002) and the fruitfly *Drosophila melanogaster* (Bernards and Hariharan 2001) are well known experimental models because of their short lifespan, well characterized development and anatomy, sophisticated genetics, fully sequenced genomes, simple transgenic analysis and susceptibility to gene inactivation by RNA interference. Many new findings in neurodevelopment and neural function have come from studies in these invertebrates. For instance, the basic mechanism of apoptosis was first found in invertebrates and subsequently in humans (Richardson and Kumar 2002).

The modeling of human diseases through transgenic expression of human genes in invertebrates has been relatively successful. We cannot expect invertebrates to exactly represent all aspects of the corresponding human disease but, in spite of various differences, there is plentiful evidence that they can provide important insights into the human disease. Human proteins can be overexpressed in transgenic models, such as

overexpression of α-synuclein in a PD model (Auluck and Bonini 2002), or of polyglutamine expansions (Warrick et al. 1998) in *Drosophila*, both of which cause neurodegenration and protein-associated cellular inclusions.

1.3 Neurodegenerative diseases

1.3.1 Huntington's disease

Huntington's disease is a well-known neurodegenerative disorder, which is caused by genetic mutations involving triplet CAG repeat expansions that lead to extended polyglutamine tracts (Ding et al. 2002). The existence of an expanded polyglutamine tract leads to protein aggregation which kills neurons in the basal ganglia. Huntington's disease is mainly caused by mutations in the Huntingtin gene. The molecular basis of this disease is expansion of the trinucleotide CAG repeat (encoding glutamine) in the Huntingtin gene. Generally, disease severity is associated with the extent of CAG expansion. This CAG sequence is repeated 6–39 times in normal individuals, whereas in Huntington's disease patients the CAG sequence is repeated 36–180 times (Rubinsztein et al. 1996; Sathasivam et al. 1997). Due to this abnormal expansion of the CAG repeat segment, the resultant huntingtin protein contains a long tract composed solely of the amino acid glutamine. This protein disrupts the normal function of nerve cells in the basal ganglia,

leading to the death of those cells in the long run. The abnormal function of these nerve cells in turn results in the signs and symptoms of Huntington disease.

The early-onset (severe) forms of HD are associated with alleles containing more than 70 repeats; the longest allele was found to contain 121 CAG repeats, and about 80% of juvenile patients inherit the mutant HD gene from their father (Zuhlke et al. 1993). The greater number of cellular divisions that take place during spermatogenesis is one possible explanation for this unstable expansion of paternal CAG repeats.

The human huntingtin (Htt) protein that carries the polyglutamine repeat expansions was expressed in mice, resulting in a progressive neurological disorder characterized by tremor, abnormal movements, and, in some cases, mild ataxia; even the brains of affected mice were slightly smaller than those of normal ones (Mangiarini et al. 1996). When these transgenic animals were analyzed they provided a shortened Htt protein with polyglutamine expansions which was prone to form cytoplasmic and intranuclear inclusions that are immunoreactive to antibodies raised against ubiquitin and the NH2- terminus of Htt (Skinner et al. 1997).

Apart from transgenic mouse models, invertebrate models have also been used. One of the polyglutamine expansion disorders has been genetically expressed in *Drosophila*. The expression of mutant Spinocerebellar ataxia type 3 (SCA3 affecting ataxin-3, also known as Machado–Joseph disease gene, *MJD*) was targeted in the eyes of *Drosophila* resulting in degeneration of the photo receptors (Warrick et al. 1998). However, a *Drosophila* Huntington's disease model is atypical, in that protein aggregation could not be detected by light microscopy (Jackson et al. 1998).

Polyglutamine expansions were also examined in *C.elegans* by expressing Green Fluorescent Protein (GFP) tagged polyglutamine fusion constructs in body wall muscle cells under the control of the powerful *unc*-54 major myosin promoter (*unc*-54::GFP:polyQ). This resulted in the formation of discrete cytoplasmic aggregates during the early stages of embryogenesis and also caused a delay in development from larval to adult stages (Satyal et al. 2000).

1.3.2 Alzheimer's disease

Alzheimer's disease (AD) is the most common neurodegenerative disease; as many as 4 million individuals are affected in the United States. It is a progressive brain disorder

that affects intellectual abilities, including loss of memory and of the ability to think and carry out daily activities. It was first described by the German physician Alois Alzheimer in 1906. Alzheimer's disease is associated with pathological changes in the brain. In AD, intramembrane proteolysis takes place where the proteolytic cleavage occurs within the lipid bilayer. AD neuropathology can be differentiated by the presence of extra-cellular Amyloid plaques and intracellular neurofibrillary tangles. The term Amyloid refers to insoluble protein deposits which possess a fibrillar, β-pleated structure. The main component found in the plaque is the β-amyloid peptide $A\beta_{1-42}$ that is cleaved by γ-Secretase from human amyloid precursor protein (APP); this peptide accumulates in the brains of Alzheimer disease patients. APP is the gene that causes early-onset familial AD (FAD).

In mammals, γ-Secretase is a multi-subunit membrane protease complex comprising of presenilin, nicastrin, aph-1 (anterior pharynx-defective 1), and pen-2 (presenilin enhancer 2). γ-Secretase is made functional through a series of molecular changes. Firstly, aph-1 and nicastrin binds to presenilin which is the catalytic subunit of γ-Secretase. Secondly, binding of presenilin stabilizes the subcomplex, which is then recognised by pen-2, to form the multi-subunit protease complex whose

activity is brought about by endoproteolysis of presenilin. Hence, the enzymatically active Presenilin cleaves the app molecule to generate $A\beta_{1-42}$ peptides within the patient's brain (Takeshi, 2004).

In *C.elegans*, the identification of sel-12 (presenilin) was a result of genetic screening of non multi-vulval revertants of lin-12 after EMS mutagenesis. Surprisingly, the sel-12 gene is similar to the S182 gene product, which has been implicated in FAD. The fact that presenilin is central to the γ-Secretase enzyme complex and that mutation of sel-12 alleles in C.elegans causes recessive egg-laying defect compels us to draw connections to the enzymatic functions of sel-12. However, this does not give direct indication of its role in the onset of alzheimer's disease in *C.elegans* (Diane and Iva, 1995).

However, the mechanism of $A\beta_{1-42}$ neurotoxicity is not clear. Amyloid aggregates also contain another protein, called tau, which normally passes on chemical messages. These proteins form intracellular neurofibrillary tangles that appear like threads twisted inside the nerve cells (Hardy et al. 1998). As the disease progresses, nerve cells start to die and the whole brain shrinks as a result of which the person starts to lose intellectual ability.

This Amyloid hypothesis has been tested in several models. Among these transgenic mice were first developed for modeling various features of AD pathology. Mutant forms of APP and Tau have been expressed in transgenic mouse models, which show evidence of Amyloid plaques as well as neurofibrillary tangles, although the relationship between the two pathways is not clear. These models exhibit several characteristics of AD, such as an age-dependent generation of Amyloid plaques, but they did not show all of the signs of neurodegeneration observed in human AD (Lewis 2000; Gotz et al. 2001; Higuchi et al. 2002; Oddo et al. 2003). Furthermore, the mouse model has a relatively long life span and therefore it is not suitable for pharmacological screening of new drugs.

Subsequently, simple invertebrate systems such as *C. elegans* and *Drosophila* were used as models for human neurodegenerative diseases because of their short reproduction time and well-characterized genomics. These model organisms are able to express human genes of interest, and genetic screening can be completed in a relatively short period of time to identify mutations that lead to age-dependent neurodegenration.

Transgenic *C.elegans* strains were engineered to express a β-amyloid peptide derived from human cDNA clones under the

control of the *unc*-54 promoter. Different sizes of Amyloid aggregates were found in the affected worms, just as seen in Alzheimer's brain. The worms became paralyzed, whereas in the transgenic mice cognitive impairment was observed. In addition, the worms lived for only 20 days (Link 1995; Link et al. 2001); A similar sequence of events was also demonstrated in a *Drosophila* model of AD (Iijima et al. 2004).

1.3.3 Parkinson's disease

Parkinson’s disease (PD) is the second most common neurodegenerative disease affecting about 1% of people over 65 years of age. In 1922 Parkinson described “shaking palsy”, a progressive neurodegenerative disorder that has an effect on movements such as walking, swallowing and writing (Parkinson 1922). As a movement disorder, it is characterized by tremor, rigidity and loss of voluntary movement, primarily due to the loss of neurons in a brain region termed the substantia nigra (Lang and Lozano 1998). These neurons produce dopamine (DA), a chemical messenger that communicates between nerve cells and muscles. In the brain, dopaminergic neurons present in the substantial nigra produces dopamine that is essential for normal motor functions. The message (dopamine) from these neurons are transmitted to the motor cortex via neuronal projection into the caudate nucleus (CN), which in turn

communicates with the neurons in the thalamus (TH) that leads to normal motor function. In Parkinson's patients, dopaminergic neurons from the substantial nigra undergo neurodegenration, as a result the message is not transmitted. This leads to abnormal motor function (Figure 1.1).

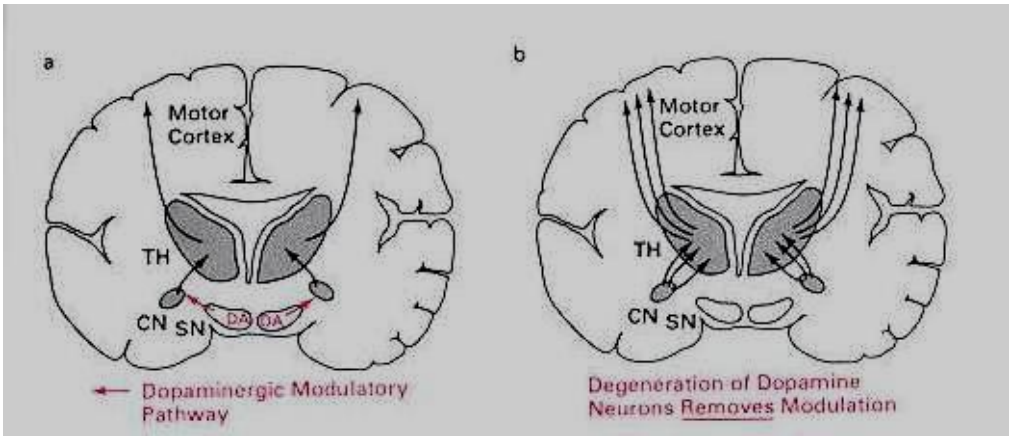

Figure 1.1: Dopamine pathways and motor functions. (Taken from the book: The Neuron, cell and molecular biology by Irwin B.L and Leonard K.K (Authors), 1997).

Neurodegeneration and loss of these Dopaminergic neurons in the substantia nigra are the key feature of Parkinson's disease (Kuwahara et al. 2006). α-synuclein aggregation and Lewy body formation are responsible for the loss of dopaminergic neurons in the substantia nigra resulting in PD (Sharon et al. 2003; Kuwahara et al. 2006). The symptoms of Parkinson's disease become evident when around 80 percent of the dopamine has been lost. 95% of cases of PD show no evidence of genetic inheritance and are termed "sporadic", whereas the remaining 5% are genetically inherited (Dauer and Przedborski 2003).

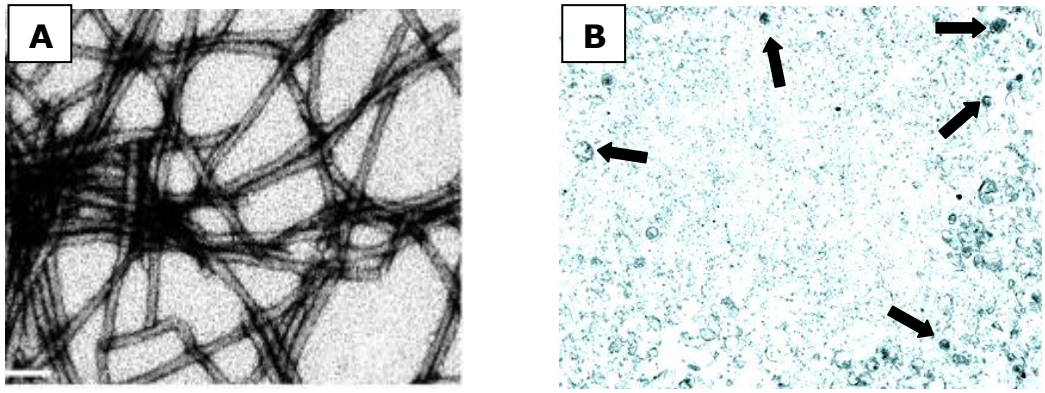

Figure 1.2: Electron microscopy pictures of (A) alpha synuclein amyloid aggregates and (B) Lewy body (arrows pointing) (adapted from Jensen et al. 2000; Antony et al. 2003)

α-synuclein is a natively unfolded protein of only 140 amino acids whose sequence is characterized by 6 imperfect repeats and a highly acidic C-terminal region. It has a tendency to form fibrillar aggregates which later develop into inclusions, such as Lewy bodies (LB), Lewy neurites (LN), and glial cytoplasmic inclusions (GCIs). The LB and LN are characteristic of Parkinson's disease (PD), and point mutations or gene amplification of *α*-synuclein are responsible for familial PD (Munoz et al. 1997; Kruger et al. 1998; Zarranz et al. 2004). α-synuclein aggregation is usually enhanced by mutations in selected genes (see below) and also by exposure to toxins (Uversky et al. 2002; Lakso et al. 2003). Mutations of α-synuclein often lead to abnormal protein folding and increased formation of LBs. Mutant forms of α-synuclein that are associated with inherited (familial) forms of PD are the A30P and

A53T variants (Tofaris and Spillantini 2005). The extent to which atypical folding and aggregation of neuronal proteins is directly toxic to the cell remains unclear (Tofaris and Spillantini 2005). Recently, a third missense α-synuclein mutation (E46K) has been shown to increase amyloid fibril formation within Lewy bodies (Choi et al. 2004; Greenbaum et al. 2005; Pandey et al. 2006).

Mutations in DJ-1/PARK7 (Parkinson disease autosomal early-onset 7), parkin (an E3 ubiquiitin ligase) and PINK1 (a mitochondria-targeted kinase) are also known to cause familial forms of Parkinson's disease (Shimura et al. 2001; Canet-Aviles et al. 2004; Silvestri et al. 2005). However, Parkin is known to be neuroprotective and helps in maintaining mitochondrial function. In the presence of oxidative stress, PINK1 accumulates on damaged mitochondria and binds to or phosphorylates Parkin triggering apoptosis of the damaged mitochondria (Narendra et al. 2010). This pathway helps in maintaining normal mitochondrial function.

A balance between mitochondrial fission and fusion is essential for normal mitochondrial function. Recruitment of Parkin to damaged mitochondria, may affect mitochondrial fission and/or fusion, leading to autophagy (Narendra et al.

2008). In *Drosophila,* Zivizni et al (2010) showed that PINK1 is essential to activate Parkin and promote degradation of the damaged mitochondria. They also found, that mitofusin (mfn) becomes ubiquitinylated on the outer surface of the mitochondria in the presence of the PINK1/Parkin complex, and upon loss of PINK1 or Parkin function, accumulation of mfn leads to elongation of the mitochondria through fusion (Ziviani et al. 2010). According to Narendra et al. (2008), these findings indicate that the PINK1/Parkin pathway has an effect on mitochondrial fission and/or fusion. Other evidence suggests an accumulation of mitochondrial DNA mutations in PD (Bender et al. 2006; kraytsberg et al. 2006).

In the past, mice and rats have been used as a model for α-synuclein overexpression; however it was not clear whether adverse effects were due to significant loss of dopaminergic terminals or to motor neuron pathology, since motor neurons are especially susceptible to α-synuclein in transgenic mice (Sommer et al. 2000; van der Putten et al. 2000)

Human α-synuclein has been overexpressed In *Drosophila*, resulting in selective loss of dopaminergic neurons (Feany and Bender 2000; Auluck et al. 2002). At the beginning of the adult stage α-synuclein causes neurodegeneration,

resulting in the gradual loss of > 50% of the dopaminergic neurons in the fly brain over several weeks of adult life. Of the three different α-synuclein isoforms tested (wild type, A30P, and A53T), all showed similar effects in this model, although A30P was slightly more aggressive and caused behavioral or locomotion defects (Feany and Bender 2000).

Human α-synuclein overexpression in transgenic *C. elegans* has been directed to different sets of neurons. When both wild type and A53T forms of human α-synuclein were expressed in dopaminergic neurons (DN cells), motor deficits, loss of dendrites and increases in neuronal process breaks, as well as loss of DN cells were all observed in the transgenic worms (Lakso et al. 2003).

The exact mechanism underlying sporadic Parkinson's disease (PD) remains mysterious but there is some evidence that environmental factors may be involved in the origin of this disorder. Exposure to metals such as manganese, copper, lead, iron, mercury, zinc (Gorell et al. 1999), cobalt, cadmium and aluminum (Altschuler 1999) have all been implicated as risk factors for PD. Pesticides (herbicides and insecticides) have also been linked to PD in various epidemiological and experimental studies.

In vitro studies show that aggregation and fibrillation of α-synuclein can be accelerated by specific pesticides and metals (Uversky et al. 2001; Uversky et al. 2002). In vivo studies show that exposure of rats and mice to pesticides such as the herbicide paraquat (Manning-Bog et al. 2002; McCormack et al. 2002) and the insecticide rotenone (Sherer et al. 2003) can cause disease-associated neuropathologies such as cytoplasmic inclusions and dopaminergic degeneration similar to human PD.

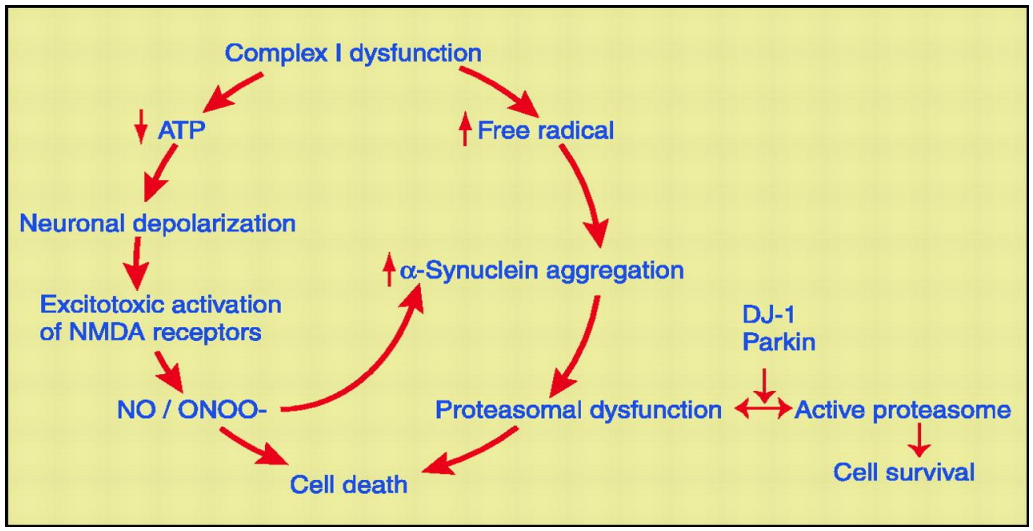

Figure 1.3: Neurodegeneration pathway in Parkinson's disease (adapted from Dawson and Dawson 2003)**.**

Dysfunction of mitochondrial complex I has been linked to sporadic PD, by causing a series of biochemical alterations such as oxidative stress, leading to increases in free radicals and reduction of ATP levels. Increased free radicals and decreased ATP both cause cell death via different pathways. Reduced ATP levels lead to neuronal depolarisation (neuronal injury) which

further leads to free radical–mediated injury involving nitric oxide (NO) and peroxynitrite (ONOO-), eventually causing cell death. Also, sustained mitochondrial complex I dysfunction leads to α-synuclein aggregation, leading to proteasomal dysfunction and also causing cell death. Parkin is an E3 ubiquitin ligase, which plays an important role in proteasomal function by recognizing specific substrates for ubiquitinylation and subsequent degradation. Thus parkin could be considered as a neuroprotective agent. In its absence cells may be unable to deal with α-synuclein aggregates via proteasomal degradation. In addition, DJ-1 is also known to be neuroprotective by a similar mechanism leading to cell survival (Dawson and Dawson 2003).

1.2 *C. elegans* as a model organism

The nematode *Caenorhabditis elegans* (*Caeno*, recent; *rhabditis*, rod; *elegans*, elegant), is a tiny multicellular, eukaryotic, non-parasitic, invertebrate, free-living organism. *C.elegans* was selected as an experimental model by Dr Sydney Brenner in 1965 to study the development and behaviour of the animal (Brenner 1974). Its anatomy is shown in figure 1.4.

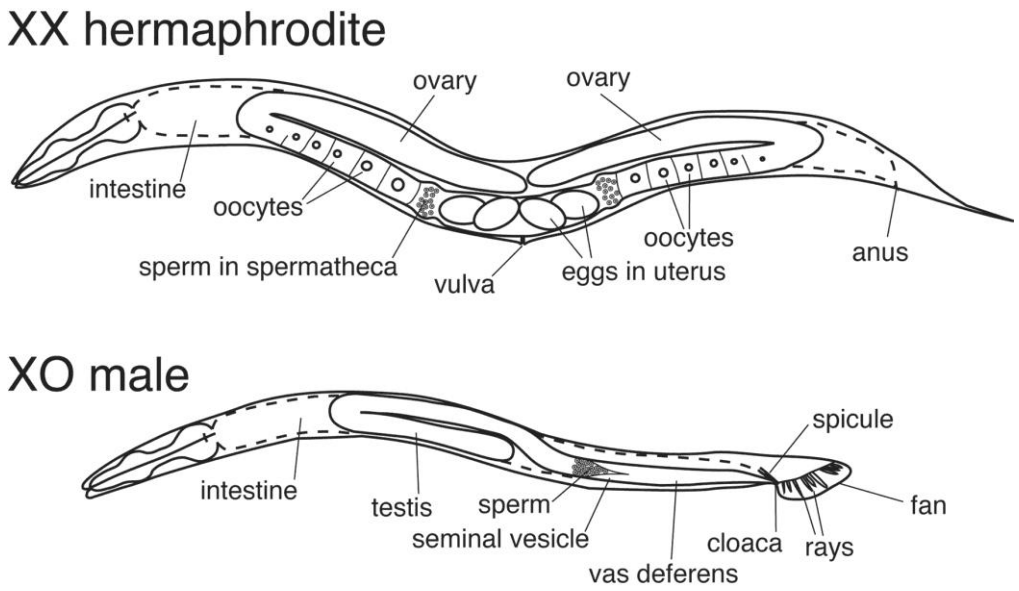

Figure 1.4: The two sexes of *C. elegans* (adapted from Sulston and Horvitz 1977).

C. elegans was used as an experimental model because of its small size physically (about 1 mm long) and genomically (~100 Mbp), its transparent body, and its ease of cultivation including economy. It develops from a fertilized egg to an adult worm with a life cycle of only 3 days at 25ºC (Angier 1995; Donald 1997). Normally it lives in compost or rotting fruit, where it feeds on micro organisms such as bacteria and fungi. It can be easily cultivated in large numbers (>10,000 worms/Petri dish) on agar plates carrying *E.coli* as food source in the laboratory; it can also be grown in liquid cultures. For long term storage, L1 larval worms can be frozen down at or below -80°C and can subsequently be revived after thawing. The developmental pattern of every single somatic nucleus (959 in the adult

hermaphrodite; 1031 in the adult male; (Sulston et al. 1983) has been traced, of which 302 are in neurons (Donald 1997; Horvitz 1997; Wood 1988). *C. elegans* has direct relevance to humans because about 83% of *C. elegans* genes (DNA or protein sequence) are similar to human sequences (Lai et al. 2000) *and* show evidence of common ancestry (i.e. the two sequences are probable orthologs by similarity of sequence). In several cases when human genes are introduced into mutant *C. elegans* they can functionally replace the *C. elegans* orthologs. Therefore, many *C. elegans* genes can function similarly to mammalian genes.

C.elegans is the first multicellular organism to have its entire genome sequenced. It has a very small genome of about 100.2Mb (100,269,912 bases) and its genes have been mapped to five autosomes and one sex chromosome (*C.elegans* Sequencing Consortium 1998). The simplicity of *C.elegans* genetics has allowed researchers to microinject DNA into the worm which can become integrated into the chromosomes, leading to the generation of stably-transformed lines (Fire 1986). This method is known as germline transformation and is used for generating transgenic *C.elegans* strains for experimental studies (see section 1.4.1 below for more details).

1.2.1 Life Cycle

The life cycle of *C. elegans* consists of an embryonic stage, four post embryonic larval stages (L1-L4) and the adult stage. At the end of each larval stage a new stage-specific cuticle is synthesized and the old one is shed (Cassada and Russell 1975). Adults mostly reproduce during the first few days of adulthood, but are characterized by a relatively long post-reproductive lifespan (living for up to 21 days in total). In this species, 99.9% are self-fertilizing hermaphrodites (see 1.2.3), but about 0.1% of the population consists of males which can outcross with hermaphrodites.

1.2.1.1 Embryogenesis

Embryogenesis involves two different stages: (i) cell proliferation and (ii) organogenesis/morphogenesis (Sulston et al. 1983).

1.2.1.1.1 Proliferation

During this initial stage cells divide from a single zygote cell to 558 essentially undifferentiated cells. This stage is further subdivided into two phases: The first phase ranges from 0 to 150 min from the time the zygote is formed to production of embryonic founder cells, and it takes place within the mother's uterus; the second phase ranges from 150 to 350 min, during which cell division and gastrulation is completed (Seydoux and

Fire 1994). At about the 30-cell stage the embryo is laid through the vulva into the surrounding medium.

1.2.1.1.2 Organogenesis / morphogenesis

The developmental event starts at approximately 5.5hrs post fertilization and completes by approximately 14 hrs post fertilization. During this stage the embryo becomes folded back on itself and the whole body of the worm becomes differentiated into distinct tissues and organs. The worm can even roll around longitudinally inside the egg during this stage (Sulston et al. 1983). Figure 1.5 shows the stages of development at 22 ºC (figure from Sulston et al. 1983).

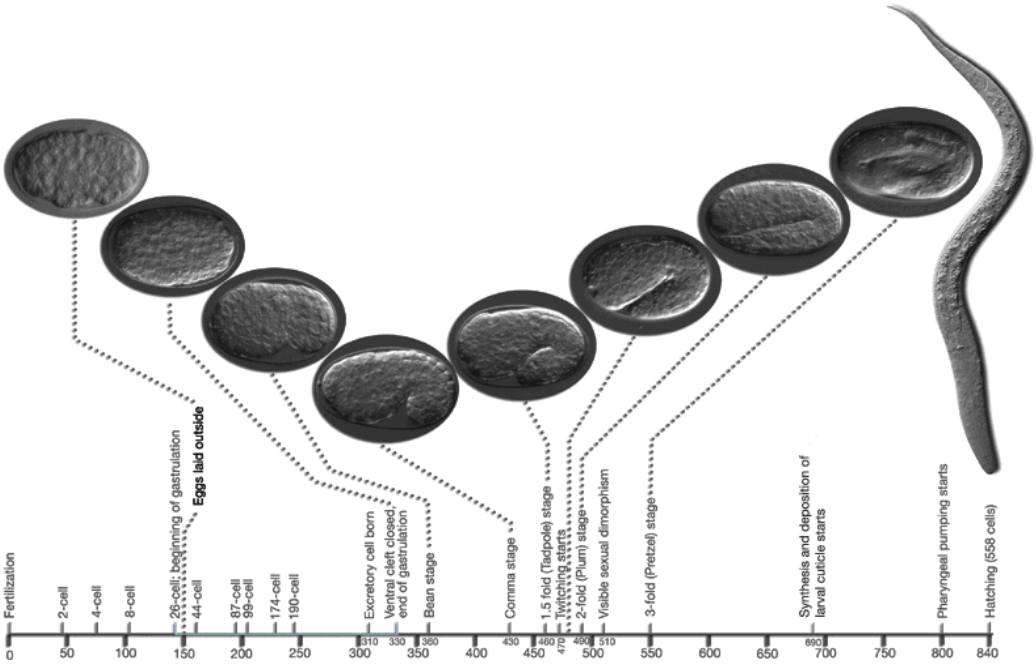

Figure1.5: Embryonic stages of development at 22 ºC (adapted from Sulston et al. 1983). The numbers below the horizontal axis show approximate time in minutes after fertilization at 22ºC. Fertilization takes place at the 0th minute. First cleavage occurs at approximately 40 min. At the 150th minute the embryo reaches the 30-cell stage. During this stage the egg is laid through the vulva. The embryo undergoes differentiation inside the egg and finally at around the 840th minute the animal is hatched out of the egg.

1.2.1.2 Postembryonic development

Postembryonic development begins 3 hours after hatching (Ambros 2000). *C.elegans* has to pass through four larval stages (L1, L2, L3 and L4) to reach adulthood, each stage lasting between 7 and 12 h at 20 ºC (Table 1). The rate of development depends on the ambient temperature (Table 1), since *C.elegans* is poikilothermic.

Table I
Growth Parameters of the *Caenorhabditis elegans* Life Cycle[a]

Temperature (°C)	Embryogenesis (h)	Molts (h posthatch)				First eggs laid (h posthatch)
		L1–L2	L2–L3	L3–L4	L4–adult	
16	29[b]	24	39	54.5	74.5	94–97
20	18[b]	15	24	34	46	59–60
25	14	11.5	18.5	26	35.5	45–46

[a] Based on Hirsh *et al.* (1976, Fig. 2).
[b] Calculated by multiplying 25°C embryongenesis time by 20 and 16°C growth rate factors of 1.3 and 2.1, respectively.

Table 1.1: Growth parameters of the C.elegans life cycle. (Taken from the book: Methods in cell biology, volume 48: *Caenorhabditis elegans;* Modern biological analysis of an organism by Henry F. Epstein (Author) and Diane C. Shakes (Editor) Academic Press,1995).

The first stage L1 larva is about 250 µm in length, and hatches from the egg at about 13.3 hrs after fertilization at 22ºC and this shorter at 25ºC and longer at lower temperatures. Again cell division starts when there is food available, though not as much as in embryos. During L2 there is an increase in growth along with some cell division and expansion of tissues. During L3 development of the gonad takes place. The size of this larval stage is somewhat larger than L2. Vulva development occurs during the late L3 and early L4 stage. The final L4 stage can be differentiated with the help of an anatomical feature known as the "Half moon" (Johnstone et al. 1997). The somatic cell lineage comes to an end at the early L4, and during this stage the animal becomes sexually mature, generating sperm cells in the hermaphrodite gonad (see 1.2.3 below). Figure 1.6 shows the

life cycle of *C. elegans* at 22ºC (figure from Cassada and Russell 1975).

1.2.1.3 Dauer

At the end of the L1 stage, the animal may enter into an alternate L2d stage which then moults into a diapause dauer larva under conditions where food is scarce and population density or temperature are high (Albert and Riddle 1988). Dauer larvae are thin and can move but their mouths are plugged and they cannot eat. Interestingly, dauers can remain viable for three months. They appear to be non-aging: dauer larvae can roam around for months without food and once they come across food they directly enter into the L4 stage and live about 15 more days (Klass and Hirsh 1976). Studying the genes involved in entry into/exit from the dauer pathway has led to the discovery of an insulin-like signaling pathway that controls lifespan via the *daf*-2 receptor which negatively regulates the *daf*-16 transcription factor (Kenyon 2010).

1.2.1.4 Adult

A newly matured hermaphrodite is formed after 45 – 50 hrs at 20º C completing its reproductive life cycle. The adult hermaphrodite switches to producing eggs in its gonad for about 3-4 days, after which they still remain fertile. During this period they normally produce about 300 self-fertilized progeny each.

The life span of a mature adult is about 21 days (Lakowski and Hekimi 1998).

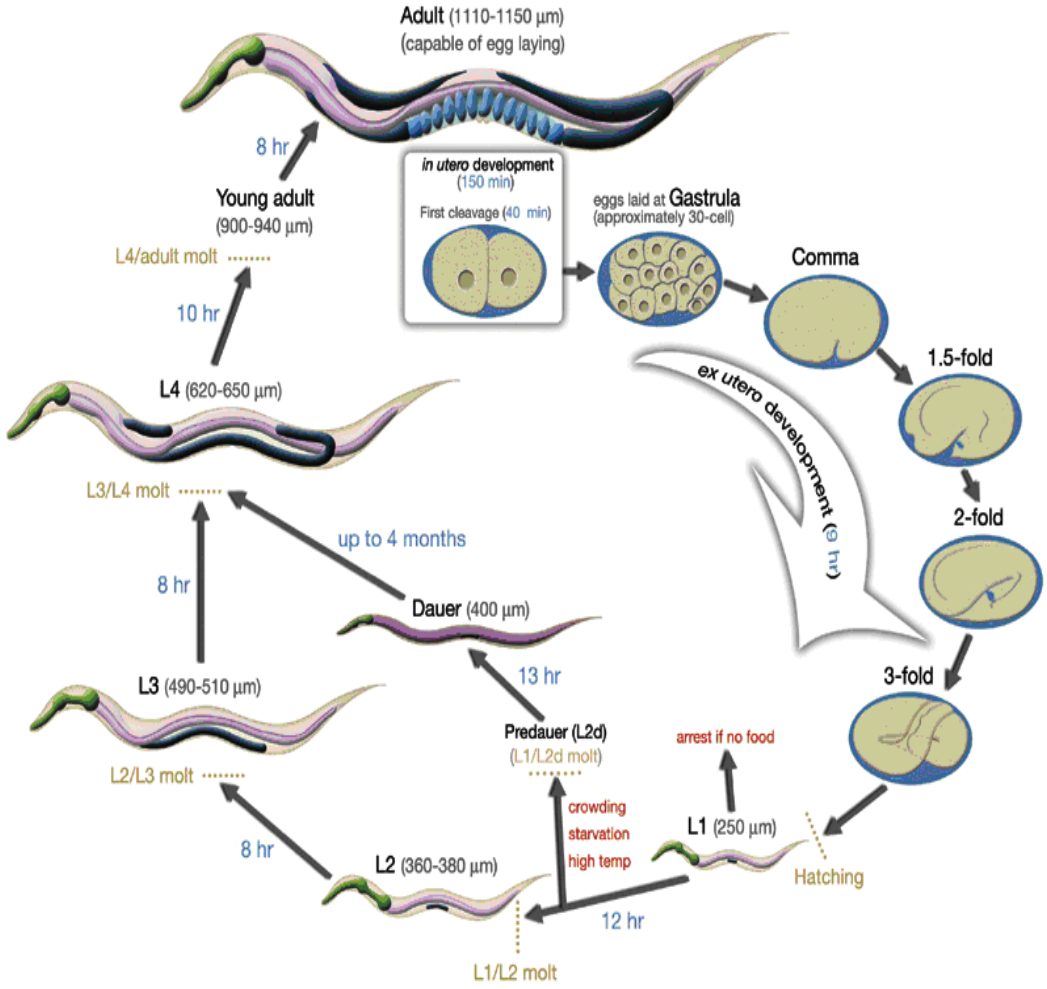

Figure 1.6: Life cycle of *C. elegans* at 22ºC (adapted from Cassada and Russell 1975). Numbers in blue next to the arrows shows that how much time is taken to complete each stage. Approximately at the 40th min, first cleavage takes place inside the egg. During the gastrula (approximately 30-cell) stage, eggs are laid out through the vulva. The length of the animal at each stage is given in micrometers.

Lifespan determinations (see 2.11) have proved an invaluable tool for exploring the effects of genetic mutations that alter life span. For example, both *daf*-2 under-expressing and

daf-16 over-expressing mutants prolong lifespan significantly (Kenyon 2010).

1.2.3 Sex determination in C.elegans

Reproduction in *C.elegans* is normally by hermaphrodite self-fertilization*. C.elegans* has both hermaphrodite and male sexes, but no female sex. The predominant sexual form of *C. elegans* is the hermaphrodite — this animal produces both sperm (during L4) and eggs (during adulthood; Maupas 1900). Males are rarely found (0.1% of population) and these produce only sperms. There are six chromosomes in *C. elegans* — five pairs of autosomes (chromosomes I, II, III, IV, V) and the sex chromosome, X. Hermaphrodites have two X chromosomes (designated XX). Males have only one X chromosome (designated XO); having only one chromosome instead of a pair is called the hemizygous state. This state can be produced by the loss of one X chromosome during meiosis or by mating (Hodgkin et al. 1979). Males cannot produce progeny on their own. However, they can cross-fertilize hermaphrodites. They are commonly used in *C.elegans* genetics for making genetic crosses. The predominance of hermaphrodite self-fertilization has advantages for maintaining genetic uniformity of strains during long-term culture. It also facilitates the recovery of homozygous recessive mutations.

1.3 Green Fluorescent Protein as a biomarker

Green Fluorescent Protein (GFP) is composed of 238 amino acids. It was originally isolated from the jellyfish *Aequorea victoria*, and when exposed to blue light it produces green fluorescence. Its excitation and emission wavelengths are 395 and 509nm respectively. GFP is used as a reporter gene to monitor gene expression and protein localization in a variety of different organisms and in cell tissue cultures. In addition, GFP can be used as a marker in living organisms during growth and development (Chalfie et al. 1994). Previous studies have used GFP as a reporter gene in *C.elegans in vivo* by fusing it to varying lengths of polyQ residues (Nollen et al. 2004). Similarly, yellow fluorescent protein (YFP) was used as a reporter gene *in vitro* by fusing it to α−synuclein (van Ham et al. 2008, 2010).

1.4 α-synuclein fusion constructs for in vivo and in vitro studies

In previous studies α−synuclein and its fluorescent-tagged variants were shown to be capable of aggregating spontaneously *in vitro* (Li et al. 2001; Goers et al. 2003). Van Ham et al (2010), showed that α−synuclein::YFP formed amyloid fibrils which were similar to those formed by wild type α−synuclein (no reporter gene) *in vitro*. In our studies, fusion constructs were created by tagging α−synuclein with two Green

Fluorescent Protein (GFP) variants, Cerulean (C) or Venus (V – for the Venus variant of YFP). Thioflavin T binding (Khurana et al. 2005) and centrifugation assays (Bodhicharla et al, submitted) showed that synuclein and synuclein-containing fusion proteins all had the ability to aggregate in vitro.

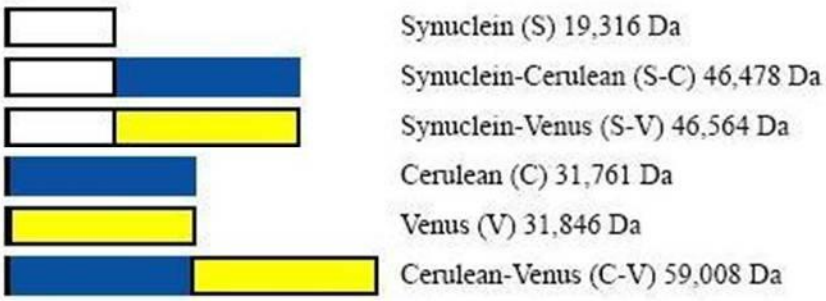

Figure 1.7: Fusion protein design (Bodhicharla et al, submitted)**.** A cartoon illustrating the construction of the fusion proteins used. The N-terminal fusion peptide from the pET-30a vector is shown as a black rectangle, human α-synuclein (S) as an open rectangle, Venus (V) as a yellow rectangle and Cerulean (C) as a blue rectangle. Each construct is identified by name and abbreviation, and the constructs are drawn approximately to scale. The fusion genes were designed, cloned and expressed in bacteria by Dr. Jody Winter.

In neurodegenerative diseases, certain proteins have the capability to aggregate *in vivo*, which is thought to be an essential factor in disease development (Dobson 2003). Among these are *α*-synuclein and its mutant forms (A30P and A53T) that are associated with inherited (familial) forms of PD (Tofaris and Spillantini 2005). However, although the aggregation process has been extensively studies *in vitro*, much less is known about the aggregation of α−synuclein *in vivo*. Van Ham et al (2008) showed formation of protein aggregates in the body walls of *C.elegans in vivo* by expressing *α*-synuclein tagged with

the reporter gene YFP (*unc*-54::YFP; strain NL5901). In our studies, transgenes encoding mixtures of both CFP- and YFP-tagged synuclein (SC+SV) were injected into the gonad of an adult hermaphrodite to generate transgenic animals. These transgenes are expressed in the body wall muscles of *C.elegans* using *unc*-54 myosin promoter (*unc*-54::SC+SV) . This strain can potentially be used to monitor α−synuclein aggregation in living worms using FRET (see below; Bodhicharla et al, submitted).

1.5 Generation of transgenic strains for use in this study

Transgenic strains are usually created by inserting the gene of interest into the animal's genome using DNA recombinant technology. This can be done in 3 different ways: DNA microinjection, retrovirus-mediated gene transfer (Jaenisch 1976) and embryonic stem (ES) cell-mediated gene transfer (Gossler et al. 1986). DNA microinjection is regarded as the first and most successful technique in mice (Gordon and Ruddle 1981) and this technique has been used in several other animal models including *C.elegans*.

1.5.1 DNA microinjection

DNA microinjection is the main technique used to make transgenic lines in *C.elegans.* A DNA construct (plasmid) is mixed with a selectable marker and injected into the syncytial distal gonad. In the case of GFP fusion genes, a selectable marker is unnecessary because expressing transgenic individuals can be identified by their fluorescence under a UV microscope. Using the *unc-54* promoter, a synuclein-YFP fusion construct was abundantly expressed in the body wall muscles of *Caenorhabditis elegans*. The injected DNA exists as an extrachromosomal array (i.e. not integrated in the chromosome; Mello et al. 1991) which segregates randomly and can be lost, but the YFP marker identifies which animals still have the array. The level of Transgene expression in multiple injected lines may vary depending on copy number and other factors; hence it is essential to ascertain phenotype homogeneity by examining multiple lines for a particular transgene.

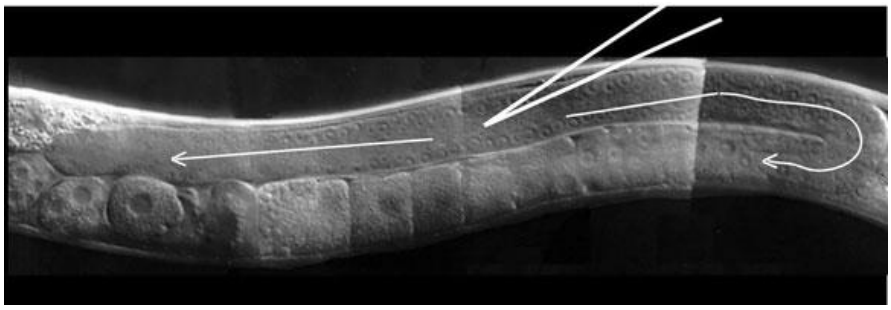

Figure 1.8: Microinjection: performed by Ademola Adenle (SV, V, C, S+V, SC+SV strains) and Declan Brady (CV, C+V, SV+C strains). (adapted from Mello et al. 1991; Mello and Fire 1995).

1.6 Permanent integrated transgenic lines

Permanently integrated transgenic lines can be achieved following gamma irradiation, which is commonly used in *C.elegans* to produce chromosomal rearrangements (Rosenbluth et al. 1985). This material is reviewed in detail in chapter 3 on radiation sensitivity.

1.7 Forster Resonance Energy Transfer (FRET)

Forster Resonance Energy Transfer is commonly abbreviated as FRET. The underlying mechanism behind FRET is the energy transfer between two fluorophores, in this study CFP (donor) and YFP (acceptor). This material is reviewed in detail in the introduction to chapter 5.

1.8 RNA Interference

RNA interference (RNAi) involves sequence-specific, posttranscriptional gene silencing mediated by double stranded RNA (dsRNA). RNAi was first discovered in *Caenorhabditis elegans* by Guo and Kemphues (Guo and Kemphues 1995). Gene silencing was activated efficiently by injecting dsRNA complementary to target mRNAs, causing their degradation. In 1998 Andrew Fire and Craig Mello published their study on the mechanism of RNA interference (Fire et al. 1998). It was previously known that antisense RNA (Izant and Weintraub 1984), but also surprisingly sense RNA (Guo and Kemphues

1995), could cause gene silencing, but the results were somewhat unpredictable. The term RNA interference (RNAi) was coined to describe the unknown mechanism (Rocheleau et al. 1997).

It soon became clear that dsRNA acts via posttranscriptional mechanisms to degrade the target mRNA during RNA interference (Montgomery et al. 1998). Within a year RNAi had been rapidly implemented as a method for selectively inhibiting gene expression in most laboratory organisms, including fruit flies, trypanosomes, plants, planaria, *Hydra* and zebrafish (Tuschl et al. 1999) as well as in mammalian cells (Elbashir et al. 2001). Thus, the general applicability of the RNAi phenomenon among eukaryotes was established very quickly.

RNAi can be initiated in *C.elegans* by delivering dsRNA into the cells of the worm (Sugimoto 2004), which can be done in 4 different ways. (1) Microinjection, (2) Soaking, (3) Harpin formation from transgenes with specific regulatory promotors and (4) Feeding.

a) Microinjection

This method involves injecting the dsRNA into either adult or larval worms (Fire et al. 1998). Although it has some

disadvantages such as being time consuming and delicate, it results in very good gene suppression.

b) Soaking

This involves soaking the worms without food for 24 hours in a dsRNA solution, before returning them to the plates and examining them or their progeny for phenotypic changes (Tabara et al. 1998; Maeda et al. 2001).

c) Harpin formation from transgenes with specific regulatory promotors

This method results in stable, heritable worm strains where RNAi can be induced (either tissue- or stage-specifically) through the use of a specific promoter and a gene construct including double stranded harpin structures in the resultant transcript (Sugimoto 2004).

d) Feeding

In this method the worms are fed with inducible dsRNA-expressing *E.coli* (Kamath and Ahringer 2003). Some of the advantages of this feeding technique are: - (i) it is much less labour-intensive than microinjection, and (ii) it can also be used for large scale applications of RNAi, saving a substantial amount of time. The feeding method is considered to work best for late

larval development, behavior and longevity studies as well as for genome-wide screening (Kamath et al. 2003).

C.elegans has been examined for RNAi resistant mutants (Tabara et al. 1999), resulting in the identification of four genes causing RNAi deficiency, termed *rde*-1/-2/-3/-4. Germline transmission of the RNAi signal requires *rde-1* but it is not required for interference (Grishok et al. 2000).

The molecular machinery involved in RNA interference can be demonstrated by introducing dsRNA into a cell. It first becomes cleaved by the enzyme Dicer to form small interfering RNAs (siRNA) which are approximately 21-25 nucleotides in length (Elbashir et al. 2001). siRNA then binds to the RNA-induced silencing complex (RISC) and is unwound. The antisense RNA forms a complex with RISC that binds to its corresponding mRNA, and the RISC complex then cuts the mRNA strand, which is subsequently degraded.

RNAi already plays an important role in *C.elegans* research, particularly since several libraries of RNAi bacterial strains are now available that cover > 80% of the known genes in *C.elegans* (Kamath et al. 2003). Figure 4 shows the mechanism of RNAi (from Lehner et al. 2004)

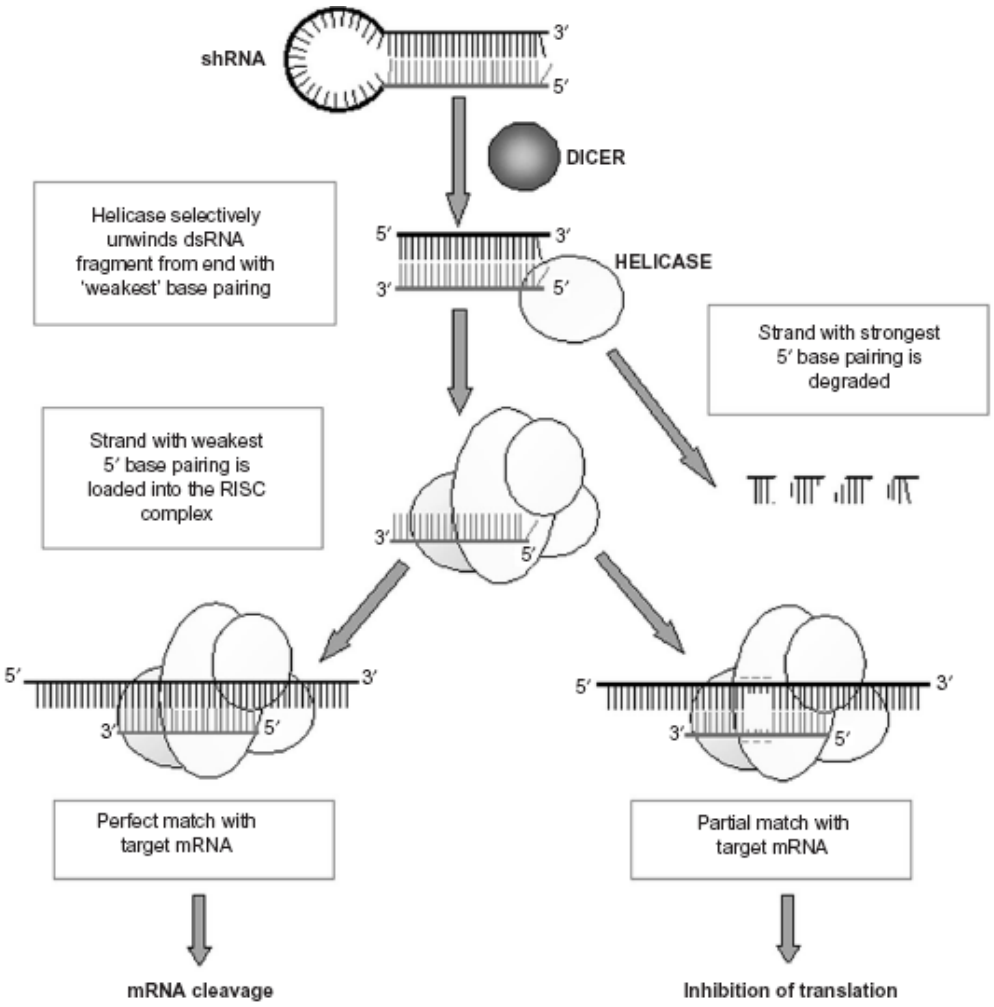

Figure 1.9: The mechanism of RNAi and RNAi delivery methods (adapted from Lehner et al., 2004). Double-stranded RNA is cut into short pieces (siRNA) by the endonuclease Dicer. The antisense strand is incorporated into the RISC complex that guides the repeated cleavage of homologous mRNAs.

1.8.1 RNAi screening of polyglutamine aggregation in *C.elegans*

Huntington's disease is a late-onset neurodegenerative condition caused by polyglutamine expansions within the human huntingtin gene (see 1.3.1). A *C.elegans* model for this disease was established by creating transgenic *C.elegans* strains with varying lengths of polyglutamine repeat sequence fused to GFP. During polyglutamine fusion protein aggregation, protein misfolding is associated with the length of the polyglutamine expansion and age-dependant changes. Genome-wide RNAi was used to identify genes that might limit or promote polyglutamine aggregation. Screening identified 186 genes, which when suppressed resulted in the premature appearance of protein aggregates (Nollen et al. 2004).

In HD patients, the mutant huntingtin protein has 34-86 CAG repeats, whereas the wild type Htt protein has only 11-34 CAG repeats (Duyao et al. 1993). At a threshold of about 36 CAG repeats, protein aggregation and cellular dysfunction increases resulting in development of HD (Karpuj et al. 1999). In order to test this hypothesis, Morley et al (2002) expressed polyQ (Q0 to Q82) in *C.elegans.* Fluorescence was diffuse in Q0, Q19, Q25, Q33 and Q35, but fluorescent aggregates could be

seen in Q44, Q64 and Q82. However, Q40 animals had a few aggregates in some cells and diffuse fluorescence in others. This shows that the higher the repeat length the more the polyQ protein aggregates. From this experimental data they were able to support the threshold hypothesis of polyQ-mediated toxicity (Morley et al. 2002).

1.8.2 RNAi screening of α-synuclein aggregation in *C.elegans*

More recently similar transgenic strains have been constructed using α-synuclein fused to the GFP sequence. Genome-wide RNAi screening was done to identify the genes and cellular processes that are involved in age-related α-synuclein aggregation. 80 genes were identified from this process, which when knocked down resulted in premature increases in the number of inclusions. Genes that are related to aging such as *sir*-2.1 and *lagr*-1 were also found during this process. This suggests that there may be a link between cellular ageing and α-synuclein aggregation (van Ham et al. 2008).

1.8.3 Comparison between previous RNAi studies

Genes that function to suppress polyglutamine aggregation (Nollen et al. 2004) were compared with those that can suppress α-synuclein aggregation (van Ham et al. 2008). A

large variety of proteasomal genes and chaperones were found to be involved in polyglutamine aggregation in *C.elegans,* and similar genes have been implicated in other protein aggregation and misfolding diseases. Unexpectedly, very few such genes were found to affect α-synuclein aggregation. Only two genes were identical in both of these aggregation studies.

Process	Cosmid no	Gene	Function
RNA synthesis and processing	Y116A80.35	Uaf-2	Similartity to splicing factor U2AF 35 kDa subunit
Energy metabolism	T14F9.1	vha-15 (phi-52)	ATPase coupled proton transport, Vacuolar ATP synthase sub

Table 1.2: Two identical genes in polyglutamine aggregation and α-synuclein aggregation (adapted from Nollen et al. 2004; van Ham et al. 2008).

However, we have identified several cases where functionally related genes (effectively carrying out a similar job), often coding for related proteins, are found in each of the two lists. This shows that the processes involved in dealing with these aggregated proteins are probably similar; in several cases these gene products may carry out a similar function in different cellular compartments because α-synuclein aggregation occurs in endomembrane-bound vesicles whereas polyglutamine

aggregation seems to occur in the cytosol and nucleus but not within inclusion bodies.

Polyglutamine Aggregation		**Alpha-synuclein Aggregation**	
Gene	**Function**	**Gene/Cosmid no**	**Funcion**
phi-53	DNA primase, small subunit	pri-2	Eukaryotic-type DNA primase, large subunit
hsp-1	Member of the heat shock HSP70 protein family/EEVD	R151.7	Hsp90 protein
hsp-6	Member of the heat shock HSP70 protein family		
Phi-4	Putative splicing factor	Rsp-7	Splicing factor, arginine/serine-rich
uaf-2	Similarity to splicing factor U2AF 35 kDa subunit	*uaf-2*	Similarity to splicing factor U2AF 35 kDa subunit
phi-11	Similarity to splicing factor 3b subunit 1		
lit-1	Serine/threonine protein kinase of the MAP kinase subfamily	F12A10.6	Serine/threonine kinase (haspin family)
phi-2	Member of the RNA helicase, DEAD-box protein family	Rcq-5	DEAD/DEAH box helicase
phi-3	Member of the DEAD or DEAH		

	box ATP-dependent RNA helicase family		
mog-5	Member of the RNA helicase, DEAH-box protein family		
phi-33	Similarity to ubiquitin carboxyl-terminal hydrolase 8	math-24	MATH domain, Ubiquitin carboxyl-terminal hydrolase 7

Table 1.3: comparison between polyglutamine aggregation and α-synuclein aggregation (adapted from Nollen et al. 2004; van Ham et al. 2008)

1.9 Environmental Toxicology in Parkinson's disease

Numerous experimental studies using animal models have shown that exposure to environmental agents may play a vital role in PD pathogenesis. Since PD pathogenesis does not develop suddenly, these animal models have usually been exposed to neurotoxic agents. Also, environmental agents such as metals, solvents, carbon monoxide and *N*-methyl-4-phenyl-1,2,3,6-tetrahydropyridine have been shown to cause PD-like symptoms (Klawans et al. 1982; Langston and Ballard 1983; Tanner 1989; Uitti et al. 1994), as well as various pesticides and herbicides. Conversely, other agents such as nicotine and

caffeine are known to alleviate the symptoms of PD (Ross et al. 2000; Ross and Petrovitch 2001; Martyn and Gale 2003).

Environmental stressors such as copper, iron, zinc, aluminium, paraquat and dieldrin (Li et al. 2001; Sun et al. 2005; Fernagut et al. 2007; Bharathi et al. 2008) have been shown to play a role either directly or indirectly in the development of Parkinson's-like symptoms both *in vitro* and *in vivo*. In addition, mixtures of metals and pesticides have been shown to act synergistically in prompting the formation of fibrils *in vitro* using purified synuclein (Uversky et al. 2002). Similarly, β-amyloid aggregation was also aggravated by metal ions both singly (Drago et al. 2008) and in combination (Ryu et al. 2008). One reason for metal and pesticide induced aggregate formation may be due to the indirect effect of reactive oxygen species (ROS) production (Allsop et al. 2008).

1.9.1 Neurotoxicity of Pesticides

1.9.1.1 Chlorpyrifos

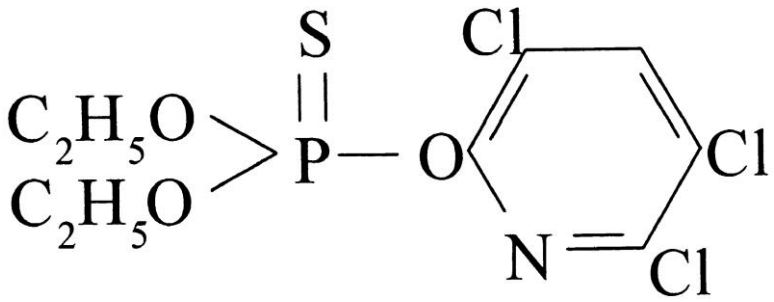

Figure 1.10: Chemical structure of chlorpyrifos (Adapted from Wu and Laird 2004).

Chlorpyrifos is an organophosphate insecticide which is commonly used in agriculture to control insect pests. Reports have also shown that chlorpyrifos exposure is lethal to fresh water fish. Since chlorpyrifos inhibits the enzyme acetylcholinesterase (AChE), one would expect that exposure to chlorpyrifos might cause severe effects in other organisms as well. In addition, chlorpyrifos may inhibit DNA synthesis and alter development (Slotkin 2004; Eaton et al. 2008). In utero exposure to chlorpyrifos caused retardation in growth (Sherman 1996), and hence its use has been restricted in households, hospitals and schools. AChE is an enzyme that breaks down acetylcholine (neurotransmitter) into acetate and choline groups in the synaptic cleft (Smegal 2000). By binding to the active site of AChE, chlorpyrifos prevents the breakdown of acetylcholine in central nervous system (CNS). As a result, chlorpyrifos leads to

neuronal cell overstimulation followed by neurotoxicity and death (Karanth and Pope 2000).

Several reports (Auman et al. 2000; Crumpton et al. 2000) have investigated the fundamental molecular mechanisms of chlorpyrifos action, in terms of inducing neuronal apoptosis. According to these authors, inhibition of acetylcholinesterase is independent of chlorpyrifos-induced apoptosis. In previous studies, rats were used as an *in vivo* model, where cortical neurons (which are particularly susceptible to neurodegeneration) were directly cultured from newborn animals. Several signalling pathways such as ERK 1/2, JNK and p38 MAP kinase are involved in neuronal apoptosis (Davis 2000; Hetman and Xia 2000). Growth and neurotrophic factors trigger the ERK 1/2 signalling pathway whereas oxidative and environmental stresses trigger the JNK and p38 signalling pathways. It was shown that JNK and p38 cause apoptosis upon activation by chlorpyrifos, while ERK1/2 (as a growth promoting pathway) defends against this apoptosis. A balance between the apoptosis pathway activated by oxidative/environmental stress and the survival pathway activated by growth/neurotrophic factors is key to determining the fate of cortical neurons (Xia et al. 1995). These findings also show that chlorpyrifos induces oxidative stress, which is a common pathway for several of the

environmental factors implicated in spordiac Parkinson's disease – including rotenone (next section), paraquat (Berry et al. 2010) and dieldrin (Kanthasamy et al. 2005).

1.9.1.2 Rotenone

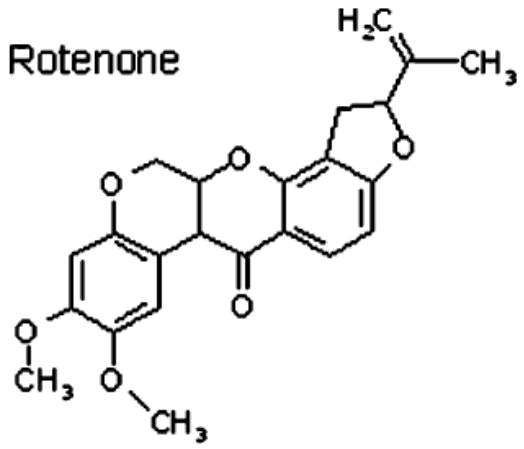

Figure 1.11: Chemical structure of rotenone (Adapted from Uversky 2004).

Rotenone is a complex ketone by nature, present in the roots of *Lonchocarpus* species. It was initially used as a fish poison but nowadays it is generally used as an insecticide. Rotenone is biodegradable and extremely lipophilic. Due to its lipophilicity, rotenone can cross cellular membranes and the blood-brain barrier without the help of transporters. Within the cell it is accumulated in the mitochondria (Talpade et al. 2000), where it blocks the electron-transport chain and hence oxidative phosphorylation (Schuler and Casida 2001). Specifically, rotenone inhibits complex I, increases ROS production, and causes oxidative damage to proteins, lipids and DNA. Fibril

formation by α-synuclein is one of the known types of protein damage induced by rotenone. As a consequence of these multiple effects, rotenone induces apoptosis of the damaged cell (Uversky 2004).

Previous studies show that intravenous exposure to rotenone causes PD like symptoms. Since rotenone is a complex I inhibitor, it suppresses the activity of mitochondria leading to depletion of dopaminergic neurons causing neuronal cell death. Rotenone also stimulates the formation of α-synuclein protein aggregates leading to cell death (Betarbet et al. 2000; Sherer et al. 2003). *In vitro* studies show that rotenone speeds up the fibril formation of α-synuclein (Uversky et al. 2001; Uversky et al. 2002).

Exposure to rotenone in rats showed severe effects on mitochondria because of its inhibition of mitochondrial complex I inhibitor (Betarbet et al. 2000). Similarly, chronic rotenone exposure in *Drosophila* caused behavioural effects, especially locomotor dysfunction due to the loss of dopaminergic neurons in the brain (Coulom and Birman 2004).

C.elegans is an excellent in vivo model to reveal the mechanisms of toxicity of pesticides (Leung et al. 2008).

Rotenone exposure inhibits mitochondrial NADH dehydrogenase present in the mitochondrial complex I. In order to confirm the role of mitochondrial NADH dehydrogenase in rotenone toxicity, a *C.elegans* mutant strain (*gas*-1) was developed. This strain contains a mutation in the 49-kDa mitochondrial complex I subunit. *Gas*-1 mutants showed increased sensitivity to rotenone, proving that NADH dehydrogenase is a key target for rotenone in the cells (Ishiguro et al. 2001).

Compound	**Strains investigated**	**Observations**	**References**
Rotenone	*gas*-1(fc21)	Increased sensitivity to rotenone under hyperoxia	(Ishiguro et al. 2001)
	pdr-1, *djr*-1.1 RNAi	Increased vulnerability to rotenone	(Ved et al. 2005)
	lrk-1 RNAi	Overexpression of wild-type human LRRK2 strongly protects against rotenone toxicity	(Wolozin et al. 2008)

Table 1.4: Rotenone toxicity to *C.elegans*

The E3 ligases *pdr*-1 (parkin orthologue) and *djr*-1.1 (DJ-1 orthologue), and the membrane associated kinase *Irk*-1 have been implicated in the pathogenesis of PD in a *C.elegans* model, and have also been reported to show sensitivity to

rotenone. Ved et al. (2005) have shown the involvement of *pdr*-1 and *djr*-1.1 in rotenone toxicity by gene knock-out experiments. To confirm the role of LRRKs (mixed lineage kinases) in PD, Wolozin et al, (2008), ablated the *C.elegans* membrane associated kinase *Irk*-1 and observed increased sensitivity to rotenone. On the other hand, over-expression of human LRRK2 in *C.elegans* was observed to confer protection against rotenone.

1.10 Oxidative stress

Oxidative stress plays a vital role in neurodegenerative diseases and especially in Parkinson's disease (Jenner 1998). When there is an imbalance in the production of reactive oxygen species (ROS), the cell is subjected to oxidative stress. ROS include peroxides, such as hydrogen peroxide and peroxynitrite, and free radicals such as the superoxide, nitric oxide and hydroxyl radicals. These are produced due to instability in the redox state of tissues and they can damage all cell components including proteins, membrane lipids and DNA through oxidation.

The superoxide radical ($O_2^{\bullet -}$) which can give rise to the more damaging hydroxyl radical ($HO^{\bullet}$) in the presence of iron and other redox-active metals (Fenton reaction). However,

superoxide radicals are normally converted by the enzyme superoxide dismutase (SOD, which exists in both mitochondrial and cytosolic forms) into oxygen and hydrogen peroxide. This latter is in turn converted into water and oxygen by catalases, or through a cyclical reaction converting two molecules of reduced glutathione (GSH) into the oxidised form (GSSG), catalysed by glutathione peroxidise enzymes (Ozgocmen et al. 2006).

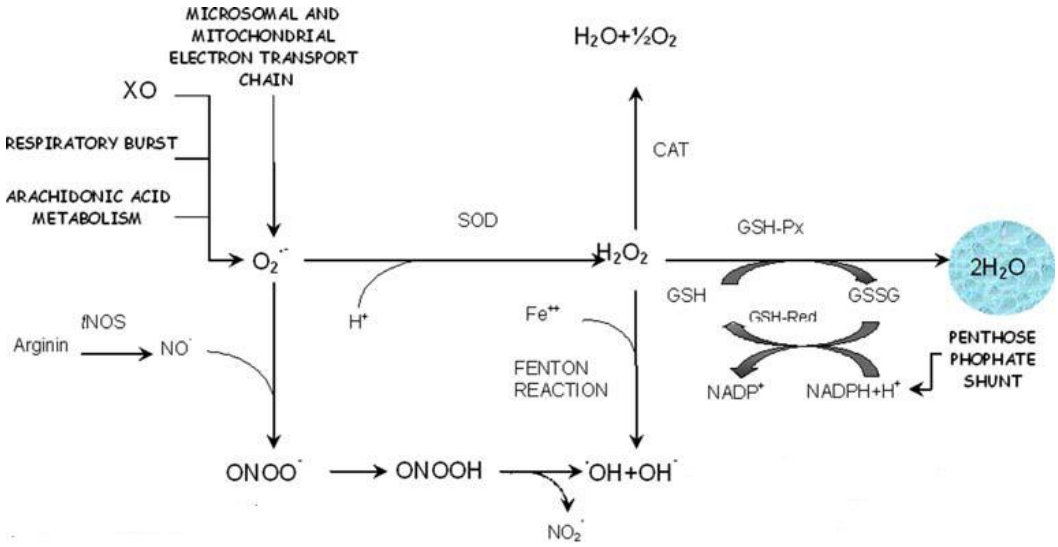

Figure 1.12: Formation of free oxygen radicals (adapted from Ozgocmen et al. 2006).

Oxidative stress can also cause cell death, either via apoptosis or necrosis (Lennon et al. 1991). In order to combat oxidative stress, every cell has several defence and repair mechanisms, including the enzymes mentioned above. Antioxidants such as vitamin C and E or reduced glutathione (GSH) are also used as a defence mechanism against the toxic effects of ROS. Oxidative stress is aggravated due to reduced

antioxidant potential. Hence antioxidants such as superoxide dismutase, glutathione peroxidise, vitamin E etc can be used as supplements to protect the cell from oxidative stress (Ebadi et al. 1996).

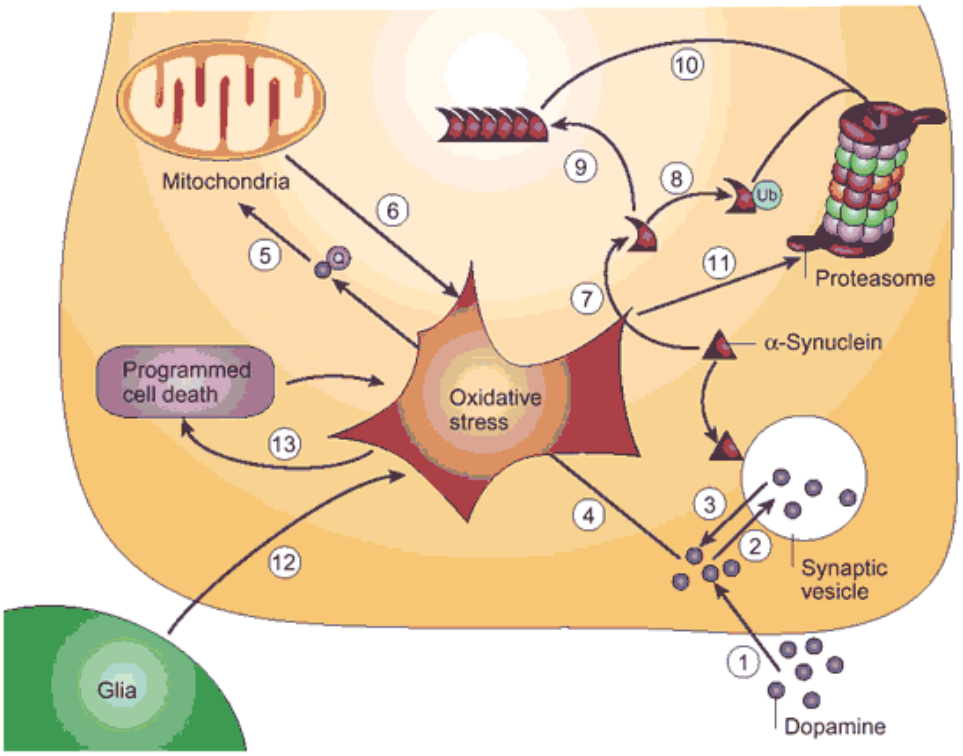

Figure 1.13: oxidative stress pathways in a dopaminergic neuron (adapted from Andersen 2004). Steps 1 to 13 are described in the text below.

.

Figure shows the oxidative stress pathways involved within a dopaminergic neuron. (1) The neurotransmitter dopamine is taken into the dopaminergic neuron by the dopamine transporter (DAT); (2) Similarly dopamine is taken into synaptic vesicles by vesicular monoamine transporter (VMAT2); (3) α-synuclein aids in dopamine release from the synaptic vesicle; (4) dopamine is oxidized to dopamine quinone

(DAQ); (5) DAQ produces potential mitochondrial inhibitors such as metabolites or conjugates of 5cysDAQ; (6) oxidative stress is produced by mitochondria; (7) α-synuclein oxidation; (8) tagging of α-synuclein by ubiquitin and subsequent degradation by the proteasome; (9) oligomerization of α-synuclein; (10) proteasomal dysfunction caused by oligomeric α-synuclein; (11) oxidative by-products such as 4-hydroxynonenol (4-HNE) interact with the proteasome further inhibiting its function; (12) glial cell production of oxidative stress; and (13) stimulation of programmed cell death (Andersen 2004).

Dexter et al (1989) showed that dopaminergic neurons in the substantia nigra undergo neurodegeneration due to oxidative stress in Parkinson's patients. Oxidative stress also causes increased protein misfolding leading to accumulation of α-synuclein aggregates in the substantia nigra (Takeuchi et al. 2002).

Aims

- To generate permanent integrated transgenic lines using gamma irradiation.
- To investigate the apparent radiation sensitivity of transgenic synuclein-expressing worms.
- Characterization of transgenic and wild type worms in terms of.
  - Life cycle
  - Brood size
  - Sterility
  - Life span
  - Pharyngeal pumping
  - Longevity
- FRET analysis for all the transgenic strains and wild type worms.
- FRET analysis for *unc*-54::SC+SV (I) fusion worms using confocal imaging.
- FRET analysis for *unc*-54::SC+SV (I) fusion worms and YFP fluorescence for NL5901 in terms of aging.
- RNA interference directed against Hip-1 in *unc*-54::SC+SV (I) fusion worms.

- Protein aggregation in *unc*-54::SC+SV (I) and positive control *unc*-54::CV (I) fusion worms following treatment with the pesticides chlorpyrifos and rotenone.
- Quantification of Reactive Oxygen Species production in *unc*-54::SC+SV (I) *and* NL5901 employing the H2DCF-DA assay.

Chapter 2. Materials and Methods

Suppliers of all materials and equipments used in this project are listed in Appendix 2.

2.1 Bacterial Preparation

Preparation of bacterial stocks was done using a laminar flow hood and a flamed platinum loop under sterile conditions.

2.1.1 *E.coli* P90C Strain

E.coli P90C is a mutant strain with the *lac*-operon deleted. This is to prevent bacterial interference with the β-galactosidase assay when using *lacZ* reporter strains. It was selected based on its *lacZ*$^-$ phenotype and it also does not possess antibiotic resistance (Miller, 1972). P90C colonies were streaked onto separate plates of S-Gal LB agar (Sigma) alongside a parallel plate with a *lacZ*$^+$ *E.coli* strain, such as HT115, and incubated overnight at 37ºC. The colonies on the *lacZ*$^+$ control plates were dense and black whereas the *lacZ*$^-$ colonies appeared off-white in colour. This was done periodically to check that the P90C strain had not become contaminated. Concentrated suspensions of P90C bacteria in 25gl^{-1} of high salt LB broth (Melford laboratories Ltd) were kept at 4°C in 50ml sterile tubes for up to 6 months for use as bacterial food.

2.2 Plate Culture of C.elegans

2.2.1 Preparation of Nematode Growth Medium (NGM) plates

Nematode Growth Medium (NGM) was prepared by adding NaCl, Agar, Peptone and Cholesterol as described below (Brenner 1974).

NaCl	3.0 $g.l^{-1}$
Agar	17.0 $g.l^{-1}$
Peptone*	2.5 $g.l^{-1}$ (*or up to 20 $g.l^{-1}$)
Cholesterol (5 $mg.l^{-1}$ stock in ethanol)	0.5 $mg.l^{-1}$

*Higher concentrations of peptone were sometimes used in high peptone plates to encourage bacterial and nematode growth.

Table 2.1: Composition of nematode growth medium

After being autoclaved, the mixture was allowed to cool to 60ºC in a water bath. Once cooled, further additions of 1M $CaCl_2$ (1ml per l), 1M $MgSO_4$ (1ml per l), and 1M potassium phosphate buffer pH 6.0 (25ml per l) were added with stirring because they tend to form insoluble calcium and/or magnesium phosphate crystals.

$CaCl_2$	1 mM
$MgSO_4$	1 mM
Potassium Phosphate Buffer pH 6.0	40 mM

Table 2.2: Additions to NGM agar (final concentrations).

The potassium phosphate buffer (1M, pH 6.0) was prepared by titrating 500 ml acidic KH_2PO_4 (1M) with basic K_2HPO_4 (1M) until pH 6.0 was reached. The resultant solution was dispensed into 150 ml aliquots, autoclaved and stored at 4ºC.

The complete NGM mixture was then poured into 3.5cm, 9cm or 14 cm Petri dishes, and allowed to solidify. Using sterile technique, a glass spreader was used to spread a dense suspension of P90C bacteria evenly over the plate. Alternatively, the NGM could be formulated with additional peptone (up to 20 $g.l^{-1}$) in order to facilitate the growth of a denser bacterial lawn. Plates were incubated overnight at 37ºC to allow the bacterial lawn to grow and then kept at room temperature for short period of time (a few days) because plates may dry out if kept for a longer periods. Alternatively, the plates could be stored in a fridge at 4ºC for up to several weeks. Plates stored at 4ºC were allowed to warm up at room temperature (15-20ºC) before use.

2.3 Worm Culture

2.3.1 Subculturing and Transferring Worms

Using sterile technique, a flamed scalpel was used to cut the agar into small pieces from a 1 week old plate containing worms. Small pieces of agar were transferred onto fresh plates containing bacteria. Individual worms could be picked up under a microscope by using the flattered tip of a platinum wire pick. This was constructed by heat sealing a small piece of 32 gauge platinum wire into the end of a glass pipette and gently hammering flat the end of the wire. This flat end of the wire was flamed first, and then dipped into the bacterial suspension to make it stickier and more attractive to worms. Once this was done the worms could be picked individually and transferred onto fresh 3.5cm plates. Worms were then incubated at either 15 or 20ºC for 3-4 days, allowing them to grow and reproduce.

2.3.2 Harvesting and Washing of Worms

2.3.2.1 K-Medium

In order to help ensure consistency between batches of K-medium, a 25 X concentrate was made up and frozen down in 40 ml aliquots. These were then defrosted and made up to 1 litre in volumetric flasks before being dispensed and autoclaved.

The final constituent concentrations in 1 X K-medium were as follows (Williams and Dusenbery 1990)

KCl	32 mM
NaCl	53 mM

Table 2.3: Components of K-Medium

2.3.2.2 M9 Buffer

For 1 Litre:

KH_2PO_4	3 g
Na_2HPO_4	6 g
NaCl	5 g
$MgSO_4$ (1M)	1 ml
dH_2O	1 L

Table 2.4: Composition of M9 Buffer

M9 buffer was prepared as above, dispensed and autoclaved for 15 minutes. Worms were harvested by washing them off the cultured plates with approximately 1-2 ml of K-medium or M9 buffer.

2.3.2.3 Transferring worms.

The worms were transferred to 50 ml centrifuge tubes and allowed to settle on ice. Normally adult worms take 10-15 minutes to settle, leaving behind a supernatant containing worm

debris and bacteria as well as some small larvae. This supernatant was removed carefully without disturbing the worm pellet and fresh K-Medium or M9 buffer was added, again allowing the worms to settle for 10-15 minutes. This whole process was repeated several times until the supernatant was clear and essentially free from bacteria. Finally the tubes were centrifuged at 2500 rpm for 2 minutes and the supernatant was removed.

2.3.3 Synchronization of Worm Cultures

2.3.3.1 Filtration

Plates containing worms were washed with either sterile K-Medium or M9 buffer (as described above) and the worm suspension passed through a sterile 5µm nylon mesh filter (Wilson Sieves, Nottingham); a population of mostly L1 and in some cases L2 larvae washed through in the filtrate (Mutwakil et al. 1997). The filtered larvae were allowed to settle on ice or at 4ºC in the fridge for at least 60 min or centrifuged at 3000 rpm for 5 minutes. After removing the supernatant, the larval pellet was resuspended with 500µl of K-medium. After resuspension equal aliquots of larvae were distributed in small drops onto fresh NGM plates and incubated at 15 to 25ºC. After several days, the developmental stage of the worms was checked to determine whether the adults were producing eggs, at which

point the worms were ready to be harvested. Adults retained in the 5µm filter were resuspended, washed and cleaned as described above.

2.3.3.2 Egg Isolation

Worms were washed off the culture plates using M9 buffer or K-medium, and the worm suspension was transferred into 50ml centrifuge tubes. Worms were then allowed to settle on ice for 30 minutes or spun at 3000rpm for 5 minutes. The supernatant was removed and 10 volumes (relative to the pellet) of freshly prepared egg isolation solution were added and vortexed thoroughly. Egg isolation solution consists of alkaline hypochlorite (described below) and is used to kill and breaks open the adult worms and larvae. Only the eggs can survive this procedure, provided that they are not exposed for more than 10 minutes in total. After 6-7 minutes, the worm suspension was centrifuged for 3 minutes at 3000 rpm, then again the supernatant was removed and fresh M9 buffer or K-Medium was added. The washing process was repeated 2-3 times until the supernatant became clear. The pellet containing the surviving eggs and worm debris was resuspended in small volume of medium to form a slurry, which was then spotted onto fresh NGM plates, and incubated at 15-25ºC.

NaOH	20 $g.l^{-1}$
NaOCl (13.5 to 16% commercial stock)	2.16-2.56%

Table 2.5: Composition of Egg Isolation Solution

NaOCl stock is at a concentration of 13.5 to 16% available chlorine (Aldrich, Dorset, United Kingdom). Due to the tendency of the sodium hypochlorite to break down over time, the egg isolation solution was made up fresh monthly and stored at 4ºC.

2.3.4 Cleaning contaminated *C. elegans* stocks

C. elegans stocks may become contaminated with other bacteria, yeasts or mould. Mould could be removed by transferring the worms onto fresh plates. Bacterial contaminants and yeast were easily removed by treating adult worms with egg isolation solution as mentioned in section 2.3.3.2, in order to kill the contaminants and all worm stages other than embryos protected within the egg shell.

In order to remove mould contaminants from *C. elegans* stock plates a scalpel or spatula was sterilized in a flame and a piece of the agar was removed from the contaminated plate. The piece of agar was placed at the edge of a clean bacterial plate. The worms were allowed to crawl off the agar and across the *E. coli* P90C lawn to the opposite side of the plate. Once the worms

have reached the other side of the plate, individual animals were picked with the help of worm picker (using a flamed scalpel or spatula) and placed near the edge of another clean plate. The whole process was repeated until the contaminants were removed.

2.4 Freezing Live Worms

Among the different developmental stages of *C.elegans,* only L1 and L2 larvae are expected to survive the freezing process. Freezing worms can be done only when the worms have very few bacteria in their gut because of the risk of rupture, which would reduce their chances of survival upon thawing. Worms were frozen down in two different ways: – (i) Culture plates were allowed to grow for 2 to 3 days at 15 - 25°C and washed with small volumes of either M9 buffer or K-Medium as above; (ii) alternatively eggs were isolated from a synchronized culture of gravid adults and allowed to hatch in M9 buffer without added bacteria for 24 hours at 15ºC. This produced a bacteria-free culture of synchronized L1 larvae. In either case, an equal volume of freezing down solution (Table 2.6) was added to the worm suspension and the mixture dispensed in 1ml aliquots into autoclaved 1.5 ml microcentrifuge tubes. These were mixed by inverting the tubes several times, then labeled, placed in polystyrene boxes and stored at -80ºC. In order to

check the degree of survival, one aliquot was taken out of the freezer, thawed quickly by hand-holding or in a 37º C water bath, and then plated onto fresh NGM plates. If very few worms survived the freezing process, then the whole procedure was repeated.

For 1 Litre:

Glycerol	240ml
NaCl	5.84 $g.l^{-1}$
KH_2PO_4 (1M) pH 6.0	50ml
dH_2O	710ml

Table 2.6: Components of Freezing down Solution

This mixture was autoclaved, and finally sterile 30 µl of $MgSO_4$ (1M) was added per 100ml of solution.

2.5 Protein Extraction from *C.elegans*

This protocol was based on that used in the Pasquinelli lab (adapted from Reinhart and Ruvkun 2001). Worms were washed off from the plates using M9 buffer and rocked for 20 minutes at room temperature to make the worms digest bacteria in the gut. Once again they were washed with M9 buffer and transferred into microcentrifuge tubes. These were centrifuged for 30 seconds at 5000 x g to give a worm pellet at the bottom of the tube. For eggs, the tubes were stood at room temperature for 2-3 minutes, and then centrifuged at 1000 x g (at higher

speeds eggs have a tendency to pellet inside the walls of the tube). Before freezing the worms/eggs in a mixture of dry ice and ethanol, the packed worm volume was noted. An equal volume of 2 X SDS buffer (Table 2.7) was added to the frozen pellet and boiled for 15 minutes; samples were vortexed once after 7-8 minutes. For eggs (only), samples were homogenized using a hand-held homogenizer before boiling. The insoluble material was then pelleted by spinning the tubes at 10,000g for 5 minutes. The supernatant containing solubilised cellular proteins was removed and stored in a separate tube.

10% SDS	2ml(4% final)
0.5M Tris HCl, pH 6.8	1ml(100mM final)
Glycerol	1ml(20% final)
dH_2O	1ml

Table2.7: 2 X SDS buffer (5ml)

2.6 SDS-polyacrylamide gel electrophoresis (SDS PAGE)

This technique, first described by Laemmli (1970) is used to separate proteins based on molecular weight. During the protein extraction excess SDS is added to denature the proteins. The denatured proteins become negatively charged when SDS binds to the amino acid chain. This negative charge is proportional to the length of the protein and hence the molecular

weight of the protein. The denatured proteins are then separated by polyacrylamide gel electrophoresis.

2.6.1 Preparation of gel

SDS-PAGE was performed using a SE 250 Mighty Small II electrophoresis kit. Before use, the glass plates were cleaned using 100% methanol to remove all traces of grease and dirt that may interfere while casting the gel. The percentage of acrylamide used in the gel was based upon the molecular weight of the proteins under investigation. Normally a 12% acrylamide gel was used in this study. Components of the resolving gel were mixed and poured between the glass plates, after the addition of 500 µl of freshly prepared 10% ammonium persulphate (APS) and 50 µl of N, N, N’, N’-Tetramethylethylenediamine (TEMED) as polymerization catalysts. Before the gel polymerized a solution of 0.1% SDS was slowly added on top of the resolving gel. This ensured that a flat interface was obtained between the resolving and stacking gels. The gel was allowed to set for about 30 minutes.

	Running	Stacking
30% Acrylamide	39.6ml	1.3ml
Distilled water	33.9ml	6.1ml
1.5M Tris-HCl pH8.8	25ml	
0.5M Tris-HCl pH6.8		2.5ml
10% SDS	1ml	0.1ml
10% ammonium persulphate (fresh)	0.5ml	0.05ml
TEMED	0.05ml	0.01ml

Table 2.8: Components of SDS-PAGE gel

Once the resolving gel had polymerized, the SDS solution was poured off from the surface of the gel. The stacking gel was made up (as above) and added on top of the resolving gel. After adding 50µl of fresh 10% APS, 10 µl TEMED was added to the stacking gel solution. Before the gel polymerized a comb was inserted into the liquid stacking gel, which was allowed to set for 60mins. The comb was carefully removed and the gel placed between baths of electrophoresis buffer before loading protein samples (see next section).

2.6.2 Sample preparation and gel electrophoresis

Protein samples for gel electrophoresis were diluted by mixing with 5x Loading buffer (0.635 M Tris HCl, pH 6.8, 4%

SDS, 25% glycerol, 500 mM DTT and 0.05% w/v bromophenol blue). These diluted samples (and also molecular weight standards) were boiled at 80-90ºC for 5 minutes and then placed on ice. The samples were briefly centrifuged to remove any insoluble material.

The upper and the lower reservoirs of the gel apparatus were filled with electrophoresis buffer (25 mM Tris-HCl pH 8.6, 1902 mM glycine and 0.1% SDS (w/v)). Prior to loading the samples, the wells were pipetted out to remove any unpolymerized acrylamide. Finally electophoresis was performed at 100 volts for 1.5 hours.

2.6.3 Coomassie Staining

The staining solution was first prepared by dissolving 0.25% Coomassie Blue R-250 in a mixture containing 40% (v/v) methanol and 10% (v/v) acetic acid in water. Prior to use this staining solution was filtered through Whatman 3MM paper, to remove undissolved solids. After electrophoresis the gel was soaked in staining solution for 20 minutes with gentle agitation. The staining solution was decanted and the gel destained using Destain solution (30% methanol and 10% acetic acid, both v/v). Once the gel had been sufficiently destained, it was placed in water for 10 minutes to fully hydrate the gel prior to drying. The

gel was dried onto Whatman 3mm paper and covered with Saran wrap, then dried for 2 hours at 80^{o}C under vacuum. Gels to be blotted were not stained with Coomassie or dried.

2.7 Western Blotting

This technique is used to identify a specific protein in a given protein sample. Gel electrophoresis is used to transfer the size-separated proteins from an SDS-PAGE gel onto a protein-binding membrane (nitrocellulose or PVDF).

2.7.1 Electrophoretic transfer

Polyvinylidene difluoride (PVDF, Immobilon P, Millipore) membranes were used for the blotting process. These have a high binding capacity and give lower backgrounds than nitrocellulose, and are therefore commonly used for blotting. The stacking gel was removed from the separating gel and discarded. The separating gel was then placed on two pieces of 3MM Whatman blotting paper pre-soaked in transfer buffer (Table 2.9). Prior to blotting a piece of PVDF was cut to the size of the gel, soaked in 100% methanol and then in 1 x transfer buffer in which it was rocked for 2-3 minutes. The membrane was then laid over the separating gel, ensuring that no air bubbles were trapped between the gel and the PVDF membrane. Two more pieces of pre-soaked 3MM Whatman blotting paper were placed over the top of the PVDF membrane and the resulting 'sandwich'

was enclosed in an Electro-transfer cassette. The blotting cassette was placed into the transfer tank with the gel side of the sandwich closest to the cathode and the membrane side closest to the anode. The tank was filled with transfer buffer and the blot was electrophoresed for 1 hour at constant 100V using plate electrodes in the high intensity position.

Tris	30.3 $g.l^{-1}$
Glycine	144 $g.l^{-1}$

Table 2.9: 10 x Transfer Buffer

10 x Transfer Buffer	100ml
Methanol	200ml
10% SDS	10ml
dH_2O	700ml

Table 2.10: 1 x Transfer Buffer

The efficiency of Western blotting was determined using prestained protein markers (SDS-7B, Sigma) which were also run on the gel. Additionally Coomassie staining could be done afterwards to show that no protein bands were left in the gel. Once the transfer was completed the blotting cassette was disassembled. The membrane was then transferred into a plastic tray containing transfer buffer to prevent the membrane from drying.

2.7.2 Developing the Membrane

Blocking of non-specific protein binding was achieved by placing the membrane in 1× Tris Buffered Saline (TBS) + 10% Marvel (non-fat milk powder) overnight. The membrane was then washed 5 times for 5 minutes in 1× Tween Tris Buffered Saline (TTBS) containing 0.05% (v/v) Tween 20. After blocking the membrane, 1× TBS + 10% Marvel +anti- synuclein primary antibody (Sigma) at a 1:2000 dilution was incubated with the membrane for 1 hour with gentle agitation. After the primary antibody incubation, the membrane was washed 5 times for 5 minutes in TTBS to remove unbound primary antibody. The membrane was then incubated for 1 hour in 1× TTBS + 10% Marvel with secondary antibody (Bio-Rad anti-Rabbit IgG at a 1:10000 dilution). After the secondary antibody incubation, the membrane was again washed 5 times for 5 minutes in TTBS.

Tris-HCl pH7.6	20 mM
NaCl	136 mM

Table 2.11: Tris buffered saline

Tris-HCl pH7.6	20 mM
NaCl	136 mM
Tween 20	0.5ml/L

Table 2.12: Tween Tris buffered saline

2.7.3 Enhanced Chemiluminescence Detection (ECL)

This followed the kit manufacturer's protocol (Thermo scientific). Equal volumes of two ECL solutions (SuperSignal West Femto Trial Kit /enhancer solution and stable peroxide solution) were mixed, and then the membrane was soaked in this ECL solution for a minute before removing the excess solution. The blot was covered with cling film, and then placed inside the gel documentation machine (Bio-Rad Chemi Doc XRS). Photographs were taken using the Chemiluminescence setting by exposing the blot with a 60 second exposure time.

2.8 Construction of Synuclein-Venus fusion

(Note: this work was performed by Dr. J.Winter prior to the start of my project, and therefore the methods used are not described in detail).

Venus-YFP (V) and human α-synuclein (S) were PCR amplified and cloned into pGEMT Easy with restriction sites added to the ends as follows:

- NcoI-Synuclein-Csp45I
- Csp45I-Venus-SacI

Cloned genes were then excised from pGEMT Easy using the above restriction enzymes, and ligated into pET-30a either

singly or in pairs. pET-30a was double digested with NcoI and SacI prior to ligation. For double ligations, NcoI-Synuclein-Csp45I and Csp45I-Venus-SacI were simultaneously ligated into pET-30a to produce gene fusions (Bodhicharla et al, submitted). The following products were subcloned into pET-30a in this way:

- Synuclein-Venus SV
- Venus V

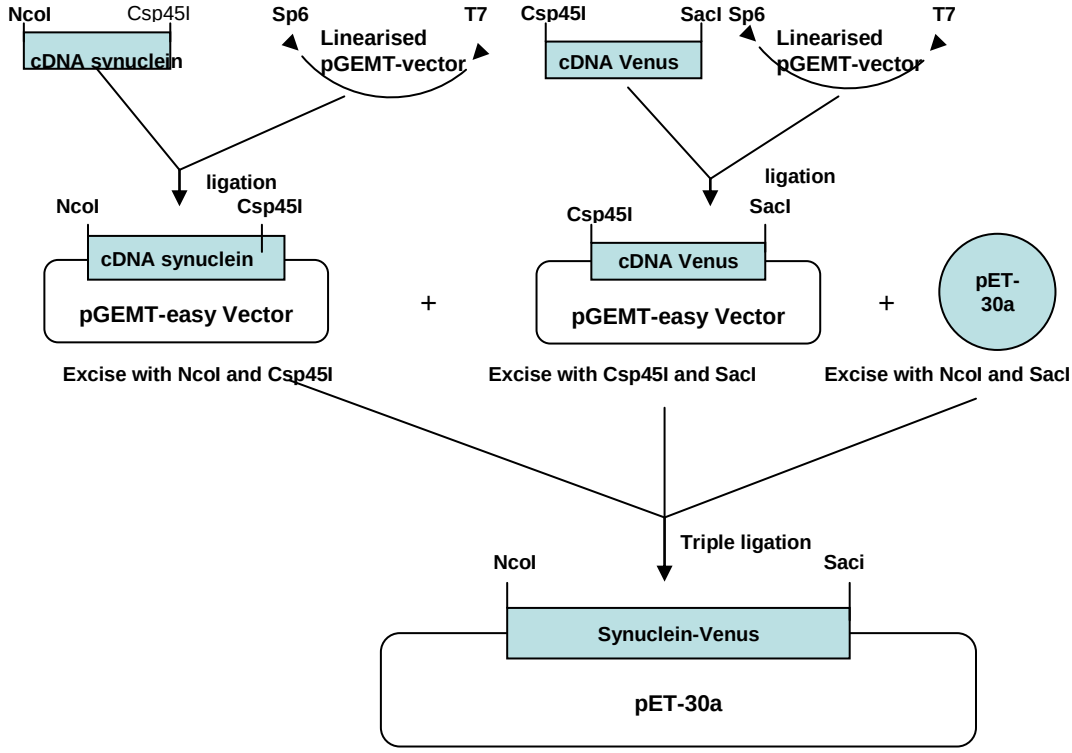

Figure 2.1: Construction of Synuclein-Venus (SV). (Adapted from Bodhicharla, 2007, MRes Thesis, University of Nottingham).

Transgene fusion constructs including Venus (V), Cerulean (C), Synuclein-Venus (SV), Synuclein + Venus (S+V), Synuclein-Cerulean + Synuclein-Venus (SC+SV), Cerulean-Venus (CV) and Cerulean + Venus (C+V) were also constructed using the same cloning procedure.

2.9 Testing of *unc*-54::S+V (NI) fusion gene transmission rate after Microinjection

Fluorescing L4 worms were identified under a fluorescence microscope (Olympus Model SZX12) equipped with filters for distinguishing CFP and YFP fluorescence. Fluorescence was measured with a CFP excitation/emission filter (440/480nm) and an YFP excitation/emission filter (500/545nm) combination. Using a platinum wire pick, a total of 10 worms were individually transferred onto 10 different 3.5 cm diameter NGM plates. After incubation at 20°C for 3 days, the worms would have started to produce F1 offspring. Because this is a non-integrated line, there will be both fluorescent and non-fluorescent offspring present. Percentage of transmission was calculated simply by counting fluorescent versus non-fluorescent worms. Out of those 10 plates, transmission rates varied between 20% and 60%. Plates with a low transmission rate were used for subsequent gamma irradiation.

2.10 Integrating extrachromosomal arrays using Gamma Radiation

An *unc*-54::S+V (NI) fusion line showing 20% transmission of the extrachromosomal transgene array was irradiated with gamma rays (Gamma cell unit with a ^{137}Caesium source; Nordion international Inc). Thirty fluorescing L4 animals

carrying the transgene array were transferred onto each of several 3.5cm plates. The plates carrying these worms were irradiated for different lengths of time to find the dose required for chromosomal integration, resulting in 100% transmission. The standard dose of gamma radiation used for this purpose in the literature is between 2000 and 4000 rad (Rosenbluth et al. 1985). After irradiation, worms were selfed onto individual plates and incubated at 20°C for 2 days. Once they started to produce offspring, several hundred F1 progeny carrying the extrachromosomal array were selfed onto individual plates and again incubated at 20°C for 2 days. After two days, all of these plates were screened for lethality and sterility. At this stage, the percentage transmission rate will be about 75%. If properly irradiated, the percentage of lethality and sterility among F1 progeny should be between 10-15%. From the F2 progeny two F2 transformants were picked from each F1 and selfed onto separate plates. These plates were screened for 100% transmission of the array to the F3; such a strain should carry a homozygous integrated array. The percentage of integrants obtained is generally very low, between 1-2%. In this way, we were able to generate a permanent integrated transgenic line for *unc*-54::S+V (I). This process (section 2.8 and 2.9) was then repeated for the following strains.

Strains		Sucess
unc-54::SV (NI)	*unc*-54 promoter fused to synuclein coding sequence tagged with YFP at its C terminus.	No
unc-54::SC+SV (I)	*unc*-54 promoter fused to synuclein coding sequence tagged with YFP at its C terminus, plus (in equal amounts) *unc*-54 promoter fused to synuclein coding sequence tagged with CFP at its C terminus.	Yes
unc-54::V (I)	*unc*-54 promoter fused to YFP.	Yes
unc-54::C (NI)	*unc*-54 promoter fused to CFP.	No
unc-54::CV (I)	*unc*-54 promoter fused to CFP linked directly to YFP.	Yes
unc-54::C+V (I)	*unc*-54 promoter fused to CFP plus (in equal amounts) *unc*-54 promoter fused to YFP.	Yes
unc-54::SV+C (NI)	*unc*-54 promoter fused to synuclein coding sequence tagged with YFP at its C terminus plus (in equal amounts) *unc*-54 promoter fused to CFP.	No

Table 2.13: Transgenic strains

2.10.1 Back-crossing

All the transgenic lines showing 100% transmission were bred with N2 males to get rid of mutations that were caused by irradiation. To begin with, 12 young N2 males were placed onto a fresh plate with several L4 stage *unc*-54::S+V (I) hermaphrodites. The plate was incubated at 20°C for 2 days. Several hermaphrodites were picked from the 1st generation and the mating process was repeated over 5- 6 generations, such that the resulting transgenic fusion strains should carry no unwanted mutations. For those strains that could not be integrated successfully, non-irradiated lines showing high transgene transmission (≥50%) were selected for culture, but did not require outcrossing.

2.11 Determination of sterility for all transgenic worm strains and N2 wild type worms after gamma radiation.

Several 3.5cm plates each carrying 30 fluorescing L4 transgenic worms were irradiated for different lengths of time (section 2.10). After irradiation these P0 worms were selfed onto individual plates and incubated at 20ºC for 2 days. Once they started to produce offspring, the worm plates were screened to check whether any of the worms were dead or sterile (not laying eggs). The offspring were allowed to develop at 20ºC until larvae

reached the L4 stage. Several hundred F1 progeny from the P0 generation carrying the extrachromosomal or integrated transgene array were selfed onto individual plates. Again these plates were incubated overnight at 20ºC for 2 days until they produced offspring. Several hundred plates were screened again to check whether any of the worms were dead or sterile.

2.12 Determination of life span for transgenic and N2 wild type worms

The life span of worms was determined by picking individual hermaphrodites at late L4 stage onto separate plates. They were left for 2 hours to produce eggs, then the adults were removed and the plate carrying the eggs was labeled with date and time. These eggs were allowed to develop at 20ºC until larvae reached the L4 stage, when they were transferred onto a separate plate and incubated overnight at 20ºC. Next day the adults were transferred onto a new plate leaving behind their offspring on the old plate. The same process was repeated until the animals stopped producing offspring (usually 3-4 days). The adult worms were allowed to grow on at 20ºC, and were monitored daily by tapping the adults on the head. Animals were considered dead if no movement was observed following repeated probing. Once the worms were identified as dead, the

date and the time were noted down. The life span of each worm was then calculated from egg until death.

2.13 Determination of motility for transgenic and N2 wild type worms

Locomotion rates were measured by picking individual adult worms from an agar plate with bacteria and transferring then onto a bacteria-free plate. Locomotion rates were determined by the number of bends each worm performs over 30 seconds. This is difficult to do on bacterial plates because the worms tend to stop moving upon encountering food. Therefore all locomotion rates were measured on bacteria free plates with 10 different worms, at room temperature (~ 20°C) using a Fluorescence microscope (Olympus Model SZX12).

2.14 Determination of pharyngeal pumping rates for transgenic and N2 wild type worms

Pharyngeal pumping rates were determined by picking 10 adult worms from an agar plate with bacteria and transferring them onto a bacteria-free plate. It was hard to observe pharyngeal pumping on agar plates with bacteria because the worms tend to hide under the bacteria and pumping sometimes also pauses. Pharyngeal pumping was observed for each of the

10 worms for 1 minute at room temperature (~ 20°C) using a Fluorescence microscope as above (Section 2.12).

2.15 Determination of sterility for transgenic and N2 wild type worms

L4 hermaphrodites of the desired genotype were individually transferred onto 3.5cm agar plates at 20°C. By the next day the L4 hermaphrodites had reached adulthood and started to produce their own progeny. They were monitored daily from embryo to L4 stage. Once they reached the L4 stage, several hundreds of them were selfed onto individual plates and each was checked for sterility. If the worms were not producing any offspring then the worms were recorded as sterile. The same procedure was repeated for all of the transgenic genotypes.

2.16 Determination of developmental time for transgenic and N2 wild type worms

The life cycle of worms was monitored by picking individual hermaphrodites at late L4 stage on to separate plates. After 2 hours they started to produce their own offspring (eggs), then the adults were removed and the plate carrying the eggs was labeled with date and time. Eggs were allowed to grow at 20ºC until larvae reached adulthood and began to lay eggs (egg-laying adults). The date and the time were again noted. The

developmental time for each worm was calculated from egg to egg laying adult.

2.17 Determination of brood size for transgenic and N2 wild type worms

L4 hermaphrodites of the desired genotype were individually transferred onto agar plates at 20°C. The hermaphrodites were transferred to fresh plates at 24 hour intervals. The progeny left behind were counted at late larval to adult stages by flaming worms one by one. An embryo was scored as being dead if the egg had not hatched after 24 hours at 20°C. The brood size of each animal was calculated as the sum of both non-hatched and hatched progeny. The same procedure was repeated for all of the genotypes.

2.18 Fluorescence Resonance Energy Transfer (FRET) Analysis for transgenic and wild type worms.

Six different worm strains (*unc*-54::C+V (I), *unc*-54::SC+SV (I), *unc*-54::CV (I), *unc*-54::C (NI), *unc*-54::V (I) and N2 wildtype worms) were washed off the plates using K-medium and transferred into 15 ml tubes. The worms were washed several times to get rid of bacteria. Equal aliquots of each strain were transferred into a black non-fluorescent 96 well

plate (Nunc Ltd, from Fischer Scientific, Loughborough, UK) with 3 replicates per strain. Worm suspensions were stirred during dispensing so that each aliquot contained roughly the same number of worms (±5-8%). Each well contained 200 µl of K-medium with 1000-2000 worms, depending on strain. While stirring one such worm suspension, several 5µl aliquots of worms were counted (53±6; n=6) to check on the consistency of these aliquots; given the inaccuracies of micro-pipetting small volumes (5 µl), it is likely that worm numbers were even more consistent across replicate wells when using larger (50 µl) samples of worm suspension. Once the worms have been transferred into the 96 well black plates, these were kept on ice for 5 minutes to allow the worms to settle. The plate was read using a Wallac Victor 1420 Multilabel Counter for detection of FRET, as described below.

The transgenic strain express one or both of the yellow (YFP; Venus, V) or blue (CFP; Cerulean, C) variants of Green Fluorescent Protein (GFP). Forster Resonance Energy Transfer (FRET) is possible from a CFP donor to a YFP acceptor only when these moieties are in very close proximity (e.g. within a protein aggregate). Fluorescence was measured with a CFP excitation filter (430nm narrow band pass) and a YFP emission filter (530 nm narrow band pass) using the Victor 1420 instrument. Each

well was scanned at the base of the U-bottomed well, where the worms settle.

2.19 FRET Analysis for *unc*-54::SC + SV (I) fusion worms during aging.

The *unc*-54::SC+SV (I) fusion worms were grown at 20 ºC for several days to allow them to produce offspring, at which point L1 filtration was performed (section 2.3.3.1) The synchronised cultures were incubated at 20 ºC for two days until the worms reached the L4 stage. The worms were washed off the plate using K-medium and transferred into 15 ml tubes, washed several times to get rid of bacteria and transferred into a 96 well black plate. After allowing the worms to settle on ice for 5 minutes, FRET measurements were taken as described above (section 2.17). After this, the worms were transferred back into fresh plates. These were again incubated at 20 ºC for 2 days for the worms to reach adulthood, and then the worms were again washed and filtered to remove the L1 larvae which might interfere with the FRET signal. FRET measurements were repeated for the adult worms as mentioned above. Further, FRET measurements were taken after another 2 days (i.e. on days 1, 3 and 5 after L4).

2.19.1 Fluorescence Imaging in *C. elegans*

After FRET measurements, the worms were immobilised using 10 mM sodium azide and 50% (v/v) glycerol and then mounted on a slide, taking care to avoid air bubbles. The cover slip was sealed using nail polish to prevent the worms from drying out. The worm slides were examined using a Leica TCS SP2 Confocal Laser Scanning Microscope (CLSM) for high resolution pictures, using Z stacking for maximum depth of field. The *unc*-54::SC+SV (I) fusion worms were imaged using a 40x lens. In order to make sure that all the images were uniform in terms of changes in fluorescence, all the samples were analyzed on the same day with the same settings on the microscope. All photographs comparing two conditions used the same gain settings and other parameters such as 8-bit images, 515x 512 pixels, field of view= 375x 375µm, 50% laser power for CFP at 458nm and for YFP at 514nm; the YFP emission filter is between 519-600, the CFP emission filter is between 470-500, the beam splitter 458/514nm, and the lens is a 40x 1.25 NA oil apochromat.

2.20 RNA Interference against Hip-1 in *unc*-54::SC + SV (I) fusion worms

25g l^{-1} of high salt LB broth (Melford Laboratories Ltd) was prepared and autoclaved, then 12.5 µg/ml w/v tetracycline

and 25 µg/ml w/v ampicillin was added to the cooled solution. A single colony of Hip-1 RNAi bacteria (kindly sent by Dr. A. van der Groot of the University Medical Centre, Groningen, the Netherlands) was scraped off the agar plate using a sterile inoculation loop and then dipped into 35 ml of sterile LB-tet-amp in a 50 ml falcon tube. The same procedure was used for similar HT115 bacteria carrying the empty L4440 feeding vector (FV) which were used as a control. The bacteria were grown overnight at 37 ºC in a shaking incubator. These overnight cultures of FV and Hip-1 RNAi bacteria were centrifuged at 3000 rpm at 4 ºC for 10 minutes to pellet the bacteria, and most of the supernatant was removed to leave a thick bacterial suspension.

NGM agar plates were prepared as usual by adding $CaCl_2$, $MgSO_4$ and potassium phosphate buffer to the cooling agar. In addition to this IPTG (1.0mM final), 12.5 µg/ml w/v tetracycline and 25 µg/ml w/v ampicillin were added. The suspension of FV or Hip-1 RNAi bacteria was then spread onto these IPTG/tet-amp agar plates. Half of the agar plates were spread with RNAi bacteria and half with empty feeding-vector (FV) bacteria. Plates were incubated at 37 ºC for 3 hours; allowing the IPTG to induce double-stranded RNA synthesis. The plates should not be kept at 37 ºC for more than 3 hrs, as this promotes overgrowth of bacteria that have lost the RNAi

construct. All plates were then cooled to room temperature for at least 1 hr.

The *unc*-54::SC+SV (I) fusion worms were grown at 20 ºC for several days allowing them to produce offspring, followed by L1 filtration to obtain a synchronised L1 population. The L1 larvae (P0 generation) were resuspended in a small volume of K-medium and then small droplets of larval suspension were added at multiple locations across both the Hip-1 RNAi and FV control plates.

The worm plates were incubated overnight at 20 ºC for several days until they produced F1 offspring. Once there were enough L1 larvae, L1 filtration was again carried out. The larval suspension was transferred onto fresh RNAi/empty feeding-vector plates.This procedure was repeated over 2 generations. The L1 larvae obtained from the F2 generation were allowed to grow for several days until they reached the L4 stage. At each generation, worms were washed off the plate using K-medium, and then transferred into a 96 well black plate, as described above (section 2.17). Both FRET measurements (section 2.17) and confocal microscopy (section 2.18.1) were performed as described previously.

2.21 Treating *unc*-54::SC + SV (I) fusion worms with Chlorpyrifos

Cultures of *unc*-54::SC+SV (I) fusion worms were grown at 20 ºC and synchronised by L1 filtration, as described above (section 2.18). Fresh agar plates with bacteria and 2 different concentrations of chlorpyrifos (20ppm and 300ppm) were prepared by spreading 300 µl of chlorpyrifos solution (20ppm or 300ppm) onto the surface of the agar plate. The L1 larvae were resuspended in a small volume of K-medium and small droplets of larval suspension were distributed onto these plates. Another fresh agar plate was used as a zero control with no added chlorpyrifos. All 3 plates were incubated for 48 hrs at 20 ºC for the worms to reach the late L4 stage. Note that ppm (parts per million) is equivalent to $mg.l^{-1}$ or $\mu g.ml^{-1}$ throughout.

Once again, FRET measurements and confocal microscopy were performed on washed worms from all 3 cultures as described previously (section 2.17 and 2.18.1).

2.22 Treating *unc*-54::SC + SV (I) fusion worms with Rotenone

Similarly, *unc*-54::SC+SV (I) fusion worms were exposed at the L1 stage to 2 different concentrations of rotenone (2ppm and 20ppm) prepared in the same way as for chlorpyrifos

(section 2.20), plus a zero control with no rotenone. All 3 plates were incubated for 24 hrs at 20 ºC until worms reached the late L2 stage. Initially rotenone treatment was done over 48 hours as for chlorpyrifos, but because rotenone causes developmental arrest, the exposure period was reduced to 24 hrs.

Once again, FRET measurements and confocal microscopy were performed on washed worms from all 3 cultures as described previously (section 2.17 and 2.18.1).

2.23 Quantification of Reactive Oxygen Species Production in *unc*-54::SC+SV (I) *and* NL5901 Employing H2DCF-DA Assay

During oxidative stress ROS production can be measured by several methods, of which the H2DCF-DA assay (Gerber and Dubery 2003) is the most effective. 2', 7'-dihydrodichlorofluorescin-diacetate (H2DCF-DA) is a non-polar compound, and measurement of hydrogen peroxide (a typical ROS) in aqueous solution can be done by using H2DCF-DA in a fluorometric assay (Keston and Brandt 1965). The principle behind this experiment is that H2DCF-DA enters the cell straight away where it is hydrolyzed to 2', 7'-dihydrodichlorofluorescin (H2DCF) by intracellular esterases. H2DCF is a non-fluorescent

polar compound which accumulates in the cell. This compound is finally oxidised to 2', 7'-dichlorofluorescin (DCF) upon encountering intracellular ROS (Rosenkranz et al. 1992). DCF is a highly fluorescent compound which can then be measured by exciting at 501nm (maximum) and reading at 521 nm emission wavelength (maximum).

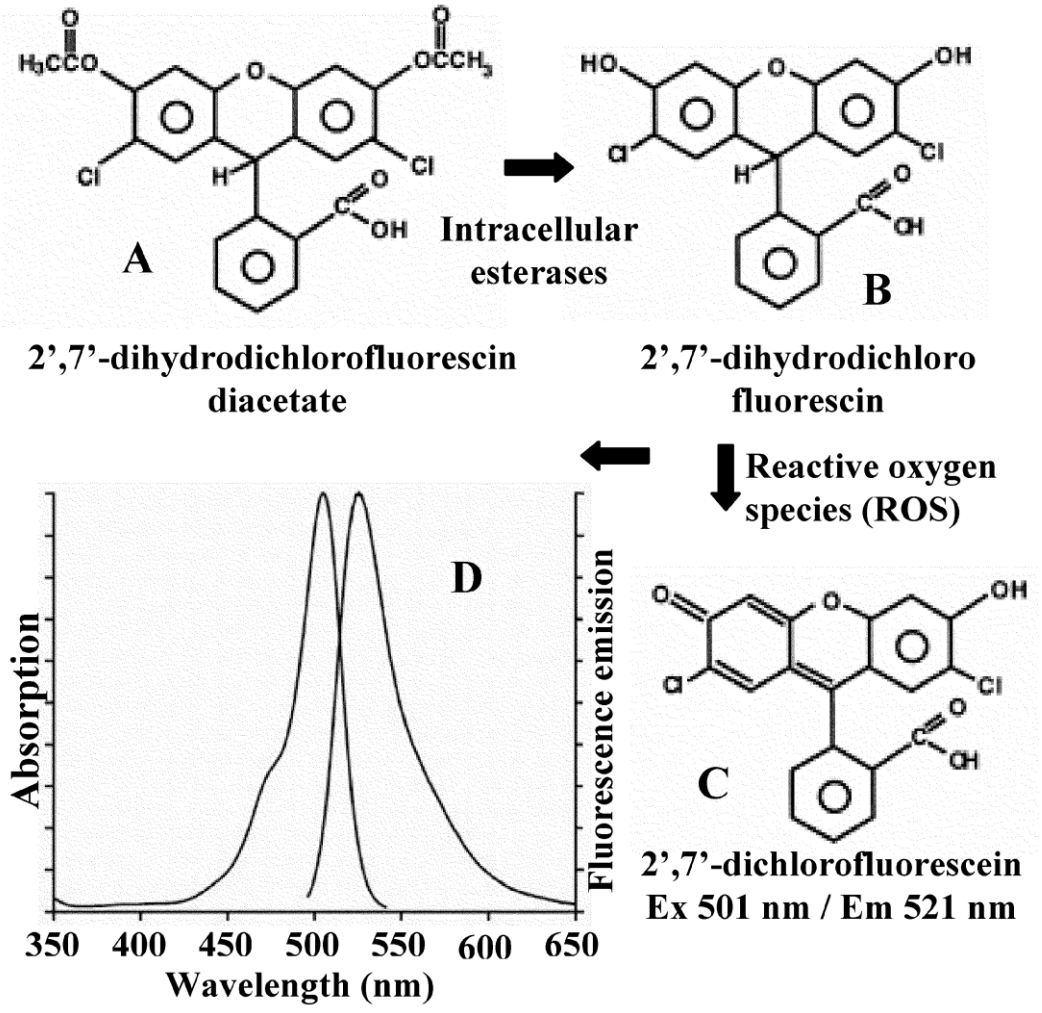

Figure 2.2: steps involved in. H2DCF-DA mediated ROS measurement. (adapted from Gerber and Dubery 2003). (A) H2DCF-DA straight away enters the cell where it is hydrolyzed to (B) 2', 7'-dihydrodichlorofluorescin (H2DCF) by intracellular esterases. H2DCF is a non-fluorescent polar compound which gets accumulated in the cell. This compound is finally oxidised to (C) 2', 7'-dichlorofluorescin (DCF) when it encounters intracellular ROS. (D) DCF is a highly fluorescent compound which can be measured by exciting at 501nm (maximum) and emission at 521 nm (maximum).

The NL5901 strain is an integrated *unc*-54::SV strain produced by the Nollen lab (van Ham et al. 2008), and was obtained from the *Caenorhabditis* Genetics Centre (CGC) at the University of Minnesota.

Long term treatments were started at the L1 stage and terminated on reaching adulthood, whereas short term treatments were given during the young adult stage itself. Synchronized L1 populations were prepared and distributed across control, chlorpyrifos (300 ppm) and rotenone (20 ppm) treated plates, as described in the preceding sections (2.20 and 2.21).

After washing, a 50 µl volume of worm suspension was pipetted out in four replicates into the wells of a black 96 well plate. 50 µl of fresh 100 µM 2', 7'-dihydrodichlorofluorescin-diacetate (H2-DCF-DA) solution was added to the suspensions (50 µM final) and immediately basal fluorescence was measured in a microplate reader (Wallac Victor 1420 Multilabel Counter) at excitation and emission wavelengths of 485 and 520 nm respectively. The plates were kept shaking at 20^0C for 1 hour, after which a second measurement was performed in the microplate reader. The difference in fluorescence readings was

determined. The resulting fluorescence was expressed as relative ROS production (Gerber and Dubery 2003).

2.24 Statistics

Graphs were generated for worm sterility caused by gamma irradiation using a non-linear regression curve with the setting log (agonist) vs. normalised response. The Prism software (version 5) also calculated the EC50 and the 95% confidence intervals allowing comparison between gamma radiation dose and sterility. For EC50 values the use of non-overlapping confidence intervals indicates statistical significance (Jeske et al. 2009). Graphs were generated using Prism software for worm lifespan using survival analysis but the P values were calculated using R statistical software with the setting Mantel-Cox test. For longevity, pharyngeal pumping, movement analysis and FRET, graphs were generated using Prism software with the setting Dunnett's multiple comparisons test.

Chapter 3 Radiation sensitivity

3.1 Introduction

In general, mutations can provide useful information for the study of gene functions. Mutations are commonly caused by radiation or mutagenic chemicals. Sometimes, they disrupt the function of the gene completely, but other mutations may reduce but not eliminate gene functions, or have no apparent phenotypic effect. The DNA repair mechanisms of an organism play an important role in protection against mutation-induced damage.

Mutagenesis is the process of inducing mutations in an organism's genome, using well-established standard mutagenesis protocols, e.g. in *Caenorhabditis elegans* (Epstein et al. 1974), *Drosophila* (Chen et al. 1993), rat (Zan et al. 2003) and mouse (Coghill et al. 2002). There are three broad types of mutagenesis, namely target-selected, spontaneous, and induced mutagenesis. Target-selected mutagenesis is also known as site-specific mutagenesis because it targets a particular sequence in a genome whose function is known. After mutagenesis these sequences have one or more mismatches which can be identified by sequence analysis (Donald 1997). Spontaneous mutagenesis is caused by natural radiation such as gamma irradiation, X-

rays, radioactive decay, cosmic rays or UV light, or by naturally occurring genotoxic (DNA-damaging) chemicals. Induced mutagenesis is caused by chemicals such as ethylmethanesulfonate (EMS), diethyl sulphate (DES) and N-nitroso-N-ethylurea (ENU) or by deliberate irradiation with any of the above—usually at doses far higher than those encountered naturally.

3.1.1 Gamma radiation

Gamma radiation is commonly used in *Caenorhabditis elegans* (Rosenbluth et al. 1985) to produce specific chromosome rearrangements such as translocations, duplications, inversions and deficiencies. Gammacell irradiators provide a large dose of γ-rays to samples. The most commonly used radioisotopes in these irradiators are Cobalt-60 or Caesium-137. The equipment used to irradiate the worms employed Caesium-137, where gamma irradiation was used to generate permanent integrated transgenic lines (section 2.10). The worms were irradiated for different lengths of time to find the optimum dose required for chromosomal integration, resulting in 100% transmission of the transgene to progeny. The standard dose of gamma irradiation normally used for this purpose is between 2000 and 4000 rads (Rosenbluth et al. 1985).

According to Baillie and others, X-rays can be used instead of gamma rays as they can cause mutations and rearrangements similar to gamma rays. The standard dose for X-rays is between 500-5000 rads. According to previous studies, stable integrated lines were successfully generated by irradiating transgenic worms with 1500 R of X-rays (Gallo et al. 2006).

3.2 Materials and methods

3.2.1 Irradiation dose

The unit of gamma radiation dose is the Gray (abbreviated as Gy) which represents the absorption of an average of one joule of energy per kilogram mass of the target material, where 1 Gray = 100 Rads.

Central dose rate = 8.13 Gy/min

Since 1Gy =100 rads

= 813 rads/min

The central dose rate is calculated to be 813 rads/min.

All other materials and methods that are related to this section are described in chapter 2.

3.3 Results

3.3.1 Gamma irradiation of Line 1:*unc*-54:: SV (NI) Fusion worms strain at different dose rates

The aim of this experiment was to determine whether line 1: *unc*-54::SV worms are sensitive to gamma radiation and to attempt integration. To achieve this, line 1:*unc*-54::SV (Table 2.13) worms were irradiated at different dose rates. The P0 parental generation was screened to find whether there were any dead worms or worms which were alive but not laying eggs. The offspring (F1) from the P0 parental generation were again screened, and the same procedure was carried out for *unc*-54::V and wildtype N2 worms. These two different strains were used as a control for the *unc*-54::SV worms.

In my previous MRes work (Bodhicharla, 2007), the dose-sterility curve of line 1: *unc*-54::SV worms was compared with wild type N2 and *unc*-54::V worms, and was shown to be far more radiation sensitive than either of the other strains. How this relates to toxicity caused by synuclein aggregation remains to be explored. A brief summary of these findings is given below (figure 3.1).

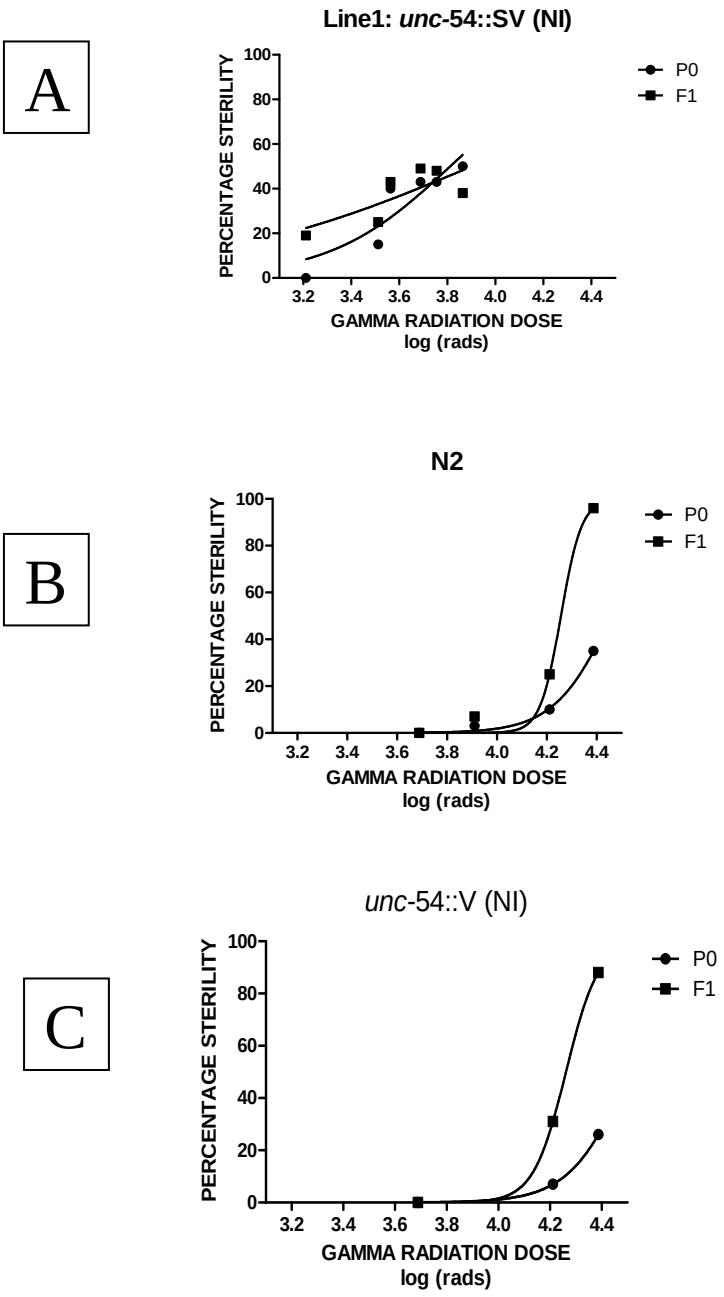

Figure 3.1: sterility dose curves (adapted from Bodhicharla, 2007).
Transgenic and wild type N2 worms were exposed at different dose rates to determine their sensitivity to gamma irradiation. P0 is the parental generation and F1 is the offspring from the P0 generation. Worm exposure to gamma radiation was in minutes and then converted to rads (central dose rate 813 rads/min). The x-axis is the log gamma radiation dose (rads) and the y-axis is the percentage sterility. Each point represents the percentage of worms found to be sterile or dead (Appendix 1). Part A is the dose response curve for the line 1: *unc*-54::SV (NI) transgenic worms, Part B is the dose response curve for wild type N2 worms, Part C is the dose response curve for the *unc*-54::V (NI) transgenic strain.

When comparing the level of radiation-induced sterility in *unc*-54::V (NI) with the wild type N2 worms we found that *unc*-54::V (NI) is similar to the control N2 worms and shows a greater radiation resistance than the *unc*-54::SV (NI) strain, resulting in lower induced sterility levels as the radiation dose increases. These results suggest that the inclusion of an α-synuclein moiety in the SV fusion protein is in some way responsible for the unusual radiation sensitivity of the *unc*-54::SV (NI) strain. The *unc*-54::SV (NI) strain was found to be significant statistically different from *unc*-54::V (NI) and N2 worms at P0 and F1 generation ($p<0.05$ by non-linear regression curve).

In order to investigate further, two further lines of *unc*-54::SV (NI) transgenic worms were irradiated at different dose rates to find out whether they are consistently radiation sensitive.

3.3.2 Gamma irradiation of Line 2 and 3: *unc*-54:: SV (NI) Fusion worms strain at different dose rates

This experiment was carried out in the same way as described above for line 1: *unc*-54::SV worms. The sterility dose curves for lines 2 and 3: *unc*-54::SV in the P0 and F1

generations (figure 3.2) show the classic pattern found for such curves, i.e. a linear relationship at low doses and a plateau at higher doses (Rosenbluth et al. 1983). Synuclein on its own is known to be toxic but the effects of its fusion to YFP and rapid aggregation in vivo are not known. Overall, the effects of γ-irradiation on F1 sterility are greater than those on P0 sterility.

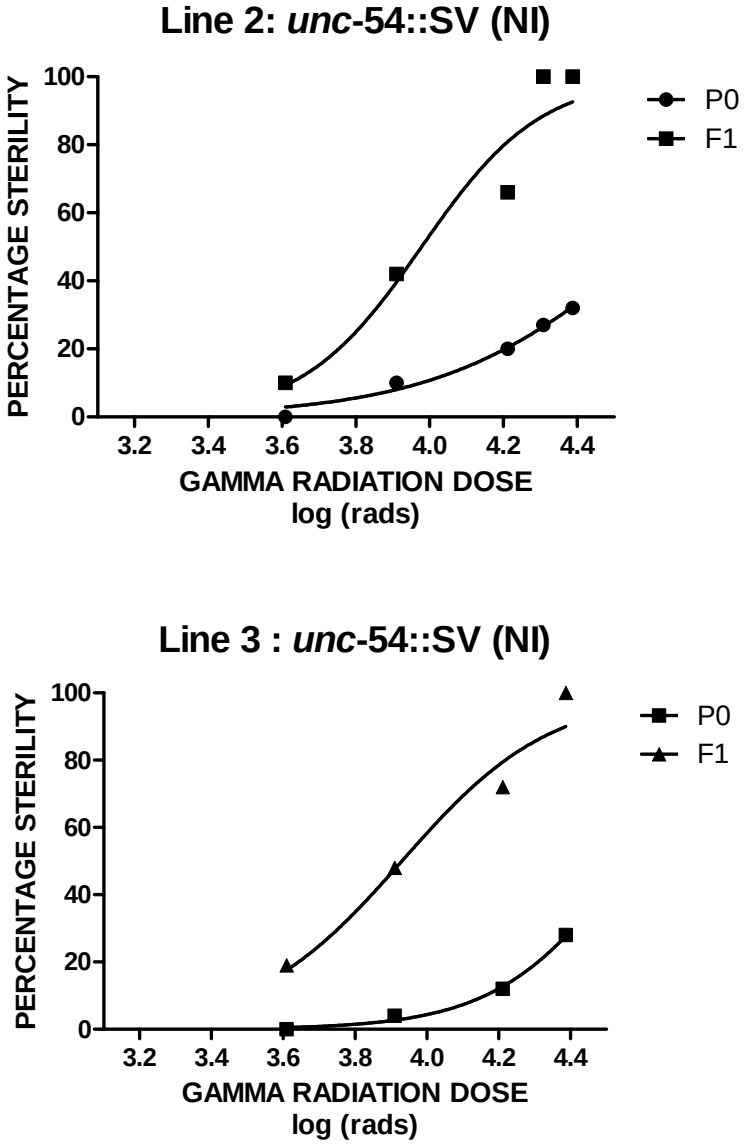

Figure 3.2: sterility curve of line 2 and 3 : *unc*-54::SV (NI).
Lines 2 and 3:*unc*-54::SV (NI) worms were exposed at different dose rates to gamma irradiation to determine their sensitivity. P0 is the parental generation and F1 is the offspring from the P0 generation. Each point represents the percentage of worms found to be sterile or dead (Appendix 1).

However**,** on comparing the effects of gamma irradiation between lines 2 and 3: *unc*-54::SV (NI) P0 worms and wild type N2 P0 worms, we found little effect on the levels of sterility in P0 worms. Figure 3.3 shows the level of sterility in the P0 generation for line 2: *unc*-54::SV (NI) and for N2 worms exposed to gamma radiation. The EC_{50} for line 2: *unc*-54::SV (NI) was 39614 rads (95% CI = 22450 rads – 69901 rads) and for N2 worms was 28833 rads (95% CI = 25230 rads – 32949 rads). Figure 3.4 shows the level of sterility in the P0 generation for line 3: *unc*-54::SV (NI) and for N2 worms exposed to gamma radiation. The EC_{50} for line 3: *unc*-54::SV (NI) was 36392 rads (95% CI = 28865 rads – 45881 rads) and for N2 worms was 28833 rads (95% CI = 25230 rads – 32949 rads). It can be seen from the analysis of the EC_{50}s that there is a large overlap in the 95% confidence intervals demonstrating that the two are not significantly different from one another. This shows that there is no effect of gamma radiation in the P0 generation, which contrasts with my earlier findings for line 1: *unc*-54::SV (NI) (section 3.3.1)

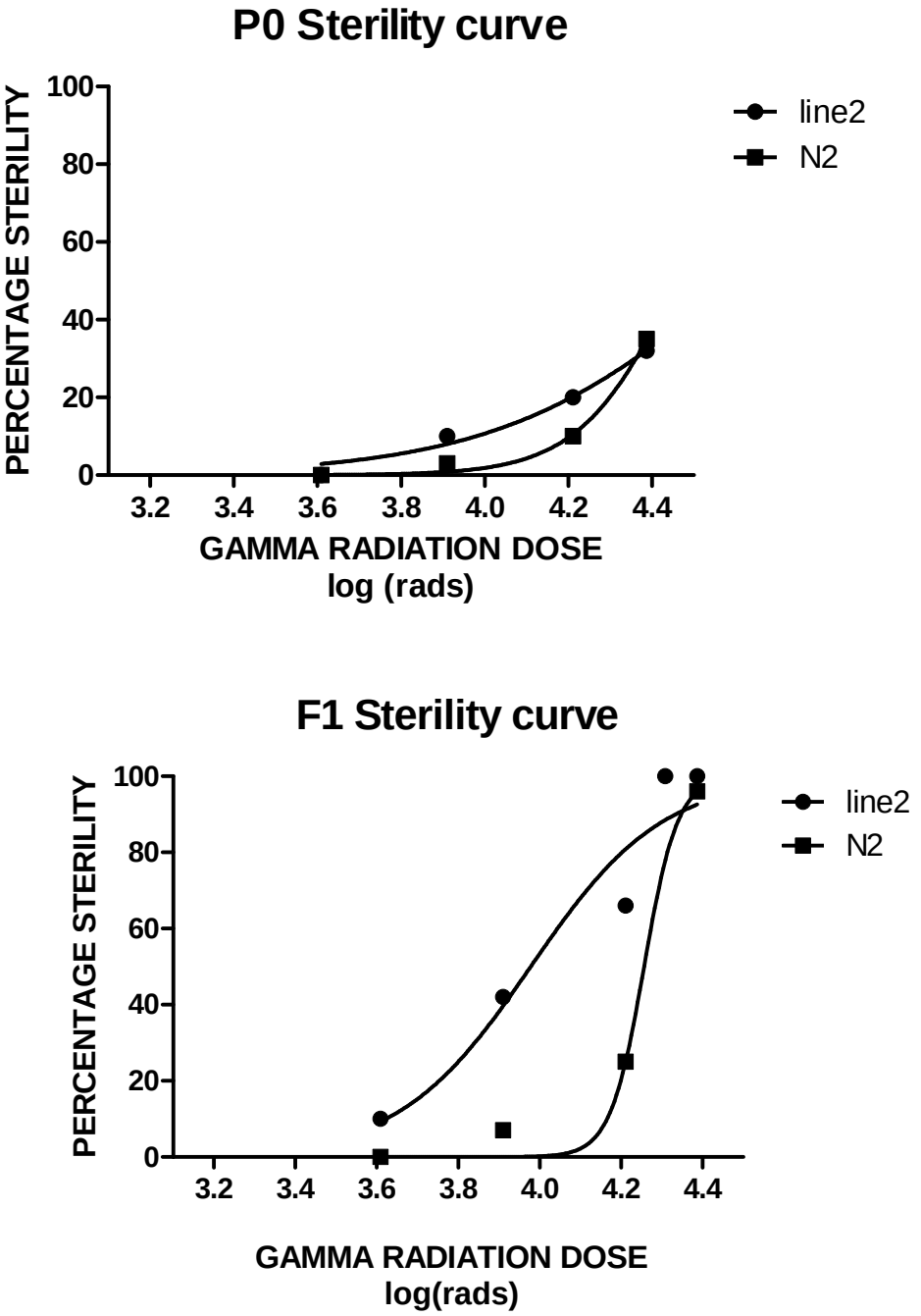

Figure 3.3: comparing the sterility curve of line 2: unc-54::SV (NI) with N2 worms. Line 2:*unc*-54::SV (NI) worms were compared with wild type N2 worms in terms of sensitivity to gamma irradiation. It was found that there was no statistical difference between line 2:*unc*-54::SV (NI) and wild type N2 worms in the P0 generation but a highly significant difference in the F1 generation.

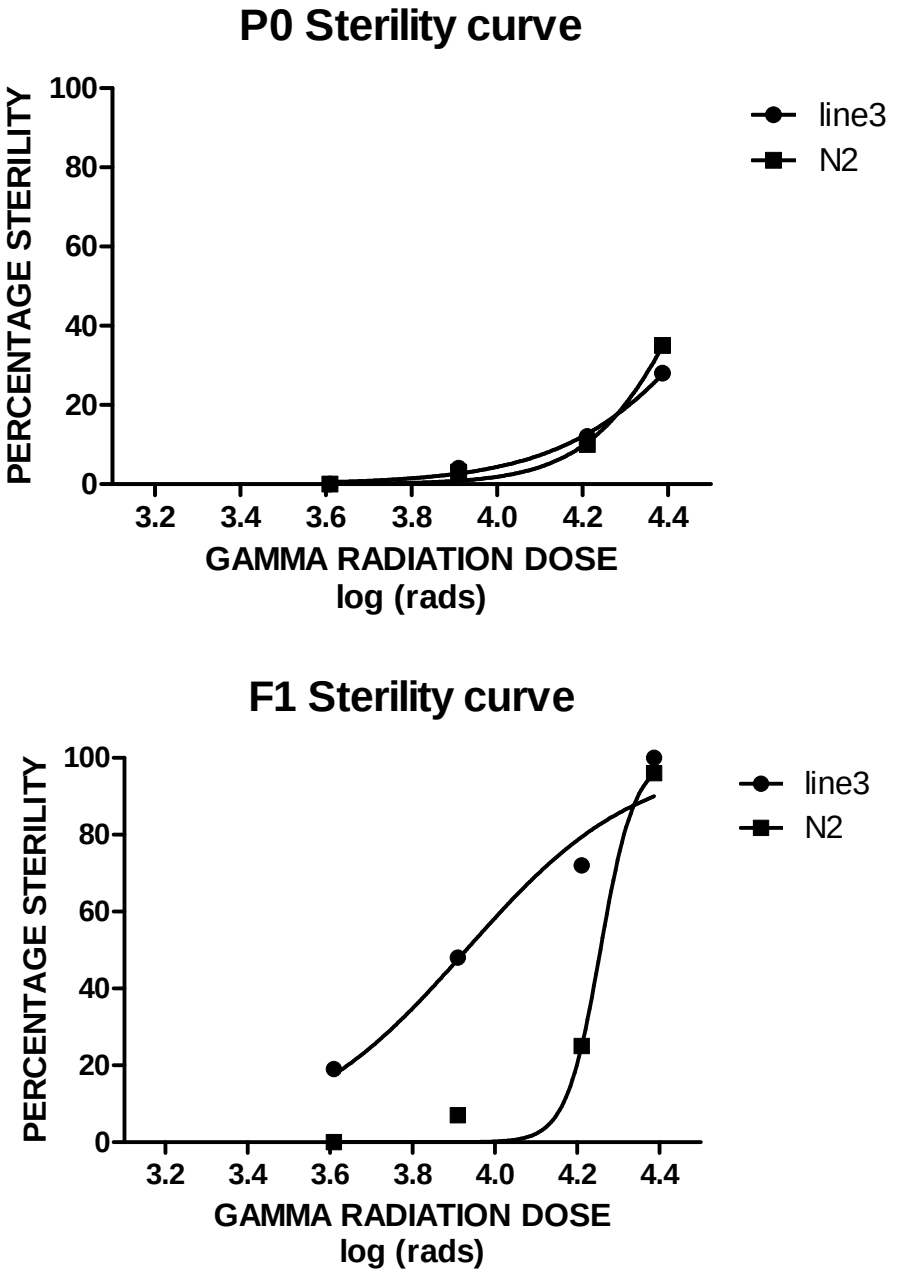

Figure 3.4: comparing the sterility curve of line 3: unc-54::SV (NI) with N2 worms. Line 3:*unc*-54::SV (NI) worms were compared with wild type N2 worms in terms of sensitivity to gamma irradiation. It was found that there was no statistical difference between line 3:*unc*-54::SV (NI) and wild type N2 worms in the P0 generation but a highly significant difference in the F1 generation.

Even so, when comparing the effect of gamma irradiation between lines 2 and 3: *unc*-54::SV (NI) F1 worms and wild type N2 F1 worms, we found evidence for a significant difference between these strains in terms of the levels of sterility in the F1

generation as compared to P0. Figure 3.3 shows the level of sterility in the F1 generation for line 2:*unc*-54::SV (NI) and N2 worms exposed to gamma radiation. The EC_{50} for line 2:*unc*-54::SV (NI) was 9505 rads (95% CI = 6105 rads – 14800 rads) and for N2 worms was 18051 rads (95% CI = 15450 rads – 21091 rads). Figure 3.4 shows the level of sterility in the F1 generation for line 3:*unc*-54::SV (NI) and N2 worms exposed to gamma radiation. The EC_{50} for line 3:*unc*-54::SV (NI) was 8518 rads (95% CI = 4987 rads –14551 rads) and for N2 worms was 18051 rads (95% CI = 15450 rads –21091 rads). It can be seen from the analysis of the EC_{50}s that there is no overlap in the 95% confidence intervals demonstrating that the two are significantly different from one another. Furthermore the data shows that the EC_{50} for sterility is doubled in line 2 and 3:*unc*-54::SV (NI) as compared to wild type N2 worms.

3.3.4 Comparison of Gamma radiation sterility between transgenic and wild type strains

The effects of gamma irradiation on sterility in the P0 generation for all transgenic worm strains gave similar results to those obtained with wild type N2 worms. Figure 3.6 shows the level of sterility (P0 generation) of all transgenic strains and for N2 worms when exposed to gamma radiation.

Strains	EC_{50}s	95% CI
unc-54::SV (NI)	39614 rads	22450 rads – 69901 rads
unc-54::S+V (NI)	37863 rads	26801 rads – 53489 rads
unc-54::SC+SV (NI)	54907 rads	27075 rads – 111350 rads
unc-54::V (NI)	32118 rads	31557 rads – 36288 rads
N2	28833 rads	25230 rads – 32949 rads

Table 3.1: EC_{50} analysis for all transgenic strains and N2 worms in P0 generation.

It can be seen from these EC_{50}s that the 95% confidence intervals overlap greatly, demonstrating that they are not significantly different from one another. This shows that there is no effect of gamma radiation in the P0 generation.

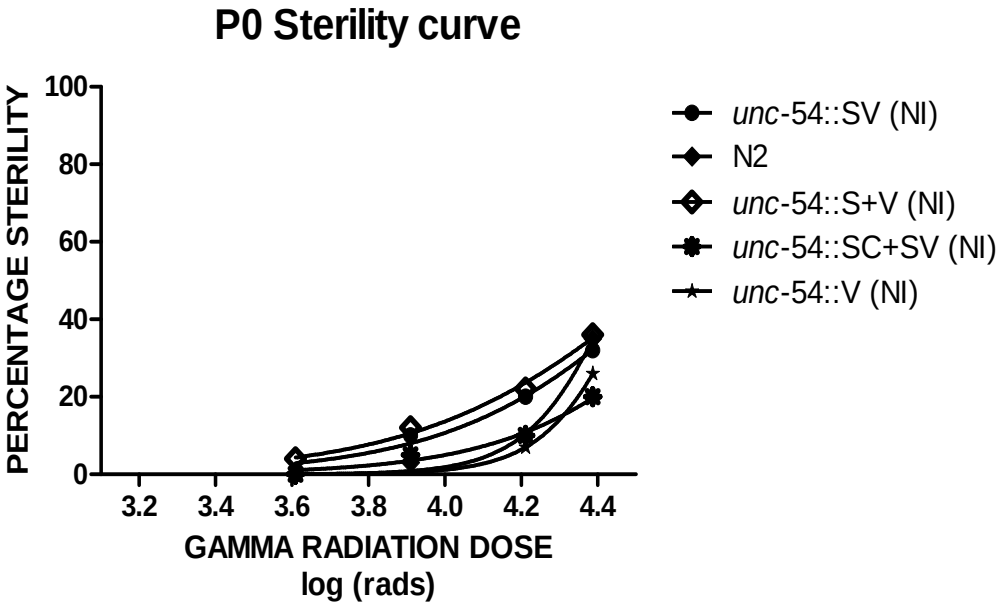

Figure 3.5: sterility curve of transgenic strains compared with wild type N2 worms in the P0 generation. Transgenic and wild type N2 worms were exposed at different dose rates to determine their sensitivity to gamma irradiation. P0 is the parental generation. Each point represents the percentage of worms found to be sterile or dead (Appendix 1).

Figure 3.6 shows the level of sterility in the F1 generation for all transgenic strains and for N2 worms when exposed to gamma radiation.

Strains	**EC_{50}s**	**95% CI**
unc-54::SV (NI)	9505 rads	6105 rads – 14800 rads
unc-54::S+V (NI)	8364 rads	4451 rads – 15719 rads
unc-54::SC+SV (NI)	11614 rads	8818 rads – 15296 rads
unc-54::V (NI)	18263 rads	18258 rads – 18268 rads
N2	18051 rads	15450 rads – 21091 rads

Table 3.2: EC_{50} analysis for all transgenic strains and N2 worms in F1 generation.

It can be seen from the analysis of these EC_{50}s that there is no overlap in the 95% confidence intervals between those strains carrying α-synuclein constructs and those that do not, demonstrating that all the synuclein-expressing transgenic worms are significantly different from both wild type N2 worms and *unc*-54::V (NI) worms.

Gamma radiation therefore has a drastic effect on the levels of sterility in the F1 generation when comparing synuclein-expressing transgenic worms and wild type N2 worms or transgenic strains lacking synuclein.

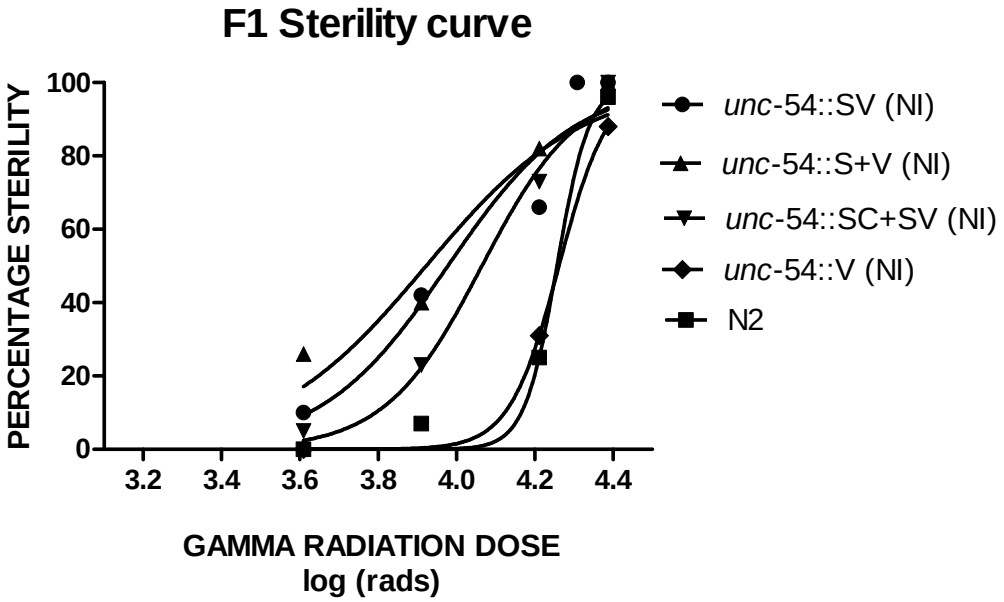

Figure 3.6: sterility curve of transgenic strains compared with wild type N2 worms in the F1 generation. Transgenic and wild type N2 worms were exposed at different dose rates to determine their sensitivity to gamma irradiation. F1 is the offspring from the P0 generation. Each point represents the percentage of worms found to be sterile or dead (Appendix 1).

3.3.5 Generating permanent integrated transgenic lines

The following transgenic lines were selected for integration:

- *unc*-54:: SV (NI)
- *unc*-54:: V (NI)
- *unc*-54:: C (NI)
- *unc*-54:: S+V (NI)
- *unc*-54:: SC+SV (NI)
- *unc*-54:: CV (NI)
- *unc*-54:: C+V (NI)

The integration procedure described in section 2.10 was carried out for all the above listed transgenic lines. Permanent integrated transgenic lines were successfully generated for *unc*-54::S+V (I)*, unc*-54::V (I)*, unc*-54::C+V (I)*, unc*-54::CV (I) and *unc*-54::SC+SV (I), but not for *unc*-54::SV (NI) and *unc*-54::C (NI), which were attempted but without success. As illustrated by pictures in figure 3.7 (below) of the *unc*-54::C+V (I) strain, all integrated worms showed YFP and/or CFP fluorescence.

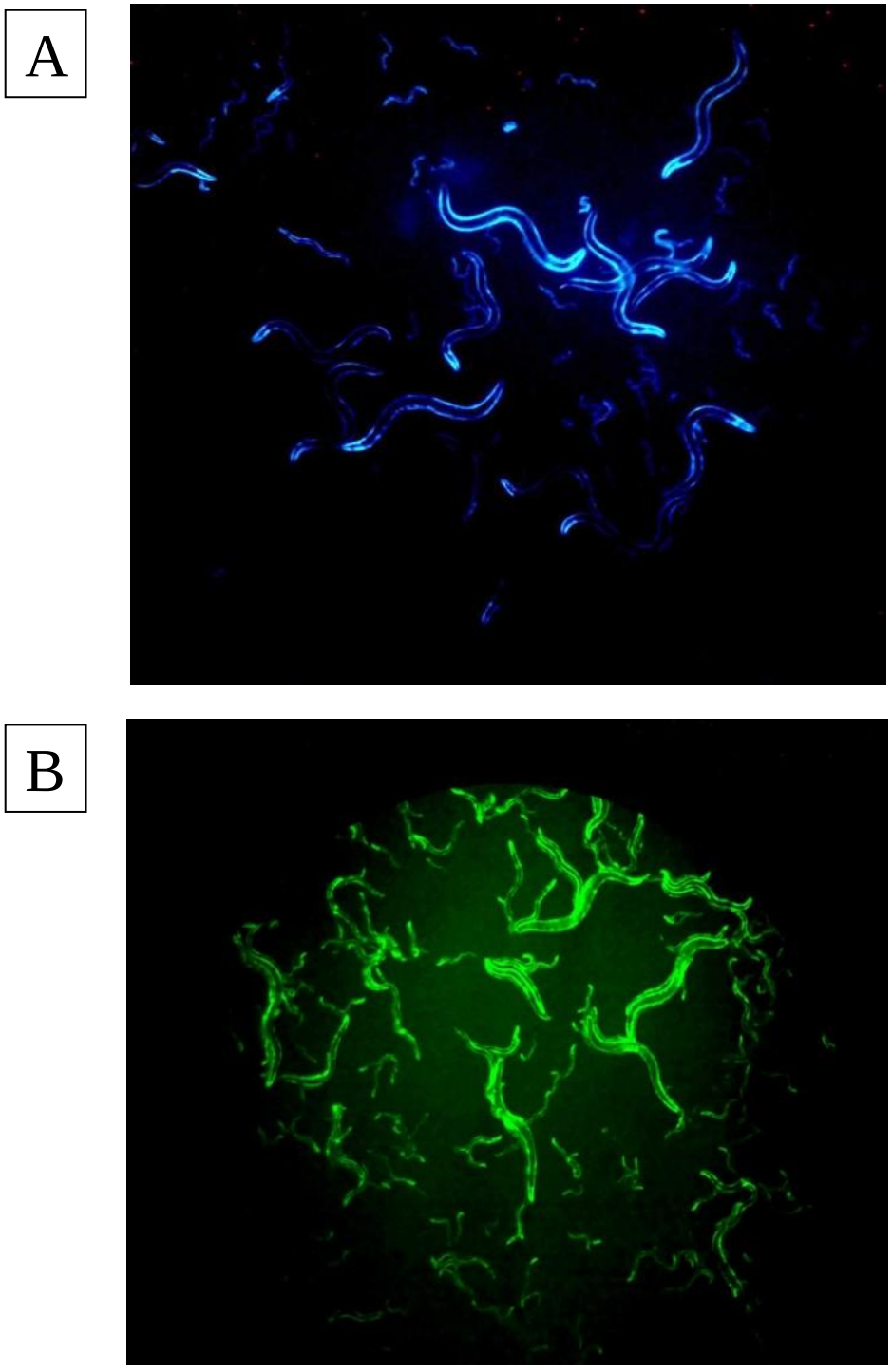

Figure 3.7: Permanent integrated transgenic lines
Permanent integrated transgenic lines were obtained for *unc*-54::S+V (I), *unc*-54:: V (I), *unc*-54::C+V (I), *unc*-54::CV (I) and *unc*-54::SC+SV (I) using the protocol described in Materials and Methods section 2.10. As an illustration of the fluorescence patterns obtained, parts A and B show that the CFP (A) and YFP (B) fluorescence is diffused throughout the body wall muscles of *unc*-54::C + V (I) worms.

3.4 Discussion

. Based on the above results, line1:*unc*-54::SV (NI) was found to be more radiation sensitive than wild-type N2 worms (figure 3.1). In order to confirm that these worms are indeed sensitive to radiation due to the presence of α−synuclein, similar experiments were performed on two further lines of *unc*-54::SV (NI) worms (line 2 and 3), providing similar results in both cases. To prove further that the radiation sensitivity of the transgenic lines was due to the presence of α−synuclein, wild type N2 worms were also subjected to gamma irradiation and shown to be significantly more resistant in the F1 (but not P0) generation. There is a possibility that radiation sensitivity might be due to generating transgenic worms rather than the presence of α−synuclein. In order to test this hypothesis, transgenic strains that do not express α−synuclein were also exposed to gamma irradiation and shown to be similar to wild type N2 worms. This suggests that in terms of radiation sensitivity in the F1 generation our α−synuclein transgenic strains are significantly more sensitive to radiation. The effect of gamma irradiation on the sterility of these worms in the P0 generation was similar to that of the N2 control (not statistically significant) whereas the F1 generation showed a large effect ($P<0.05$; using non-linear regression curve).

In general, gamma irradiation causes DNA strand-breaks that are often repaired by the cell's DNA repair systems. DNA repair systems work well after low radiation-dose exposure but are much less efficient following high radiation-dose exposure—and the damage caused by very high doses may not be repairable at all. There is also evidence (Herman 1978; Meneely and Herman 1979) that high doses cause a great deal of sterility among the F1 generation in *C.elegans*. Interestingly, my results show that even at relatively low doses of gamma irradiation, α−synuclein transgenic strains were found to be sterile, in F1 generation. Therefore, it could be speculated that presence of α−synuclein aggregation in the cell may contribute via a yet unknown mechanism(s), to render these transgenic worms sensitive to irradiation. Also, another possibility is that the presence of α−synuclein DNA as a transgene in the gonads may compromise the DNA repair machinery during irradiation mediated integration. As a result, the F1 and may be F2 generation might have aneuploid genome causing sterility or even lethality. To understand, if this epigene (α−synuclein) may be toxic to the cell, a control experiment using sham DNA could be parallel injected into the gonads and F1 observed for sterility. However, further experiments will have to be performed to study the actual status of DNA repair systems of these transgenic worms upon exposure to gamma irradiation.

Chapter 4 Behavioral changes triggered by synuclein expression in transgenic worms

4.1 Introduction

Nearly all animals undergo weakening of muscle strength due to normal aging, leading to functional disorders of motility. Even though the apparent changes in motility during aging are clear, very little is known about the cellular changes that are linked with aging and motility disorder in vertebrates (Kamel 2003). Therefore, to study such a complex mechanism, a simpler model organism would be ideal. *Carnorhabditis elegans* was selected as an experimental model to study development and behavior (Brenner 1974), and particularly motility and longevity (Guarente and Kenyon 2000).

Ageing also has an effect on general motor functions such as pharyngeal pumping. The nematode *C.elegans* has a neuromuscular organ called the pharynx, which is situated in the head region. The pharynx is a complex organ composed of 9 marginal cells, 5 gland cells, 5 epithelial cells, 20 neurons and 34 muscle cells (Albertson and Thomson 1976). Several other soil nematodes including *C.elegans,* feed on bacteria such as E.coli in

laboratory culture. The rhythmic contraction of the pharynx (pharyngeal pumping) is used for pumping food into the digestive tract of the worm. Since *C.elegans* is a transparent animal, this process can be observed under a light microscope. The number of times the pharynx pumps is ~ 200- 300 times/ min in a young adult, but gradually decreases during aging (Bolanowski et al. 1981; Huang et al. 2004).

Figure 4.1: *C.elegans* Pharynx (picture from Haun et al. 1998).

4.2 Materials and methods

All the materials and methods that are related to this section are described in chapter 2.

4.3 Results

4.3.1 Life cycle analysis for all transgenic strains and N2 worms

Life cycle analysis was done at 20ºC to find out how much time the worm needs to grow from egg to egg laying adult. From this data it was confirmed that all the strains took 70 – 80 hrs to reach adulthood, and there were no statistically significant difference between strains ($p>0.05$, Dunnett's test against N2 as control).

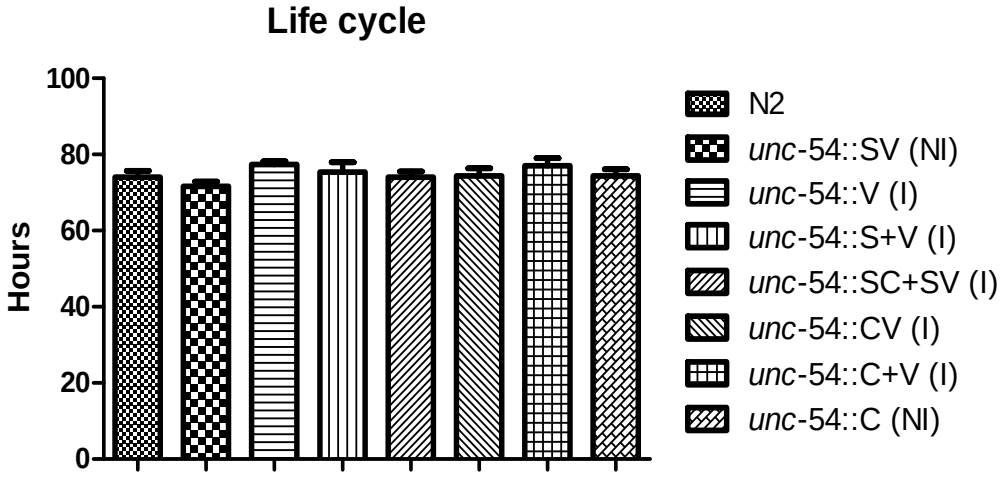

Figure 4.2: Life cycle analysis for all transgenic strains and N2 worms

4.3.2 Brood size analysis for all transgenic strains and N2 worms

Analysis of brood size was done to check whether all the transgenic strains were similar or different to wild type N2 worms. It was confirmed that the brood sizes for all the strains

were close to 300 thus confirming that they are all normal (Hirsh et al. 1976). There were no statistically significant difference between strains ($p>0.05$, Dunnett's test against N2 as control). Refer to Appendix 1 for detailed analysis.

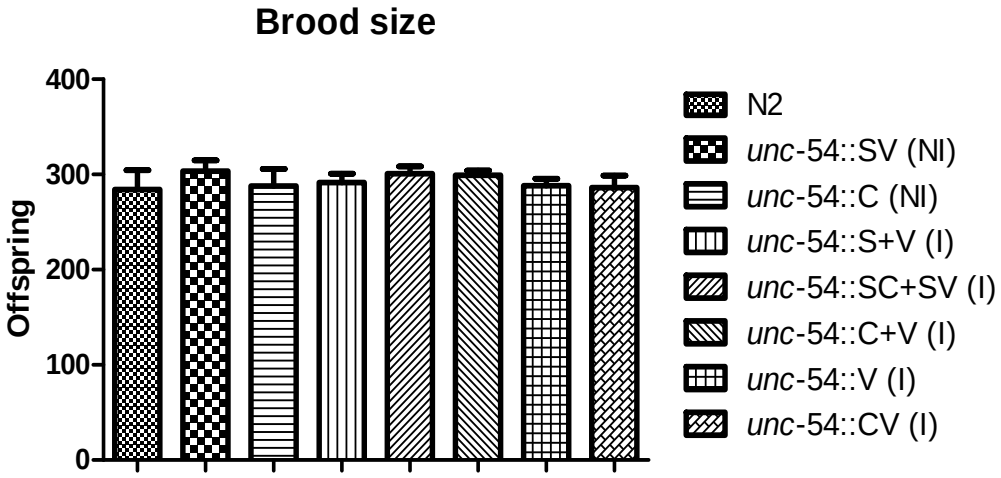

Figure 4.3: Life cycle analysis for all transgenic strains and N2 worms

4.3.3 Sterility analysis for all transgenic strains and N2 worms

Mid-L4 larvae of eight different strains of worms were grown for 48 h and scored for embryo production. For each strain, 20 animals were scored. We found that none of their progeny were sterile. From this data it was confirmed that all these transgenic strains at least were normal in respect to fertility.

Strains	% steriltiy
unc-54::SV (NI)	0
unc-54::SC+SV (I)	0
unc-54::V (I)	0
unc-54::C (NI)	0
unc-54::CV (I)	0
unc-54::C+V (I)	0
N2	0

Table 4.1: Sterility analysis for all transgenic strains and N2 worms

4.3.4 Life span analysis of line 2: *unc*-54::SV (NI)

This aim of this experiment was to determine whether line 2:*unc*-54:SV (NI) worms have a shorter life span. Life span was measured at 20 °C on standard nematode growth medium (NGM) agar plates. The life span of each worm was then calculated from egg until death. Worm survival was assayed using 25 worms per line as described in Materials and Methods. The survival fraction (i.e. percent remaining alive) is plotted against total life time in days in figure 4.4. This experiment concluded that line 2:*unc*-54:SV (NI) worms have a shorter maximum life span of 14 days as compared with N2 (19 days).

The life span of line 2:*unc*-54::SV (NI) worms at 20 °C is significantly reduced when compared to wild type N2 worms. The

statistical significance of the difference between N2 and line 2:*unc*-54::SV (NI) was determined using the Mantel-Cox test, and the difference between them was found to be highly significant (P<0.0001).

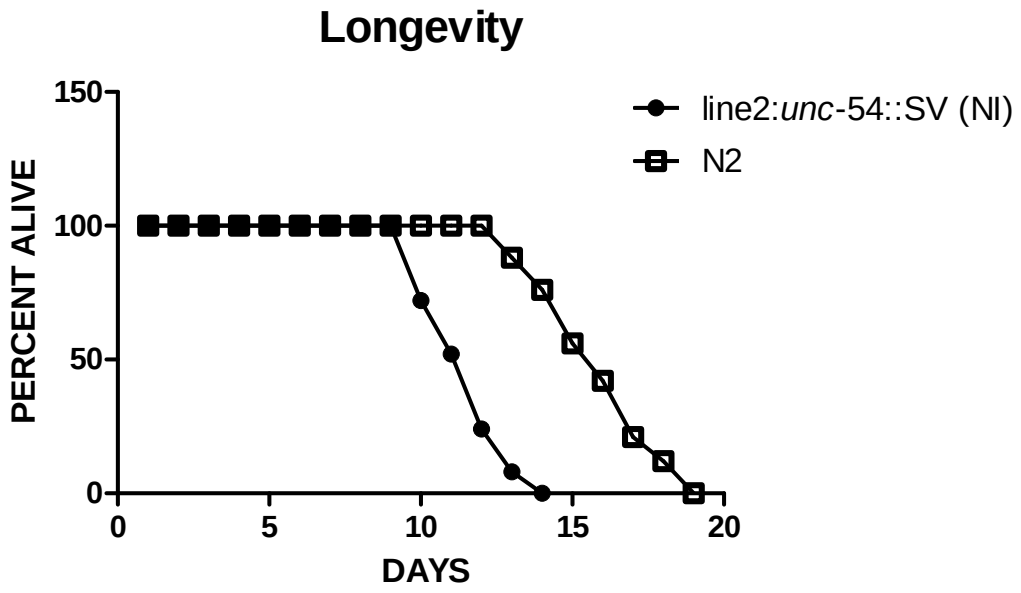

Figure 4.4: Longevity of line 2: *unc*-54::SV (NI) worms
25 Synchronized L4 line 2:*unc*-54:SV (NI) worms were picked onto a NGM plate. After 2 hours of incubation when they begin to lay eggs, the date and the time were noted. The life span of each worm was then calculated from egg until death. The worms were monitored on a daily basis. Once the worms were identified as dead, the date and time were noted. A graph was plotted showing the percent alive against time.

4.3.5 Life span analysis of line 3: *unc*-54::SV (NI)

Similarly the life span of line 3:*unc*-54:SV (NI) was measured using the same procedure (figure 4.5). The life span of line 3:*unc*-54::SV (NI) worms at 20 °C is also significantly reduced when compared to wild type N2 worms. The statistical significance of the difference between N2 and line 3:*unc*-54::SV (NI) was determined by the Mantel-Cox test, and the difference

between them was again found to be highly significant (P<0.0001).

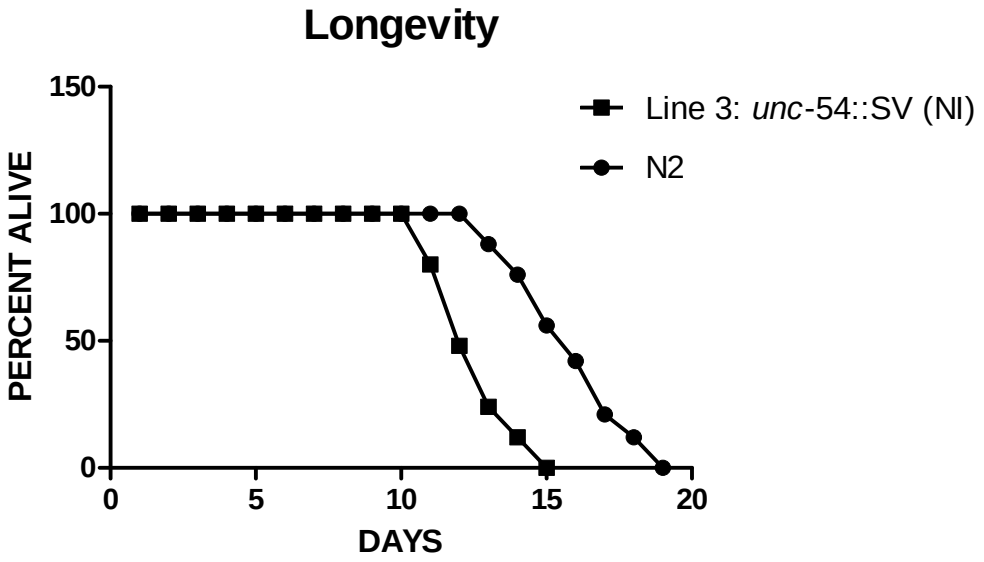

Figure 4.5: Longevity of line 3: *unc*-54::SV (NI) worms
The life span of each synchronized L4 staged worm was calculated from egg until death. The graph shows percent alive against time.

4.3.6 Comparison of life span between transgenic and wild type strains

Figure 4.6 compares the life spans of all transgenic worms lacking synuclein (V, CV and C+V) with wild type N2 worms at 20 °C. We found that the lifespan of these transgenic worms was similar to that of wild type N2 worms. Using the Mantel-Cox test, these transgenic worms were found not to be statistically significantly different from N2 worms (P > 0.05). The 3 lines expressing one or both fluorescent markers (V, CV and C+V) showed only a slight (1-2 day) and non-significant (p =

0.08, 0.137 and 0.555; Mantel-Cox test) reduction in lifespan as compared to N2 worms.

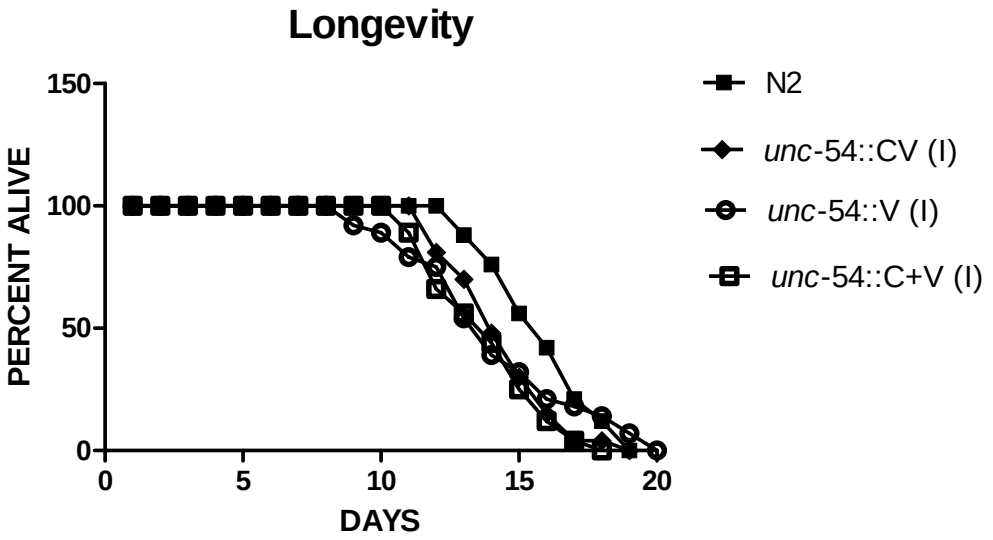

Figure 4.6: Longevity of different transgenic strains lacking synuclein compared with wild type N2 worms. The life span of each synchronized L4 staged worm was calculated from egg until death. The graph shows percent alive against time.

Figure 4.7 compares the life spans of all synuclein expressing transgenic worms with wild type N2 worms at 20 °C. We found that the lifespan of synuclein-expressing transgenic worms was significantly reduced when compared to wild type N2 worms. Using the Mantel-Cox test, the life spans of synuclein expressing transgenic worms were found to be statistically significantly different from N2 ($P < 0.0001$). The 3 lines expressing α-synuclein (S+V, SV and SC+SV) showed a marked decrease of ~5 days in lifespan as compared to N2 ($P < 0.0001$ fpr all 3 strains; Mantel-Cox test). Therefore over-expression of

α-synuclein in these worms caused significant toxicity and reduced lifespan.

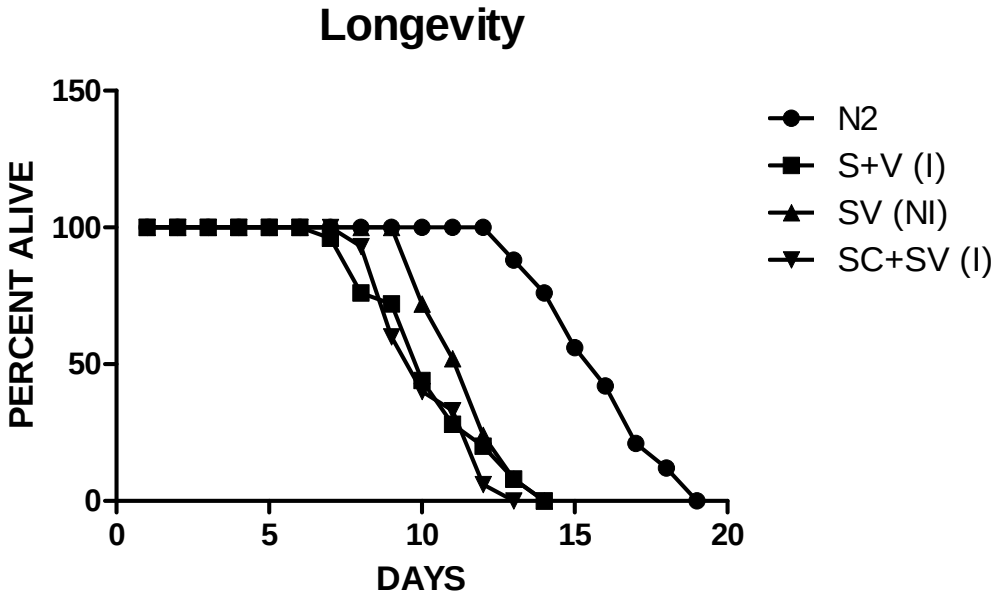

Figure 4.7: Longevity of synuclein expressing transgenic strains compared with wild type N2 worms. The life span of each synchronized L4 staged worm was calculated from egg until death. The graph shows percent alive against time.

This might be due to the aggregation of synuclein on its own or as a fusion protein, possibly affecting lifespan either directly or indirectly (e.g. through reduced motility and/or pharyngeal pumping rate; see sections 4.3.7 and 4.3.8)

4.3.7 Comparison of locomotion rate between transgenic and wild type strains

Locomotion rate was averaged across 25 individual worms, as determined by the number of bends each worm performs in 30 seconds (see Materials and Methods section

2.13). From the results obtained we found that transgenic synuclein-expressing worms have a slower locomotion rate as compared with the transgenic strains lacking synuclein or wild type N2 worms. Using Dunnett's multiple comparisons test, the transgenic synuclein worms (S+V, SV and SC+SV) were compared with the control wild type N2 worms and found to be statistically significantly different ($P<0.001$ for all 3 strains), whereas the strains lacking synuclein (V, CV and C+V) were not ($P>0.05$).

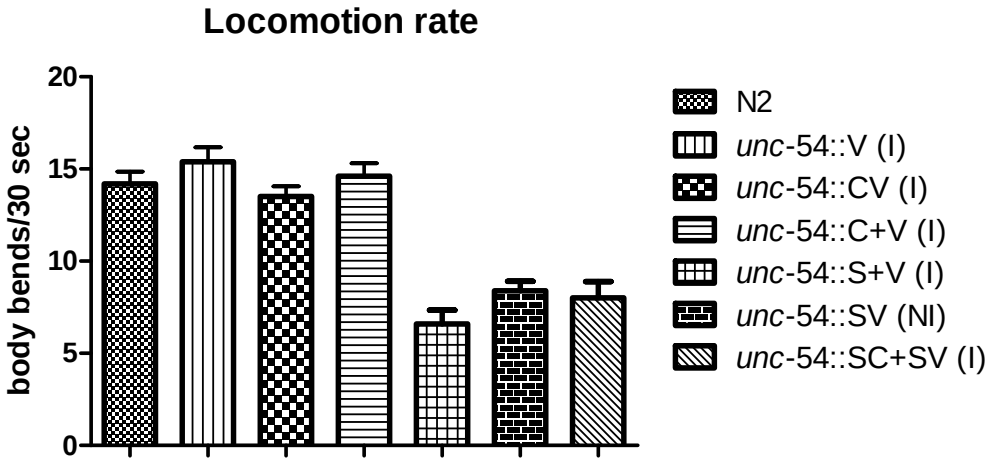

Figure 4.8: Locomotion rate of different transgenic strains compared with wild type N2 worms. 10 adult worms were picked onto a bacteria free plate. The locomotion rates were determined by the number of bends each worm performs in 30 seconds.

4.3.8 Comparison of Pharyngeal pumping rates between transgenic and wild type strains

Pharyngeal pumping rates were measured for 25 individual worms for 1 minute each as described in Materials and Methods (section 2.14). From the results obtained we found that

transgenic synuclein-expressing worms have slower pharyngeal pumping rates when compared with the transgenic strains lacking synuclein or with wild type N2 worms. Using Dunnett's multiple comparisons test, the transgenic synuclein worms (S+V, SV and SC+SV) were compared with the control wild type N2 worms and they were found to be statistically significantly different ($P<0.01$, $P<0.001$, $P<0.05$), whereas the strains lacking synuclein (V, CV and C+V) were not ($P> 0.05$).

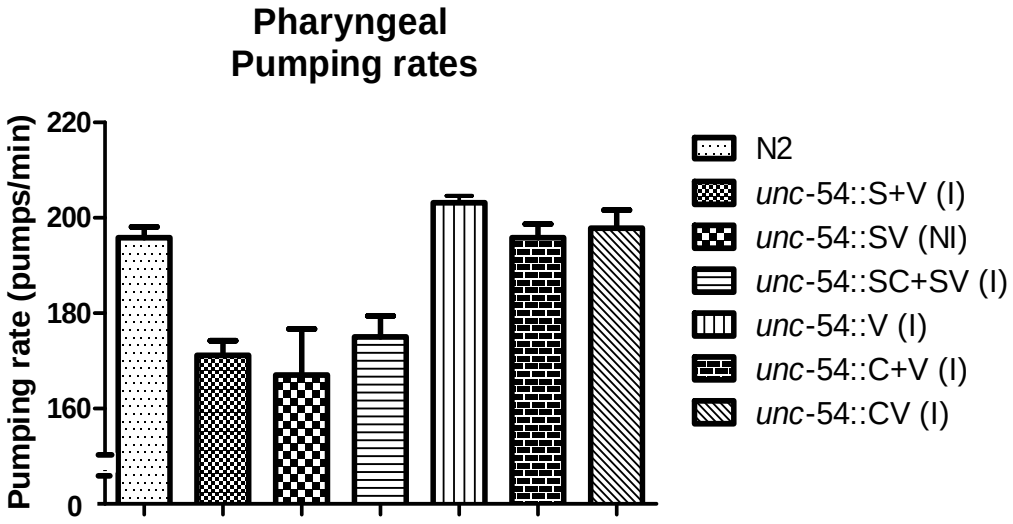

Figure 4.9: Pharyngeal pumping rates of different transgenic strains compared with wild type N2 worms. 10 adult worms were picked onto a bacteria free plate. The pharyngeal pumping rates was observed for each worm for 1 minute.

4.3.9 SDS-PAGE and Western Blotting to detect α-synuclein expression.

Two SDS-PAGE (sodium dodecylsulfate polyacrylamide gel electrophoresis) gels were run followed by Western blotting to identify the α-synuclein protein using primary and secondary antibodies. Total proteins were extracted from *unc*-54::SC+SV (I)*, unc*-54::S+V (I) and *unc*-54::SV (NI) *strains*. These protein samples were run on a 15% SDS gel and stained with Coomassie blue, as described in Materials and Methods. The proteins were then transferred from a parallel gel onto a PVDF membrane.

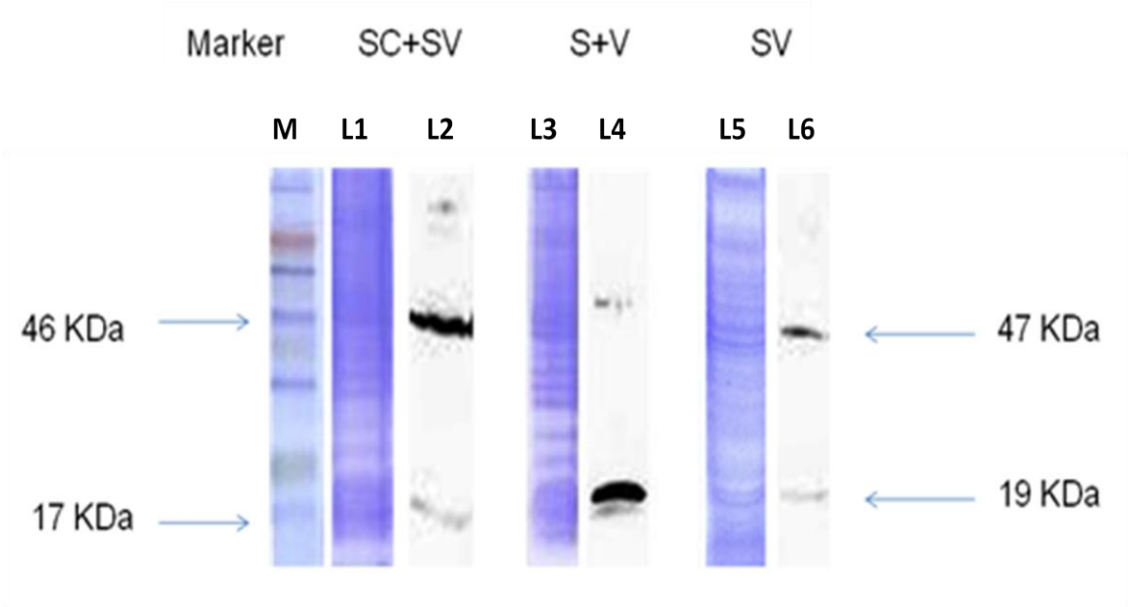

Figure 4.10: SDS- PAGE and Western Blotting to detect α-synuclein
SDS-PAGE followed by Western blotting to detect the α-synuclein protein. Molecular weight markers shown in lane M; Lanes 1, 3 and 5 show the stained Coomasie gel of SC+SV, S+V and SV strains. Lanes 2, 4 and 6 show the parallel lanes of SC+SV, S+V and SV strains following Western blotting and probing for α-synuclein.

Finally, Western blotting was used to detect α-synuclein among the total proteins extracted from these 3 transgenic strains. In figure 4.10 the sizes of the major bands identified by the antibody are indicated as 47 kD (SV/SC) and 19 kD (S alone), as estimated from the molecular weight marker lane (M). The cartoon shown previously in the introduction (Figure 1.6) illustrates the construction of the fusion proteins, where the expected sizes of α-synuclein (S; 19.3 kD) and α-synuclein fusion proteins (SV and SC; 46.5 kD) are shown. The Western blot in lane 2 of the SC+SV fusion strain shows the expected fusion protein size of ~47 kD together with a small amount of cleaved monomeric α-synuclein (19 kD) also present. Lane 4 similarly shows monomeric synuclein from the S+V strain at the expected protein size of ~19 kD. Finally, lane 6 shows again the expected fusion protein size of ~47 kD for the SV fusion strain, together with some cleaved monomeric α-synuclein. The cleaved monomeric α-synuclein was not our main concern because the majority of α-synuclein protein expressed in the SC+SV and SV worms remains in the CFP-/YFP-tagged fusion form.

4.4 Discussion

This chapter shows that our α−synuclein transgenic strains are characterized by a reduction in pharyngeal pumping, motility and life span. Other parameters such as life cycle, brood size and sterility are not affected in these strains. In order to confirm that the above mentioned changes are indeed due to the effect of α−synuclein, parallel experiments were carried out on wild type N2 worms. Also, Western blotting was used to confirm the expression of intact α−synuclein protein (with or without reporter tags) in these transgenic worms. Using anti-α−synuclein, some cleavage of the tagged α−synuclein was inferred from the presence of a smaller band at ~19kD in lanes 2 and 6 of figure 4.10. However, in this worm model, the problem of cleavage appears much less than that observed by McLean et al. (2001) using GFP-tagged α−synuclein fusions expressed in transfected cultures of mouse primary neurons.

Interestingly, these results show changes in cellular characteristics pertinent to neurodegeneration in human conditions such as Parkinson's disease. Since these effects are observed in α−synuclein transgenic worms, one could plausibly attribute these effects to α−synuclein aggregation. However, a small but significant reduction (~20%) in pharyngeal pumping is also observed in these transgenic worms, which is unlikely to be

a direct effect of α−synuclein expression, because the α−synuclein is expressed in the body wall muscles under the control of *unc*-54 promoter, whereas other major myosin genes (such as *myo*-2) are expressed in the pharynx. Reduced pharyngeal pumping has been previously reported in ageing animals (Bolanowski et al. 1981; Huang et al. 2004). One of the several contributing factors is structural deterioration of the pharynx muscles (Garigan et al. 2002; Herndon et al. 2002). It has also been suggested that cellular damage due to stress (such as ROS byproducts and mitochondrial dysfunction) may cause a decline pharyngeal pumping rate (Chow et al. 2006).

Chapter 5 Forster Resonance Energy Transfer (FRET)

5.1 Introduction

FRET is a well-known technique for investigating the interactions between two proteins labeled with different fluorophores, and can be performed *in vitro* or *in vivo*.

In our FRET experiments, we used two colour variants of GFP, Cerulean Fluorescent Protein (CFP) and Yellow Fluorescent Protein (YFP) as donor and acceptor. Transfer of energy takes place from an excited donor to an adjacent acceptor. CFP and YFP protein interactions allow bimolecular fluorescence by means of exchange of energy from CFP to YFP (Miyawaki 2003; Zhang et al. 2004).

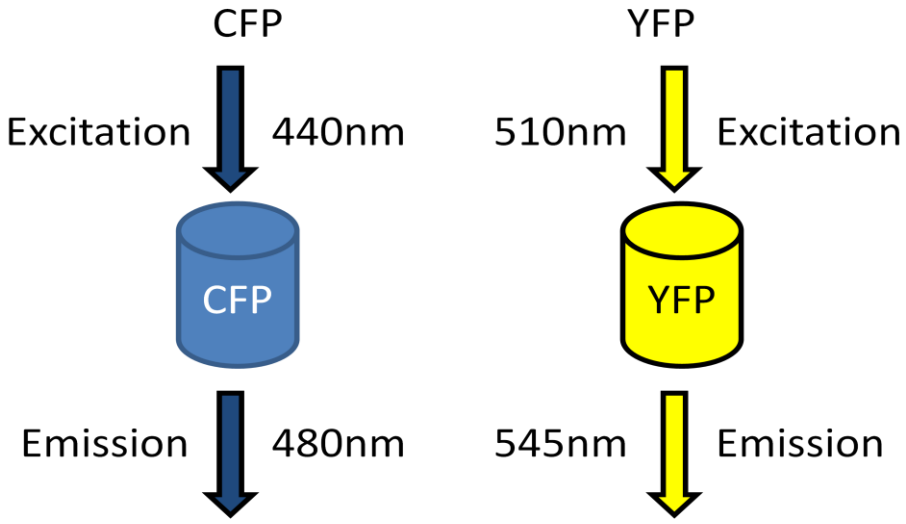

Figure 5.1: Excitaiton and emission wavelengths for CFP and YFP

A FRET signal can be observed by exciting the CFP fluorophore at 440nm using a CFP excitation filter, and the emission from YFP is captured using a YFP emission filter at ~545nm. These are the two types of filter combinations which we used for FRET, and are called FRET channels.

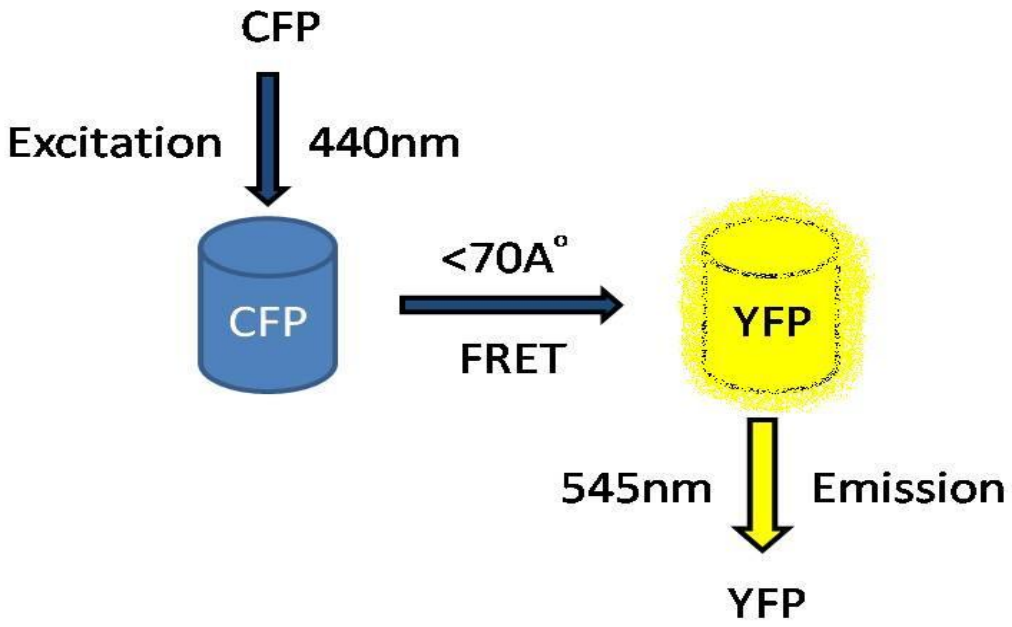

Figure 5.2: Mechanism of FRET

Two conditions are obligatory for obtaining a FRET signal:

(i) The CFP and YFP fluorophores must be very close to each other (<70 Å). (ii) The proteins are properly adjusted to facilitate dipole–dipole interactions between fluorophores, for which they must be parallel to each other so that the transfer of energy takes place between these fluorophores (Miyawaki and Tsien 2000; Miyawaki 2003).

In the *unc*-54::SC+SV (I) strain, genes encoding the two colour variants of GFP (CFP and YFP) are incorporated into the genome of *C. elegans* as gene-fusions to the human α−synuclein coding sequence, such that the CFP and YFP moieties are fused to the C-terminus of the synuclein protein sequence in both cases. Both fusion genes are abundantly expressed in the body-wall muscles, as a result of using the *unc*-54 major myosin promoter. However, the CFP and YFP can only interact when the α-synuclein moieties come close together (<70 Å) in the form of protein aggregates, producing FRET signals when the fluorophores are oriented parallel to each other.

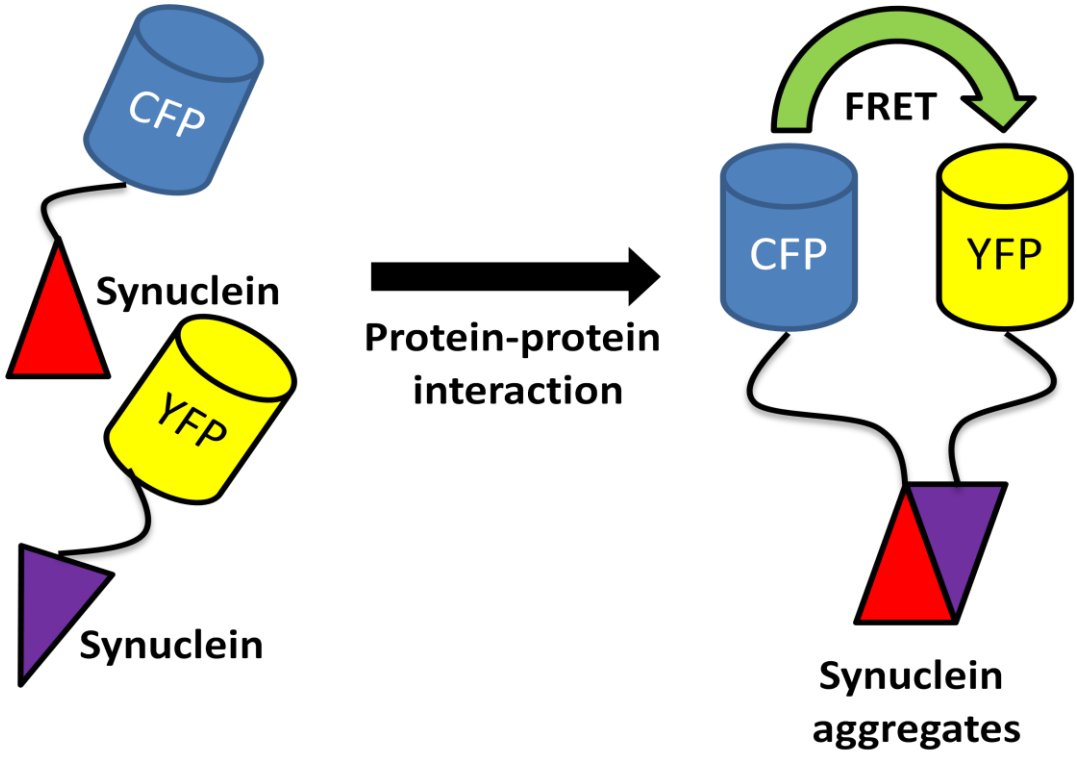

Figure 5.3: Protein-protein interaction (adapted from Zhang et al. 2002). CFP and YFP can only interact when the attached α-synuclein moieties come close together in the form of aggregates, producing FRET signals.

FRET measurements can be done in two different ways:

1. Direct measurement of FRET
2. Indirect measurement of FRET

When two protein fluorophores are close enough, transfer of energy takes place from the donor to the acceptor and hence the intensity of donor fluorescence is reduced in the process. However, when the acceptor is photobleached it blocks the transfer of energy from the donor to acceptor resulting in increased donor fluorescence intensity. Measuring the intensity of donor fluorescence before and after acceptor photobleaching is an indirect method for measuring FRET signals. On the other hand, direct FRET measurement can be done by measuring the acceptor emissions in the presence or absence of excitation for the donor (Brignull et al. 2006). In our experiments we used this direct mode of measuring FRET signals on a standard microplate fluorometer (Wallac Victor 1420 Multilabel Counter) equipped with narrow bandpass filters for CFP excitation (430nm) and YFP emission (530nm). This also allows us to quantify the FRET signal.

5.2 Materials and methods

All Materials and Methods related to this section are described in chapter 2.

5.3 Results

5.3.1 FRET analysis for all transgenic strains

Alpha-synuclein has a known tendency to aggregate *in vivo,* as shown in previous studies using transgenic worms (Brignull et al. 2006; van Ham et al. 2008). The objective of this work is to show that synuclein aggregation can be monitored in *unc*-54::SC+SV (I) worms using FRET. Synchronized young adult worms were washed off the plate and transferred in equal aliquots into a microplate. Each well usually has around 1-2000 worms –but the range in worm numbers between replicates for any given strain is only ±5% (see 2.18). A standard microplate fluorometer (Wallac Victor 1420 Multilabel Counter) was used with an excitation wavelength of 430nm for CFP and an emission wavelength of 530nm for YFP. All data have been normalized per 1000 worms for each strain. As shown in figure 5.4, the FRET signal from wildtype N2 (control) worms was very low when compared with the other transgenic strains. The *unc*-54::C (NI) strain expressing CFP and *unc*-54:V strain expressing YFP showed a low level of FRET signal that was nevertheless considerably higher than N2 worms. This represents a minority of the emissions spilling over into the YFP emission range (for *unc*-54::C (NI)), or some part of the CFP excitation causing direct excitation of the YFP (for *unc*-54:V (I)). Only 1% of the

YFP signal shows through in the CFP channel when excited for YFP, whereas 30-35% of the CFP signal shows through in the YFP channel when excited at CFP. This is unavoidable using the filters we had available from PerkinElmer. The negative control *unc*-54::C+V (I) worms expressing both CFP and YFP showed a slight increase in the FRET signal when compared with *unc*-54:C (NI) and *unc*-54:V (I). The positive control *unc*-54::CV (I) expressing CFP fused with YFP in the same construct showed a very high FRET signal when compared with the other transgenic strains – since the CFP donor and YFP acceptor are always in very close proximity. The *unc*-54::SC+SV (I) worms showed FRET signals intermediate between the negative and positive control strains. This suggests that both CFP and YFP moieties may be brought close together due to the aggregation of α-synuclein in this double transgenic strain.

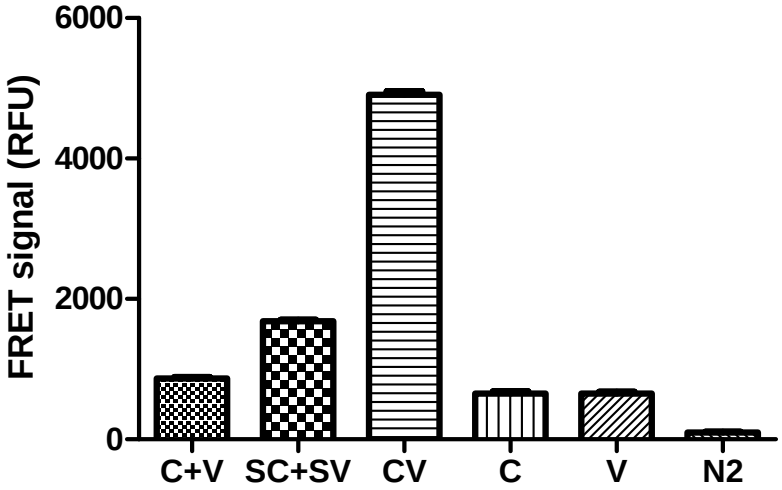

Figure 5.4: FRET signal for all transgenic strains. Using a standard microplate fluorometer (Wallac Victor 1420 Multilabel Counter), the FRET signal was measured by excitation at a wavelength of 430nm for CFP and measuring emission at a wavelength of 530nm for YFP. C, V and N2 are controls; C+V is the negative control, CV is the positive control. The FRET signal for SC+SV is intermediate between the negative and positive controls. The graph is normalized per 1000 worms for each strain.

5.3.1.1 Confocal microscopy of *unc*-54::SC+SV (I) showing FRET

The *unc*-54::SC+SV (I) and the control *unc*-54::C (NI) worm pictures were taken using a Leica TCS SP2 Confocal Laser Scanning Microscope (CLSM) with Z-stacking to confirm FRET in *unc*-54::SC+SV (I) worms. A 458nm laser was used to excite CFP which in turn excites YFP giving the CFP and FRET images shown in part A (panels i and ii) for *unc*-54::SC+SV (I) worms. Subsequently, a 514nm laser was used to excite the YFP directly, although no CFP can be seen (part A panels iv and v). To confirm that FRET in *unc*-54::SC+SV (I) worms was not due to crossover, unc-54::C (NI) worms were also used. Again

458nm laser was used to excite CFP, but there is no sign of FRET in *unc*-54::C (NI) worms because of the absence of YFP (part B panels i and ii). A 514nm laser was used but in the absence of YFP no fluorescence could be observed for either CFP or YFP (part B, panels iv and v).

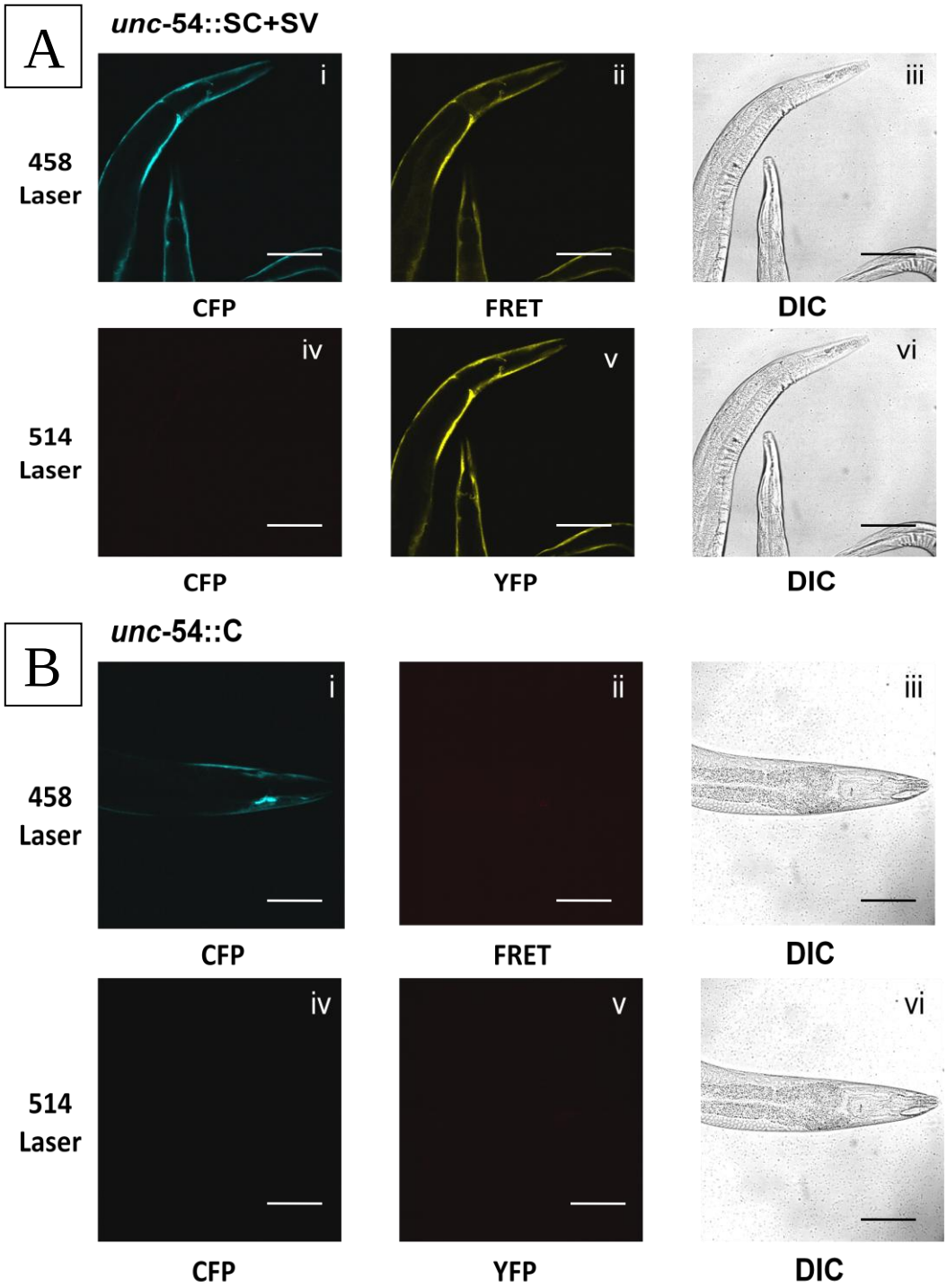

Figure 5.5: Confocal microscopy of *unc*-54:: SC+SV (I) and *unc*-54:: C (NI). *(A) unc*-54::SC+SV worms showing FRET signal (B) control *unc*-54::C worms showing the absence of FRET signal. All photographs comparing two conditions used the same gain settings:- pinhole=0.9 airy doses (long Z-depth), point spread function (PSF) = 0.451 µm in Z sampled into PMT#2 gain 837.0 V, offset 1.8%, PMT#3 gain 677.0 V, offset -1.1%, Transmission DIC gain 170.2V, offset -2.5%, scale bar=100µm.

5.3.1.2 Confocal microscopy of *unc*-54:: SC+SV (I)

Pictures of *unc*-54::SC+SV (I) worm were taken using the same confocal settings as above (5.3.1.1) to confirm that α-synuclein is aggregating inside the worm to bring the CFP and YFP moieties close together. Figure 5.5 shows the head region of a young adult worm expressing both CFP (A) and YFP (B), showing fluorescent granular aggregates.

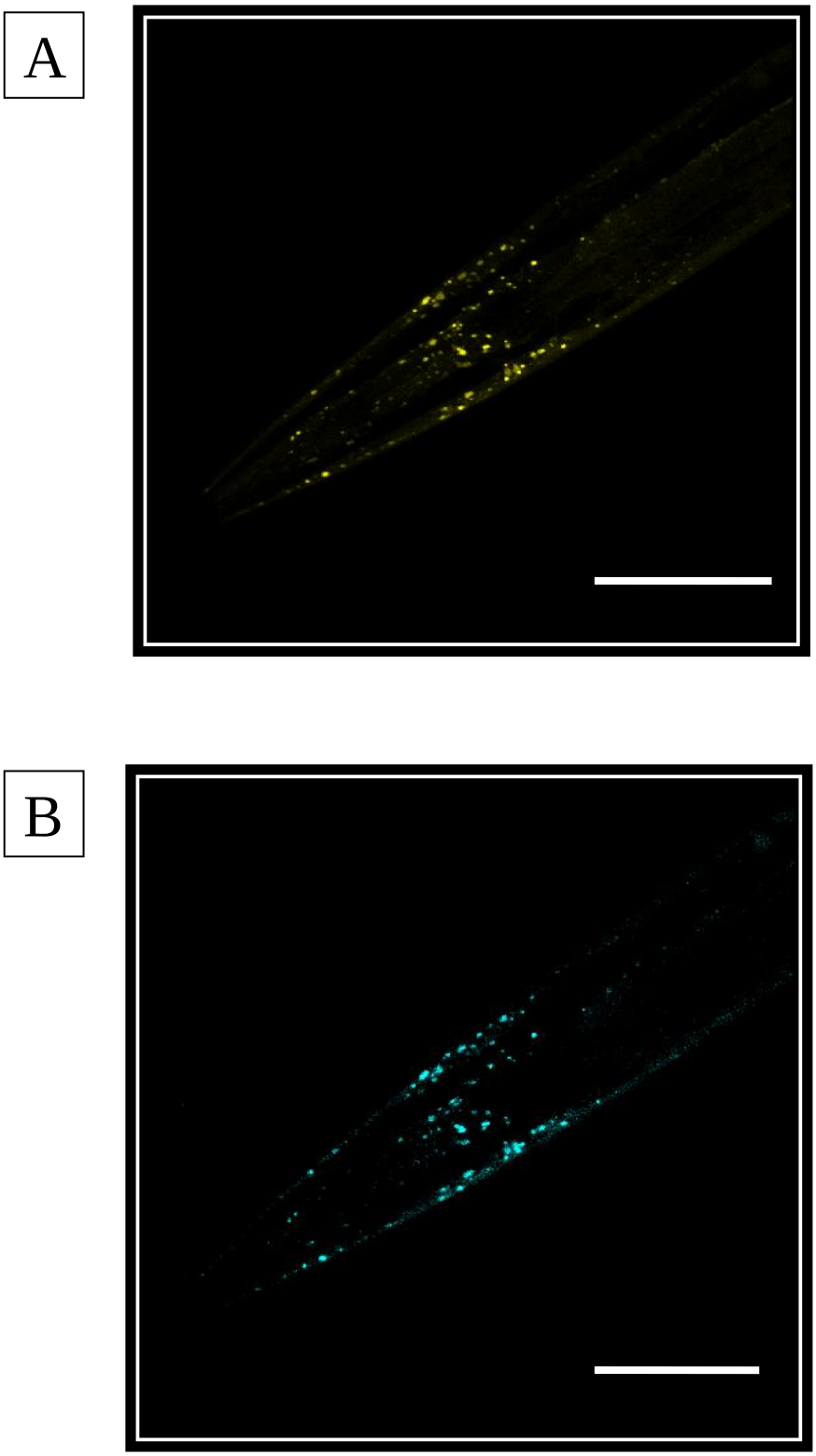

Figure 5.6: Confocal microscopy of *unc*-54:: SC+SV (I)
Head region of a young adult worm with Z-stacking for CFP (A) and YFP (B), showing aggregated fluorescent granules. The excitation and emission wavelength of CFP and YFP used in the confocal microscope to capture images are 458/485 and 514/545. Photographs comparing these two conditions used the same gain settings:– pinhole=0.9 airy doses (long Z-depth), point spread function (PSF) = 0.451 µm in Z sampled into PMT#2 gain 460.4 V, offset 2.4%, lens=63x 1.25NA oil apochromat, scale bar=100µm.

5.3.1.3 Confocal microscopy of *unc*-54:: SV+C (NI)

Pictures of *unc*-54::SV+C (NI) worm were taken using the same confocal settings as above (5.3.1.1) to confirm that synuclein tagged with YFP is aggregating inside the worm whereas CFP show a diffuse distribution along the body wall muscles.

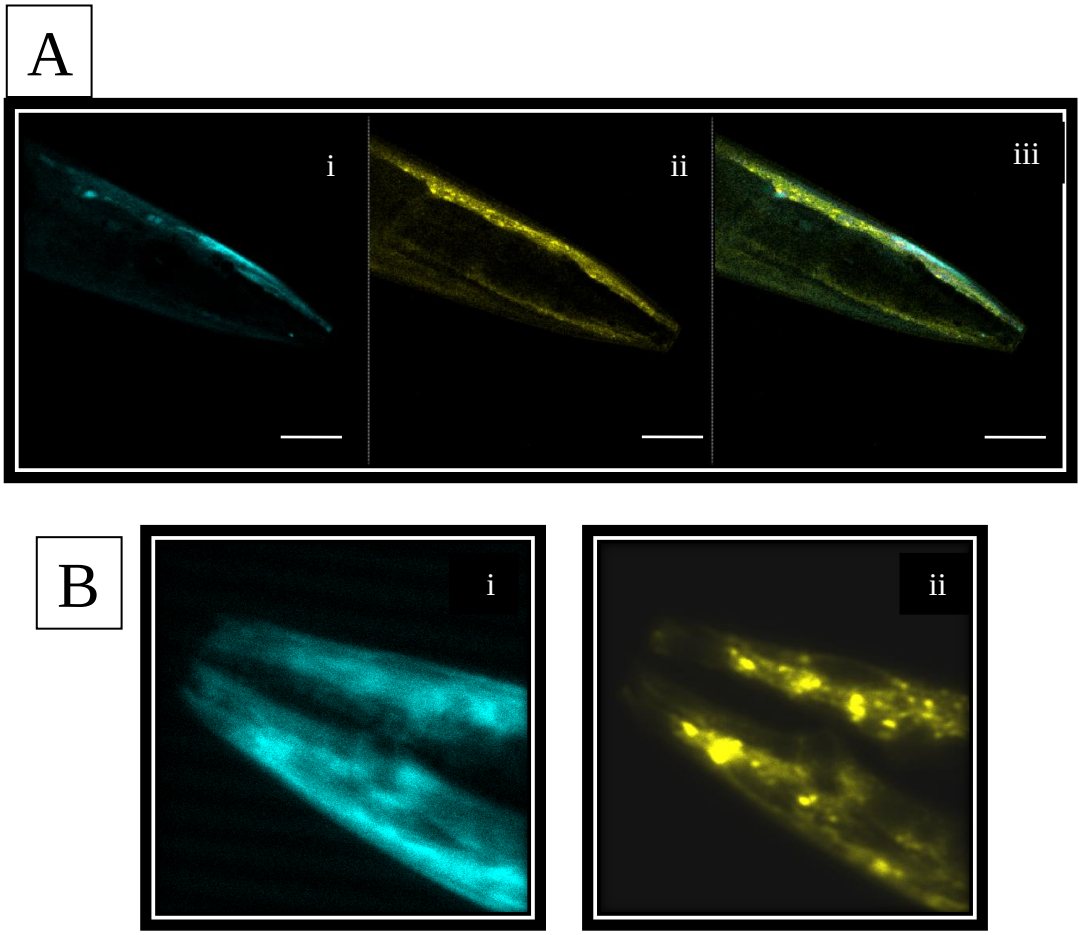

Figure 5.7: Confocal microscopy of *unc*-54:: SV+C. (A) Shows the head region of a young adult worm showing diffuse CFP and YFP aggregates (B) The head region of the worm is magnified (x40) to show aggregated fluorescent granules of YFP and diffuse CFP. The excitation and emission wavelength of CFP and YFP used in the confocal microscope to capture images are 458/485 and 514/545. All photographs comparing two conditions used the same gain settings:– pinhole=2.75 airy doses (long Z-depth), point spread function (PSF) = 1.379 µm in Z sampled into PMT#2 gain 610.7 V, offset 1.4%, PMT#3 gain 710.1 V, offset -0.4%, zoom=12.3, scale bar=100µm.

Figure 5.7 part (A) shows the head region of a young adult worm showing diffuse CFP (panel i), YFP-tagged synuclein aggregates (panel ii) and merged image showing CFP together with aggregate YFP (panel iii). Part (B) shows another worm under 40 x magnification, where the head region of the worm is enlarged to show fluorescent YFP-tagged aggregates (panel ii) and diffuse CFP fluorescence (panel i).

5.3.2 FRET Analysis for *unc*-54::SC+SV (I) fusion worms and YFP fluorescence for NL5901 in terms of aging

We measured the FRET signal from synchronized L4 larvae through the first few days of adult life. As shown in figure 5.8 Part (A), we observed a >3 fold increase in FRET signal, which was maintained through several days of adult life. This shows that, as the worms grows from the larval L4 stage to adulthood, the aggregation of α-synuclein increases rapidly. The mechanisms underlying this sudden onset of α-synuclein aggregation in young SC+SV adults require further investigation. In Part (B), worms of the NL5901 strain (which are similar to our *unc*-54::SV strain but fully integrated; van Ham et al. 2008) showed only a slight (~30%) increase in YFP fluorescence. This might be due to the expression of the *unc*-54 gene during the

early adult stage, but cannot account for the much larger increase in FRET signal (Part A). Because filtration was required to remove small larvae from the adult population, some worm losses are inevitable; this probably accounts for the slight drop seen after 5 days in part A, and possibly for the larger drop seen in part B (which may also reflect reduced *unc*-54 gene expression in mature adults).

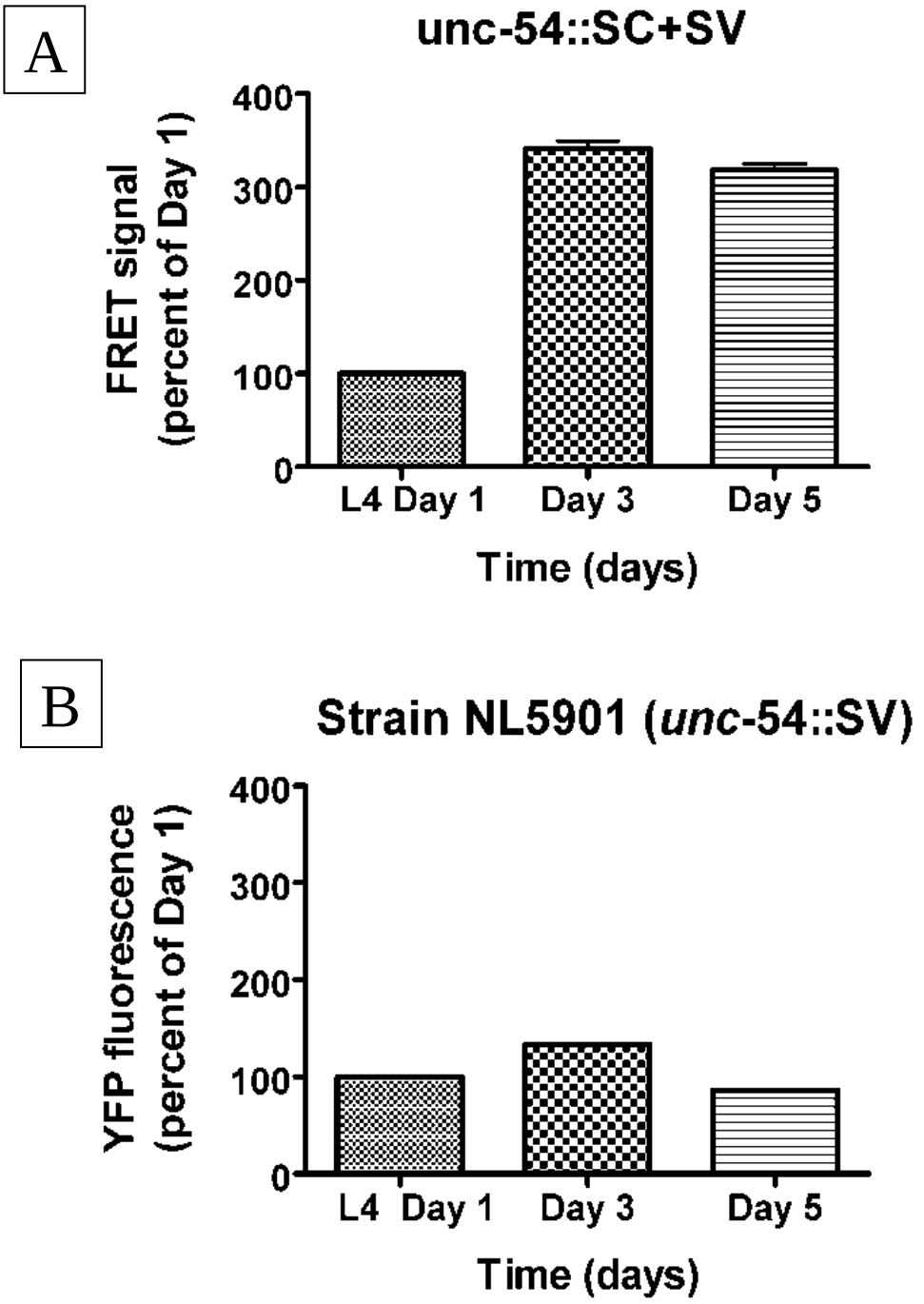

Figure 5.8: FRET signal for *unc*-54::SC+SV (I) and YFP fluorescence for NL5901 strains from the larval L4 stage through the first few days of adult life. The FRET signal was measured for larval L4 stages of *unc*-54::SC+SV (I) strain and YFP fluorescence for NL5901 strain. After 2 and 4 days (once the worms reached adulthood) the FRET signal was again measured for *unc*-54::SC+SV (I) worms and YFP fluorescence for NL5901 worms using the same worm population.

5.3.2.1 Confocal microscopy of *unc*-54:: SC+SV (I) during the larval L4 and adult stage

Confocal images of *unc*-54::SC+SV (I) worms were captured as above (5.3.1.1), showing that α-synuclein aggregates rapidly between the larval L4 stage and adulthood. Figure 5.9 part (A) shows small granules of aggregated YFP-labelled α-synuclein along the body wall muscles of a larval L4 stage worm, whereas part (B) shows a clear increase in the size and intensity of such aggregates (after merging together) as the worms mature from L4 larvae to adults.

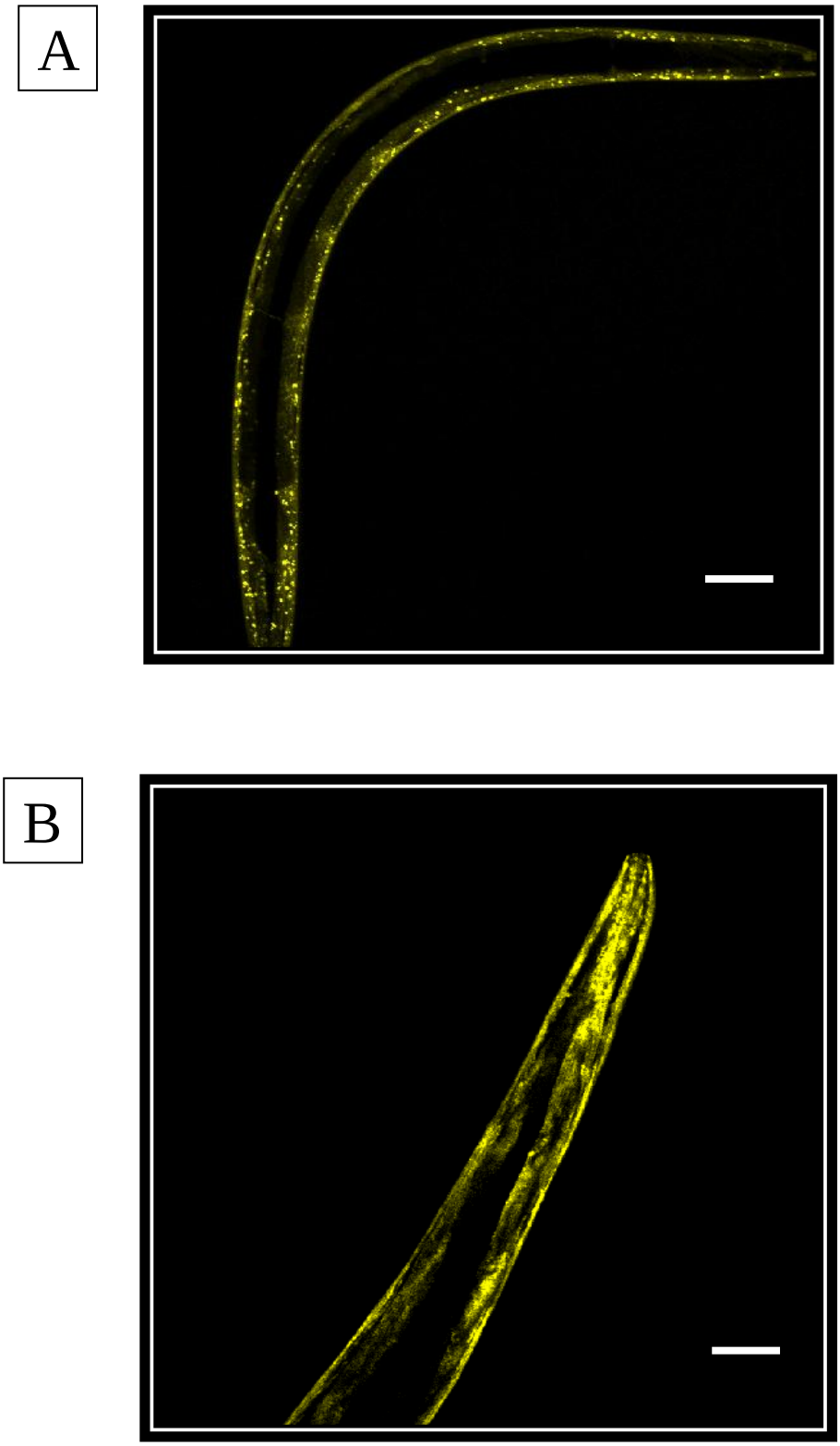

Figure 5.9: Confocal microscopy of *unc*-54:: SC+SV (I) larval L4 and adult stage. Body wall muscles of a Larval L4 stage worm with Z-stacking for YFP (A), showing small fluorescent granules; (B) showing larger granules along the body wall muscles of an adult worm. The excitation and emission wavelength of YFP used in the confocal microscope to capture images are 514/545. All photographs used the same gain settings:- pinhole=0.9 airy doses (long Z-depth), point spread function (PSF) = 0.451 µm in Z sampled into PMT#2 gain 460.4 V, offset 2.4%, scale bar=100µm.

5.3.3 Effect of RNAi against Hip-1 for *unc*-54:: SC+SV (I) fusion worms.

Roodveldt et al (2009) used RNA interference (RNAi) to target the co-chaperone Hip-1 (T12D8.8) to knock down its function, and showed that this could promote an increase in the number of YFP-tagged α-synuclein inclusions in the OW40 (effectively *unc*-54::SV) transgenic strain. However, this effect was only apparent in second-generation RNAi worms due to maternal expression of the Hip-1 gene (Roodveldt et al. 2009). In the experiment shown below, Hip-1 RNAi bacteria were fed continuously from the L1 stage of P0 worms for 2 generations in order to block Hip-1 function effectively. Parallel control worms were fed with HT115 bacteria containing the empty feeding vector L4440 (FV). When compared with the control, the FRET signal was increased at least 2-fold in the *unc*-54::SC+SV (I) worms fed with Hip-1 RNAi bacteria.

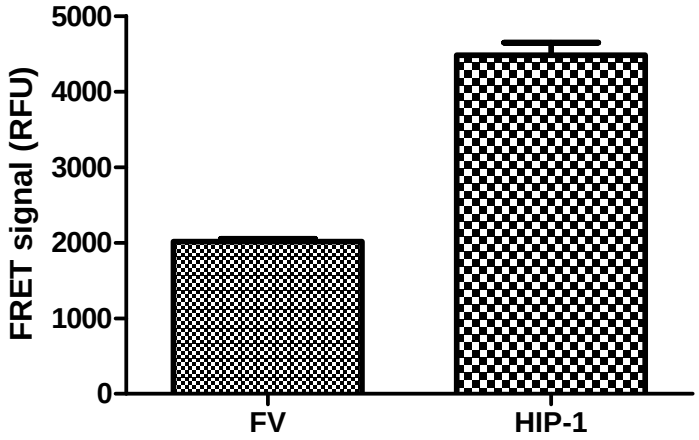

Figure 510: FRET signal for *unc*-54: SC+SV (I) strain targeted against co- chaperone Hip-1 using RNAi. The function of co-chaperone Hip-1 was inactivated by using Hip-1 RNAi. The FRET signal was increased by 2 fold in the worms fed with Hip-1 RNAi bacteria when compared with those fed with feeding vector controls (FV).

5.3.3.1 Confocal microscopy of *unc*-54:: SC+SV (I) worms fed with Hip-1 RNAi and empty feeding vector (FV)

Confocal images of *unc*-54::SC+SV (I) worm pictures were again captured as described previously (5.3.1,1). Figure 5.11 part (A) shows a few small granules of aggregated CFP-tagged α-synuclein in the head region of *unc*-54::SC+SV (I) worms fed on bacteria expressing the L4440 empty feeding vector, through most of the CFP fluorescence is diffuse. The head region of this particular worm was magnified for a clearer picture of these small aggregates. In part (B), these CFP-tagged α-synuclein aggregates increased markedly in size as well as number in worms fed for 2 generations with Hip-1 RNAi bacteria,

and diffuse CFP fluorescence is much reduced. Again, an enlargement of part of the head region emphasizes this difference. Note that the fluorescent granules in part B will appear fainter because of FRET (emissions being absorbed by the acceptor YFP).

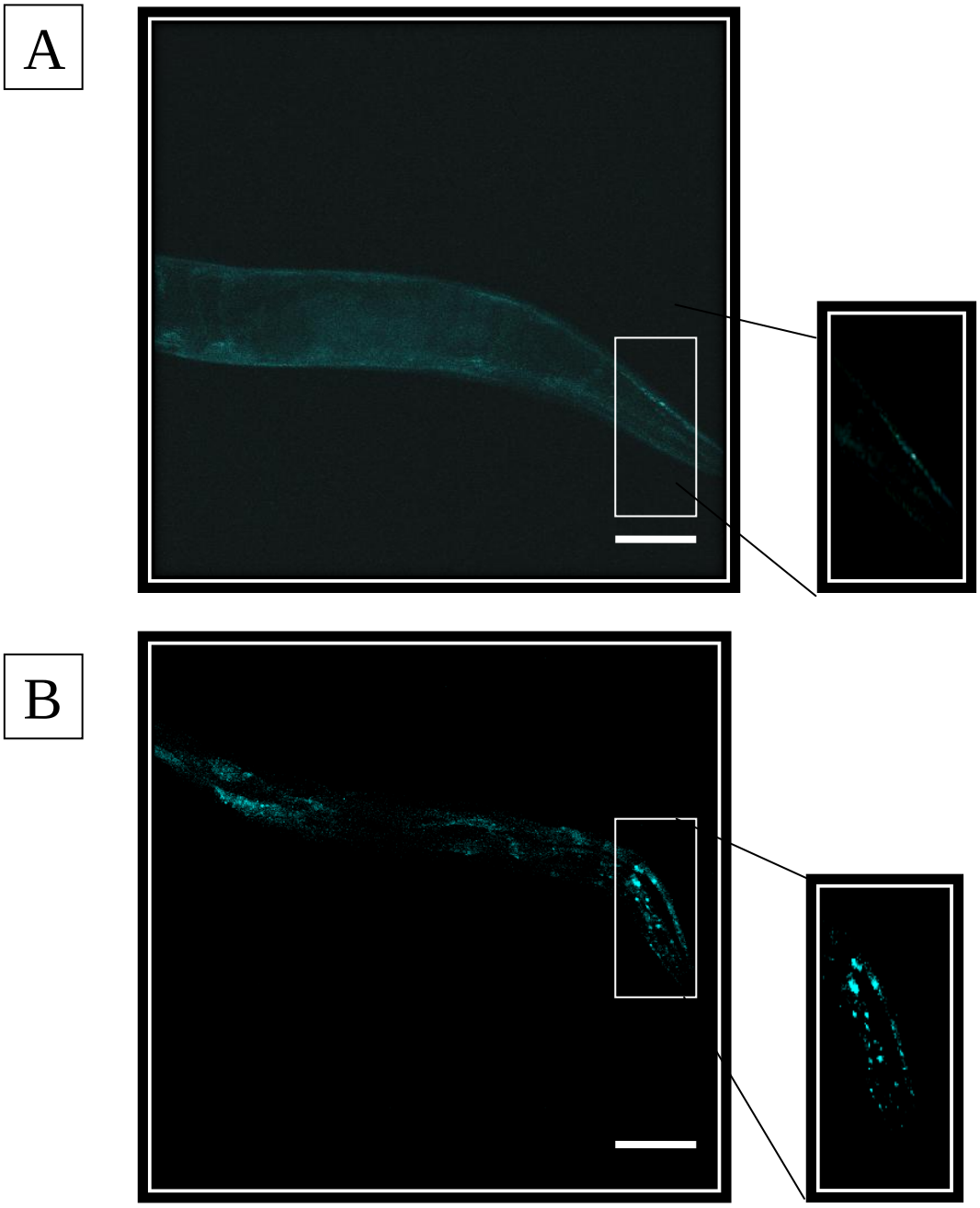

Figure 5.11: Confocal microscopy of *unc*-54:: SC+SV (I) worms fed with Hip-1 RNAI bacteria and empty feeding vector (FV)
Confocal images showing the head regions of young adult *unc*-54::SC+SV (I) worms: (A) fed on empty feeding vector L4440 showing CFP fluorescence; (B) fed on Hip-1 RNAi bacteria; inserts show head regions of each worm magnified. The excitation and emission wavelength of CFP used in the confocal microscope to capture images are 458/485. All photographs used the same gain settings: - pinhole=0.5 airy doses (long Z-depth), point spread function (PSF) = 0.250 µm in Z sampled into PMT#2 gain 566.2 V, offset -7%, scale bar=100µm.

5.3.4 Effects of pesticide treatment on *unc*-54::SC+SV (I) and positive control *unc*-54::CV (I) worms

Exposure to several neurotoxic pesticides such as rotenone, dieldrin, paraquat and chlorpyrifos has been shown to stimulate Parkinsonism in various animal models (Betarbet et al. 2000; Davis 2000; Hetman and Xia 2000; Ishiguro et al. 2001; Boyd et al. 2009). We have tested both chlorpyrifos and rotenone, and found that both stimulate α-synuclein aggregation in *unc*-54::SC+SV (I) worms.

5.3.4.1 Chlorpyrifos treatment on *unc*-54::SC+SV (I) worms

Synchronized *unc*-54::SV+SV (I) L4 larvae were exposed to two different concentrations of chlorpyrifos (20ppm = mg l^{-1} and 300 ppm = mg l^{-1}) for 48 hours. We found a 2-fold increase in the FRET signal at the higher concentration of chlorpyrifos (300 mg l^{-1}) but there was no detectable increase at the lower concentration (20 mg l^{-1}). Using Dunnett's multiple comparisons test, the effect of high but not low chlorpyrifos doses was found to be significant ($P < 0.01$) at 300 mg l^{-1} ($P > 0.05$ at 20 mg l^{-1}).

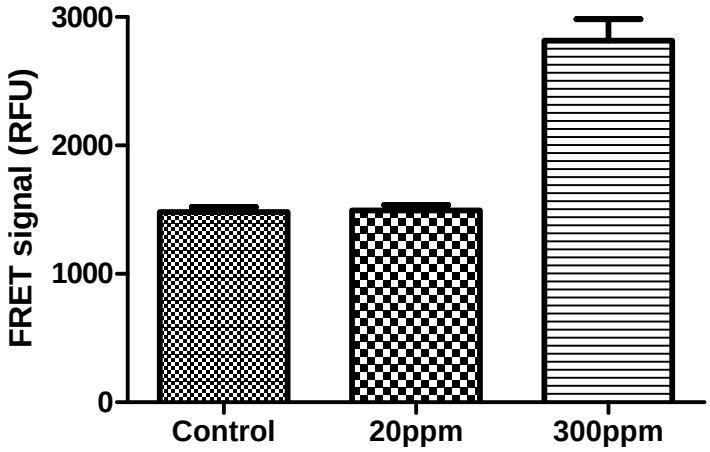

Figure 5.12: FRET signal for *unc*-54::SC+SV (I) worms exposed to chlorpyrifos. Synchronized L4 larvae were exposed to chlorpyrifos for 48 hrs at two different concentrations (20ppm and 300ppm). The FRET signal was increased by 2 fold in worms exposed to 300ppm as compared with the control (0ppm).

5.3.4.2 Chlorpyrifos treatment of positive control *unc*-54::CV (I) worms

Synchronized *unc*-54::CV (I) L4 larvae were exposed to the same two concentrations of chlorpyrifos (20 ppm = mg l^{-1} and 300 ppm = mg l^{-1}). We found similarly high FRET signals in the control and in both concentrations of chlorpyrifos. Using Dunnett's multiple comparison test, the effects of high and low doses of chlorpyrifos on *unc*-54::CV (I) worms were not significant ($P > 0.05$).

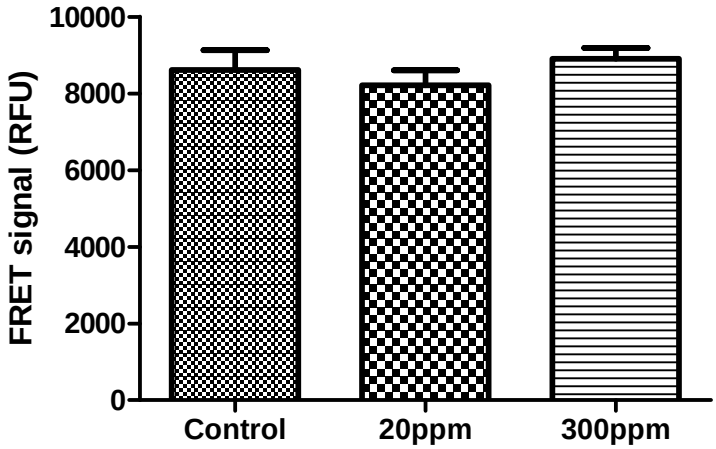

Figure 5.13: FRET signal for *unc*-54::CV (I) worms exposed to chlorpyrifos. Synchronized L4 larvae were exposed to chlorpyrifos for 48 hrs at two different concentrations (20ppm and 300ppm), using *unc*-54::CV worms as a positive control.

5.3.4.3 Confocal microscopy of *unc*-54::SC+SV (I) exposed to chlorpyrifos

Figure 5.13 part (A) shows the head region of an *unc*-54::SC+SV (I) worm with small granules of YFP-tagged α-synuclein aggregates in the absence of chlorpyrifos (control); much of the fluorescence appears diffuse. The head region of this worm was magnified for a clearer picture of small aggregates. Part (B) shows much larger and brighter granules of YFP-tagged α-synuclein aggregates following exposure to chlorpyrifos at 300ppm.

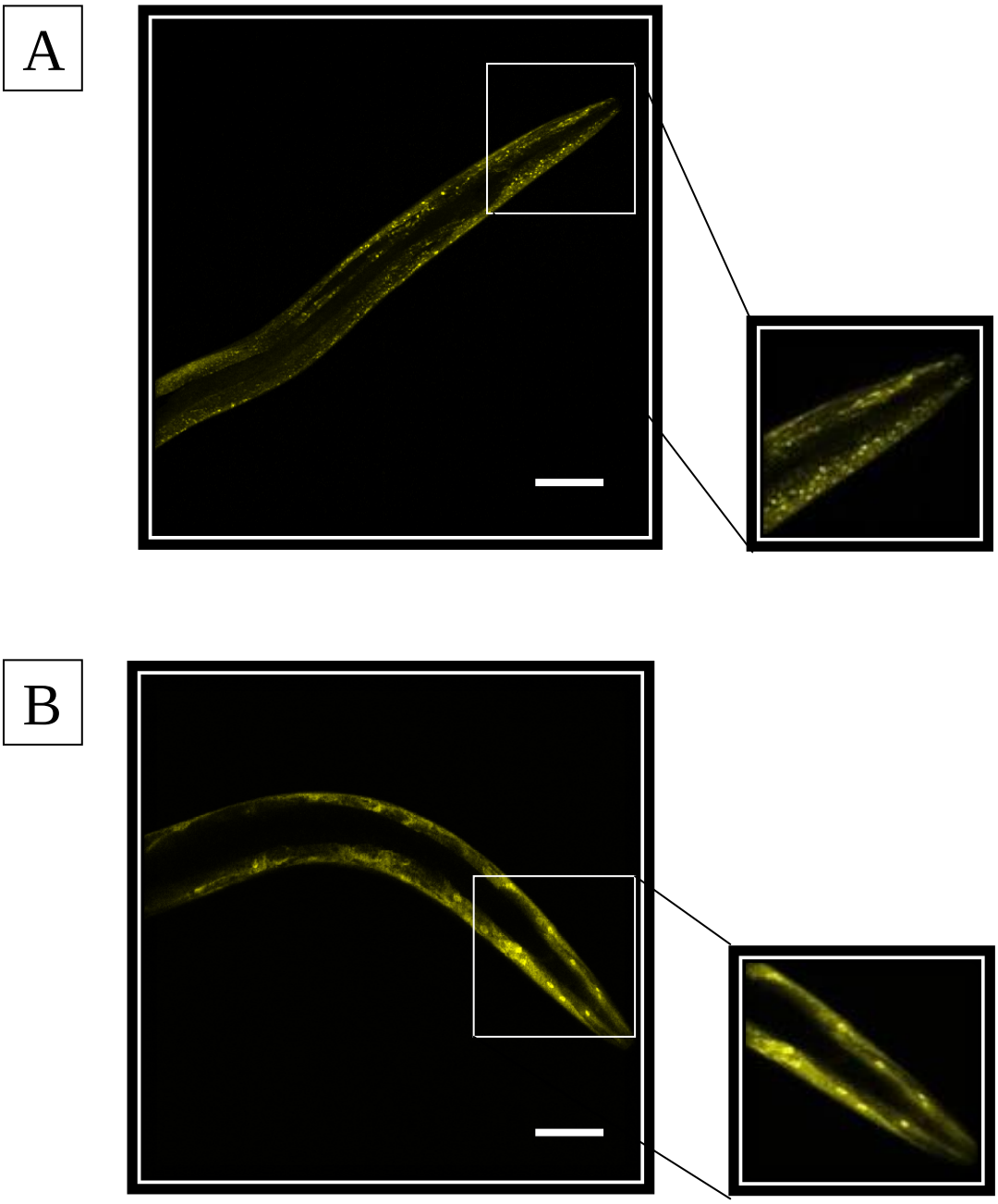

Figure 5.14: Confocal microscopy of *unc*-54:: SC+SV (I) worms exposed to chlorpyrifos. Exposure of L4 larvae to 300ppm chlorpyrifos for 48 hrs versus control (no chlorpyrifos):- (A) showing YFP fluorescence in a control worm with small faint granules, and (B) showing a chlorpyrifos-treated worm (300ppm) with larger, brighter granules. The excitation and emission wavelength of YFP used in the confocal microscope to capture images are 514/545. All photographs used the same gain settings:- pinhole=0.9 airy doses (long Z-depth), point spread function (PSF) = 0.451 µm in Z sampled into PMT#2 gain 460.4 V, offset 2.4%, scale bar= 100µm.

5.3.4.4 Rotenone treatment of *unc*-54::SC+SV (I) worms

Rotenone was found to cause developmental arrest of worms after the L2/L3 stage, so synchronized L1 larvae were tested for a shorter (24 hour) exposure. Two different concentrations of rotenone (2ppm/ mg l^{-1} and 20 ppm/ mg l^{-1}) were used to treat synchronized L1 larvae of the *unc*-54::SC+SV (I) strain for 24 hours. We found a 2-fold increase in the FRET signal at the high concentration of rotenone (20ppm) but again there was no detectable increase at the low concentration (2ppm). From the Dunnett's multiple comparisons test, the effect of the high rotenone dose was significant ($P < 0.01$) at 20 mg l^{-1}, but the low dose was non-significant ($P > 0.05$) at 2 mg l^{-1}.

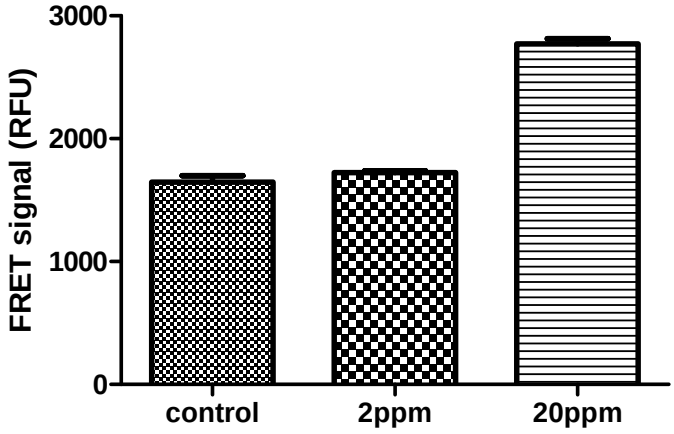

Figure 5.15: FRET signal for *unc*-54::SC+SV (I) worms exposed to rotenone. Synchronized L1 larvae were exposed to rotenone for 24 hrs at two different concentrations (2ppm and 20ppm). The FRET signal was increased by 2 fold in the worms exposed to 20ppm as compared with the control (0ppm).

5.3.4.5 Rotenone treatment of positive control *unc*-54::CV (I) worms

As before, two different concentrations of rotenone (2ppm = mg l^{-1} and 20 ppm = mg l^{-1}) were used to treat synchronised L1 larvae of the *unc*-54::CV (I) positive control strain for 24 hours. We found similarly high FRET signals in the control and in both concentrations of rotenone. Using Dunnett's multiple comparisons test, the effects of both high and low doses of rotenone on *unc*-54::CV (I) worms were not significant (P > 0.05).

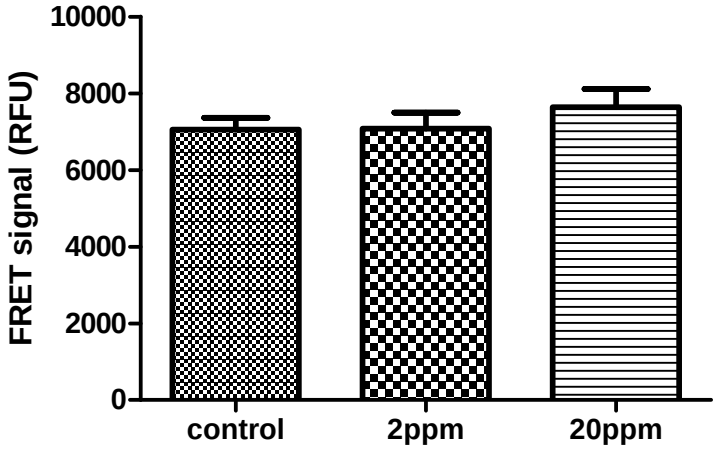

Figure 5.16: FRET signal for *unc*-54::CV (I) worms exposed to rotenone. Synchronized L1 larvae were exposed to rotenone for 24 hrs at two different concentrations (2ppm and 20ppm), using *unc*-54::CV (I) worms as a positive control.

5.3.4.6 Confocal microscopy of *unc*-54:: SC+SV (I) exposed to rotenone

After 24 hours of exposure to rotenone, confocal images of *unc*-54::SC+SV (I) strain were captured as described above (5.3.1.1). Figure 5.15 part (A) shows small granules of YFP-labelled α-synuclein aggregates in the head region of an *unc*-54::SC+SV (I) control worm (not exposed to rotenone). Part (B) shows an increase in the size and number of fluorescent synuclein aggregates following exposure to rotenone at 20ppm. Part (C) shows an arrested L1 larva following rotenone treatment – again with larger and brighter granules.

A

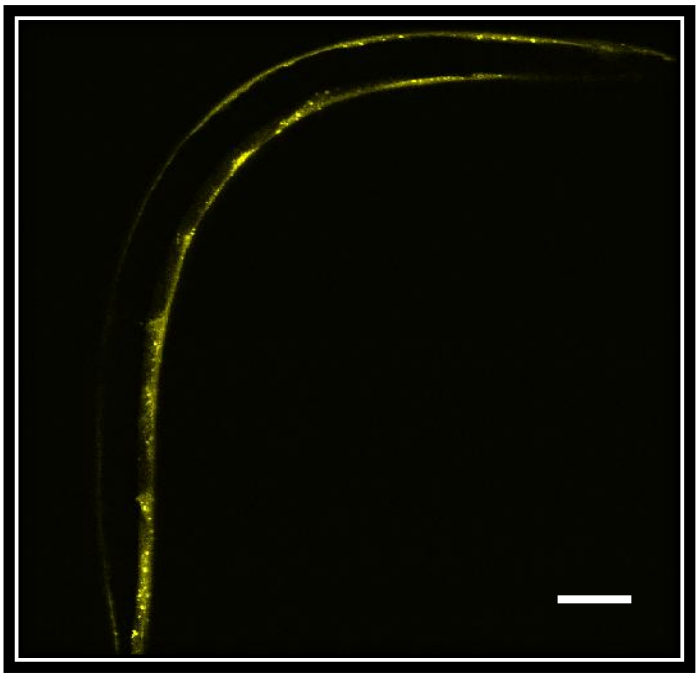

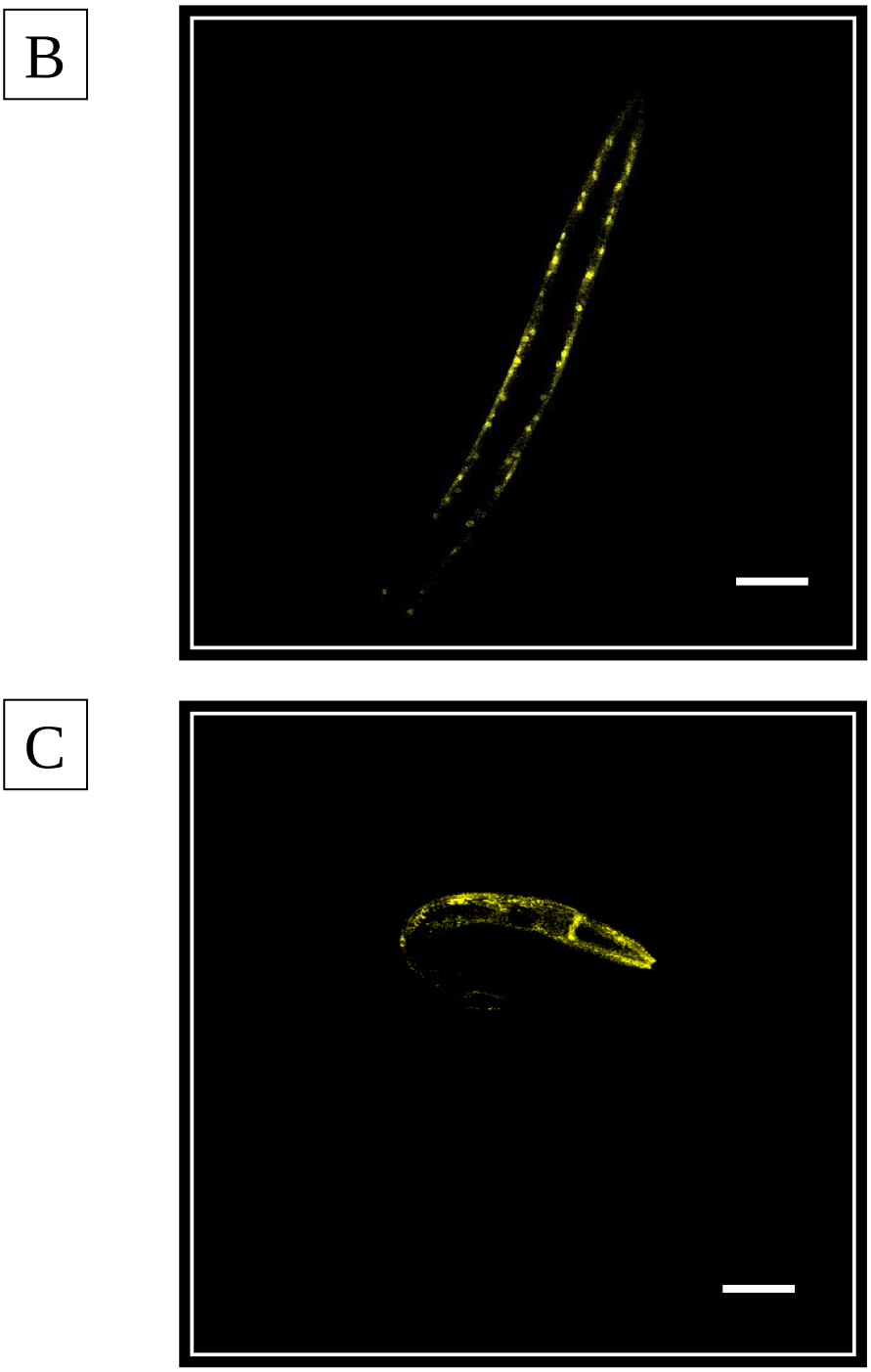

Figure 5.17: Confocal microscopy of *unc*-54:: SC+SV (I) worms exposed to rotenone. Exposure of L1 larvae to rotenone for 24 hrs at 20ppm:- (A) showing YFP fluorescence in a control worm (0ppm) with small faint granules, (B) showing a rotenone-treated worm (20ppm) with larger, brighter granules and (C) showing an arrested L1 larvae also with larger and brighter granules. The excitation and emission wavelength of YFP used in the confocal microscope to capture images are 514/545. All photographs used the same gain settings:- pinhole=1.2 airy doses (long Z-depth), point spread function (PSF) = 0.601 µm in Z sampled into PMT#2 gain 566 V, offset -7.1%, scale bar= 100µm.

5.3.5 Effects of Rotenone and Chlorpyrifos on the induction of Reactive Oxygen Species (ROS) in *unc*-54::SC+SV (I)

This experiment used only the highest test concentrations of rotenone (20ppm = mg l^{-1}) and chlorpyrifos (300 ppm = mg l^{-1}) to determine whether or not these pesticides induce oxidative stress. Synchronized L1 larvae were exposed to each pesticide for 24 hours alongside zero controls (no pesticide). As mentioned earlier, the highest concentration of rotenone causes developmental arrest after the L2/L3 stage. The change in DCF fluorescence/worm was increased by 5-fold at the high concentration of chlorpyrifos (300ppm) but there was only a small increase at the high concentration of rotenone (20ppm). Dunnett's test showed that the effect of chlorpyrifos was significant ($P < 0.01$), but that of rotenone was not ($P > 0.05$).

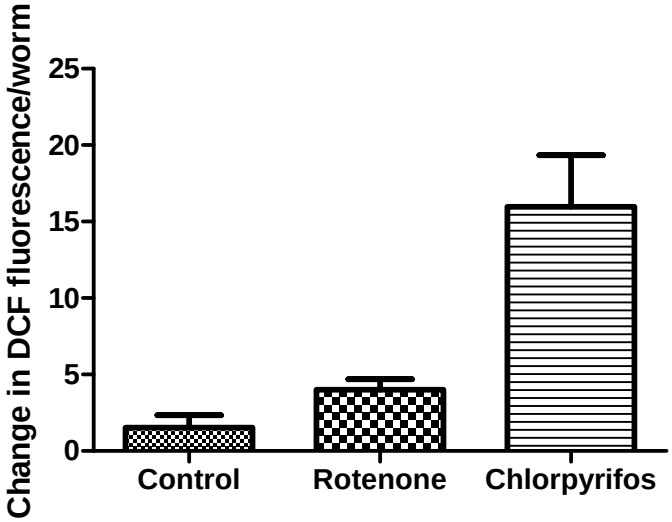

Figure 5.18: oxidative stress in *unc*-54::SC+SV (I) worms exposed to rotenone and chlorpyrifos. Synchronized L1 larvae were exposed to rotenone and chlorpyrifos for 24 hrs at high concentrations. Change in DCF fluorescence/ worm was measured using the H2-DC-DA assay. There was a 5 fold increase in DCF fluorescence in worms exposed to chlorpyrifos (300ppm) and a slight increase when exposed to rotenone (20ppm) compared to the control (0ppm).

5.3.6 Effect of Rotenone and Chlorpyrifos on the induction of ROS in a transgenic *C.elegans* model of Parkinson's disease (NL5901 Strain).

A similar experiment was done to show the effect of Rotenone and Chlorpyrifos on the induction of ROS in a different transgenic *C.elegans* model of Parkinson's disease (NL5901; effectively an integrated *unc*-54::SV strain). We found similar results except that rotenone had a significant effect in this NL5901 strain. There was a > 2-fold increase in DCF fluorescence caused by chlorpyrifos (300ppm) and a > 3-fold increase caused by rotenone (20ppm). Here Dunnett's test

shows that both pesticides have a statistically significant effect ($P < 0.01$).

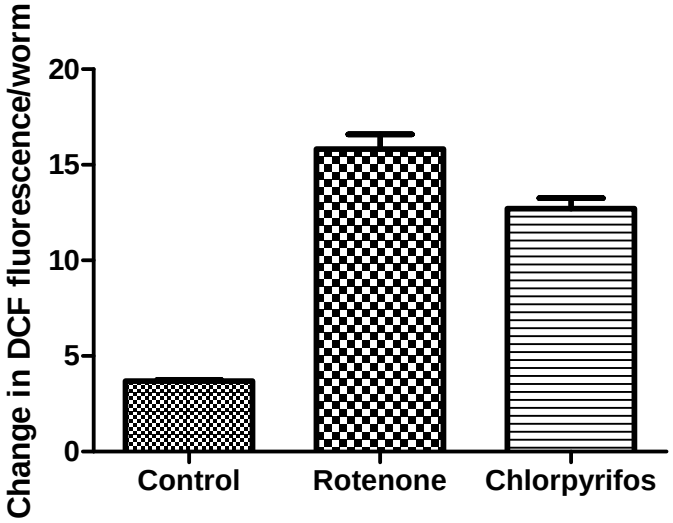

Figure 5.19: oxidative stress in NL5901 strain exposed to rotenone and chlorpyrifos. Synchronized L1 larvae were exposed to rotenone and chlorpyrifos for 24 hrs at high concentrations. Change in DCF fluorescence/ worm was measured using the H2-DC-DA assay. There was a 2 fold increase in the DCF fluorescence in worms exposed to chlorpyrifos (300ppm) and a 3 fold increase when exposed to rotenone (20ppm) compared to control (0ppm).

5.4 Discussion

Our key purpose in creating the *unc*-54::SC+SV (I) strain is to elucidate the role of α-synuclein aggregation in Parkinson's disease. Measuring FRET signals in the *unc*-54::SC+SV (I) strain serves as a surrogate indicator of α-synuclein aggregation. From our results, the *unc*-54::SC+SV (I) strain showed intermediate FRET signals compared to negative control strains (C, V and C+V) and the positive control (CV) strain. This is because the fluorophores CFP and YFP can be brought together by α-synuclein aggregation in the SC+SV (I) strain, whereas they are locked together in the CV fusion. Confocal images were generated to confirm the presence of FRET. Furthermore, a 3-fold increase in FRET signal in *unc*-54::SC+SV (I) strain was observed during early adult life as compared to L4 larvae. This was confirmed by confocal images showing larger and brighter aggregates after several days of adulthood. Therefore the accumulation of α-synuclein aggregates seems to be age-dependent. To confirm that the FRET signal is genuine, the NL5901 (*unc*-54::SV) strain was used as a control. We observed only a slight increase in YFP fluorescence between L4 and adult stages. This accounts for any change in the expression of the *unc*-54 gene, and hence the remainder of the observed fluorescence increase seen in SC+SV worms was genuine FRET signal.

In addition, RNAi against Hip-1 showed an increase in α-synuclein aggregation, as monitored by FRET, supporting the proposed role of the co-chaperone Hip-1 in protein homeostasis. In agreement with previous findings (Roodveldt et al. 2009), this consequence of knocking down Hip-1 function was only apparent in the second generation, apparently because maternal expression ensures continued Hip-1 function in the first generation worms Similarly, a 2-fold increase in FRET signal in *unc*-54::SC+SV (I) worms was observed upon exposure to the pesticides chlorpyrifos and rotenone, consistent with the possible role of these toxicants as environmental risk factors for Parkinson's disease. Again, confocal images of the *unc*-54::SC+SV (I) strain confirm the presence of fluorescent α-synuclein aggregates. Notably, these YFP-tagged α-synuclein aggregates were brighter and larger in size following exposure to high doses of chlorpyrifos or rotenone as compared to untreated controls.

Finally, an increase in DCF fluorescence indicated oxidative stress in both *unc*-54::SC+SV (I) and NL5901 strains upon exposure to rotenone or chlorpyrifos, although the response to rotenone in *unc*-54::SC+SV (I) worms was lower than that in NL5901 worms.

Chapter 6 Discussion

Our overall aim in this project was to generate a double transgenic strain (*unc*-54::SC+SV (I)) and to monitor FRET signals as a biomarker of α-synuclein aggregation. This was achieved through expression of human α-synuclein fused at its C-terminus with CFP and/or YFP in the body wall muscles of *Caenorhabditis elegans* (*in vivo* model) driven by the *unc*-54 myosin promoter. Worms expressing α-synuclein show greater sensitivity to gamma irradiation, shorter lifespan, reduced pharyngeal pumping and slower motility, whereas expression of CFP and/or YFP without α-synuclein had little or no effect. We observed increases in FRET signal in this *unc*-54::SC+SV (I) strain during ageing from L4 to adult, following RNAi against Hip-1, and following exposure to pesticides (chlorpyrifos and rotenone). Finally, an increase in the levels of reactive oxygen species (ROS) was observed in the *unc*-54::SC+SV (I) strain when exposed to chlorpyrifos and possibly rotenone.

6.1 Effect of gamma irradiation on *C.elegans*

Hartman and Herman (1982) were the first to identify the genes involved that respond to radiation damage in C.elegans. *C. elegans* has a large number of DNA repair genes which function in highly conserved pathways. For the purpose of

examining the radiation response, reporter analysis of DNA repair gene expression would be of interest. Following gamma irradiation, DNA strand-breaks are generated, which the cell can repair up to the limit of its capacity. DNA repair systems work well after low-dose exposure but are much less efficient following high-dose exposure—and the damage caused by very high doses may not be repairable at all. There is also evidence (Herman 1978; Meneely and Herman 1979) that high doses cause a great deal of sterility among the F1 generation.

Our work has demonstrated that moderate gamma irradiation does not have much effect on worm's sterility in the P0 generation, whereas it has a large effect on the F1 generation. When comparing the different transgenic strains with wild type N2 worms, we found that there is no statistically significant difference ($P>0.05$) in the P0 generation, but these differences become statistically significant ($P<0.05$) in the F1 generation. This applied to all transgenic strains expressing α-synuclein compared against wild-type N2 worms but not for those strains expressing CFP and/or YFP only. The synuclein fusion strains are more sensitive to gamma irradiation as compared with the wild type N2 worms. Synuclein on its own is known to be toxic but the effects of its fusion to YFP on the rate of aggregation *in vivo* are not known.

In an analysis of the dose response of *C.elegans* to gamma radiation, Rosenbluth et al. (1983) observed that at low doses, the curve was non-linear (Fig. 4.1). Their data show that low doses of radiation are non-damaging, apparently due to DNA repair mechanisms which can deal effectively with low doses of radiation (figure 6.1).

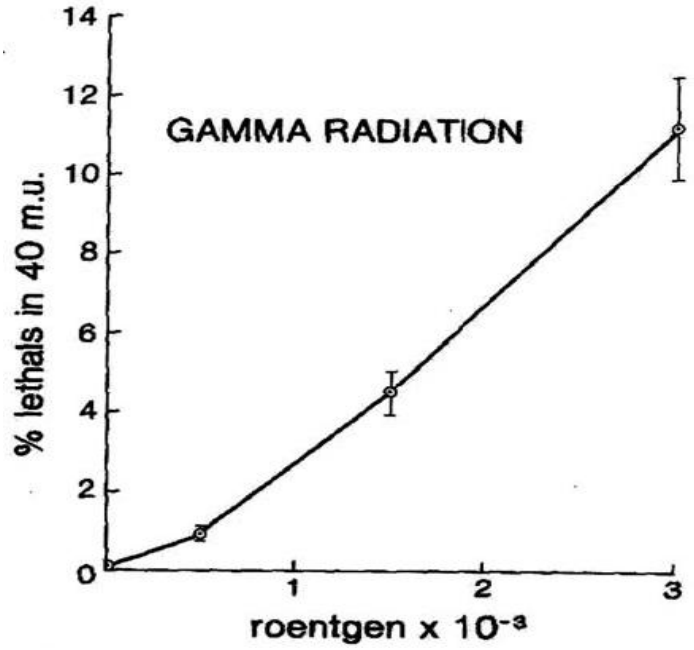

Figure 6.1: Dose response curve for gamma radiation in *C.elegans*. Data from Rosenbluth et al. (1983).

In choosing a mutagen dose for integrating transgene arrays, it is necessary to weigh up the desirability of screening as small a population as possible (using a relatively high dose) against the desirability of limiting the frequency of secondary

mutational events associated with the selected rearrangement (using a low dose).

Interestingly, our data show that our α−synuclein transgenic strains became sterile even at low doses of gamma irradiation. Hence, α−synuclein aggregation in the cell may cause radiation sensitivity to these transgenic worms through an unknown mechanism(s). Also, another possibility is that the presence of α−synuclein DNA as a transgene in the gonads may compromise the DNA repair machinery during irradiation mediated integration. Further experiments will be required to study the relation between DNA repair systems and exposure to gamma irradiation in these transgenic worms.

6.2 Behavioral defects in *C.elegans* linked to α-synuclein expression

The decreased lifespan observed in our transgenic *C. elegans* strains expressing α-synuclein (Figure 4.7) reflects a characteristic decreased lifespan in Parkinson's patients (Diamond et al. 1990; Marttila and Rinne 1991). A similar effect was observed upon expression of human α-synuclein (A53T) in mice, with neurological abnormalities and shortened lifespan (Lee et al. 2002). However, surprisingly it has been reported that worms carrying human α-synuclein fused with GFP and

overexpressed from an *aex-3* (pan-neuronal) promoter (*aex-3*::human synuclein:GFP) have a longer life span compared to control or non-transgenic worms (Vartiainen et al. 2006). One of the reasons for this increased life span is correlated with decreased pharyngeal pumping (Lakowski and Hekimi 1998; Walker et al. 2005), and a significant reduction of pharyngeal pumping was observed for the *aex-3*::human synuclein:GFP transgenic animals suggesting that they were under dietary restriction even though they were raised on thick bacterial lawns (Vartiainen et al. 2006). Taken together, these results suggest that dietary restriction may be a contributing factor for the observed increase in lifespan (Klass 1977; Hosono et al. 1989). Our transgenic strains expressing α-synuclein have increased levels of α-synuclein expression throughout the body-wall muscles, leading to a loss of motor function, resulting in greatly impaired mobility (figure 4.8). Along with reduced longevity, there seems to be reduction in pharyngeal pumping rate as well, but this is most likely an indirect effect, since *myo*-2 (but not *unc*-54) myosin is expressed in the pharynx. Our data (Figure 4.5) suggest that motility is more strongly affected by α-synuclein expression (~50% reduction) than pharyngeal pumping (~20% reduction); the effect of the former may outweigh the latter, contributing towards an overall reduction in life span.

Changes in oxygen concentration also affect the life span of *C. elegans* (Honda and Honda 2002). At high concentrations of oxygen, worm life span is shortened, whereas at low concentrations of oxygen, the life span increases. In addition, a strain with reduced levels of superoxide dismutase was more susceptible to the damaging effects of oxygen. These results indicate that oxidative damage can also speed up the ageing process in *C. elegans*.

According to Morley et al. (2002), polyQ aggregation and cellular toxicity are correlated with ageing in *C. elegans*. Accumulation of aggregates of polyQ expansions (Q19, Q25, Q33, Q35, Q40, Q44, Q64, and Q82) during ageing leads to increasing levels of cellular toxicity. Loss of motility has also been correlated to polyQ aggregate formation, due to the expression of polyQ expansions in *C. elegans* muscles.

So far, ten genes have been linked to inherited forms of human PD; of these, α-synuclein and Parkin have been studied most thoroughly (Polymeropoulos et al. 1997; Kitada et al. 1998). Parkin is an E3 ubiquitin ligase, which plays an important role in the protein degradation process. Previous studies show that a glycosylated form of α-synuclein may be degraded with the help of Parkin (Shimura et al. 2001) Mutations in the Parkin gene are known to cause Autosomal

Recessive Juvenile Parkinson disease (ARJP) resulting in death of dopaminergic neurons (Mouradian 2002). Reduced life span, loss of climbing activity and decreased flight were observed in *Drosophila* on deletion of Parkin (Greene et al. 2003). Similarly climbing ability was reduced in transgenic flies over-expressing both wild type and mutant forms of α-synuclein in transgenic flies (Feany and Bender 2000). Our data shows reduced life span and slower motility in transgenic *C.elegans* strains over-expressing α-synuclein. This could possibly reflect impaired *pdr*-1 (parkin ortholog in *C.elegans*) function, leading to reduction in α-synuclein degradation and hence slower motility and reduced life span, in our transgenic strains. Reduced climbing ability in *Drosophila* and slower motility in *C.elegans* may be caused by muscle degeneration, which is one of the characteristics of PD.

6.3 Detection of α-synuclein using Western blotting

α-synuclein(s) is a 19kD protein and both CFP and YFP are 31 kD proteins. The fusion of CFP and synuclein should yield a protein size of about 47 kD. Likewise, YFP-synuclein should also give rise to a band of about 47 kD in SDS PAGE. We have confirmed that most of the immunoreactive α-synuclein present in both *unc*-54::SC+SV (I) and *unc*-54::SV

(NI) worms is of the CFP-/YFP-tagged fusion-protein size (~47 kD). However, a small proportion of cleaved α-synuclein was also detected whereas the synuclein present in *unc*-54::S+V (I) worms is of the expected untagged 19 kD size. This suggests that cleavage of the fusion proteins is not a major problem in our strains because the majority of α-synuclein protein expressed in the *unc*-54::SC+SV (I) and *unc*-54::SV (NI) strains remains in the CFP-/YFP- tagged fusion form.

Our findings show interesting similarities and differences to a study by McLean et al (2001) where they expressed α-synuclein tagged with EGFP (α-synuclein:EGFP) in primary neurons. Using anti-α-synuclein antibodies directed against the C- terminal of α-synuclein and they found a 49kD α-synuclein fusion protein and truncated 27kD band which is larger than the α-synuclein 19 kD band alone. Probing the blot with anti-GFP antibody (C-terminal) recognized a 16kDa band, suggesting cleavage of EGFP from the α-synuclein:EGFP fusion protein (McLean et al, 2001), so the truncated 27kD protein was in fact a fusion of α-synuclein (19kD) and the N-terminus of EGFP (truncated). This proved that EGFP was cleaved whereas the α-synuclein was not. In our study, there is some evidence that α-synuclein (19kD) may became cleaved from the YFP and/or CFP tags (figure 4.10, lanes 2 and 6) in a

minority of fusion proteins, but there is no evidence for cleavage within the YFP or CFP protein sequence. Overall, cleavage of the fusion proteins appears to be far less of a problem in *C.elegans* (this study) as compared to the mouse primary neuron culture system described by McLean et al (2001).

6.4 FRET measurement in double transgenic *C. elegans* strain (*unc*-54::SC+SV (I))

Our key purpose in creating these double transgenic *C. elegans* strains expressing α-synuclein was to develop a rapid-throughput assay for exploring the role of environmental and genetic factors in promoting α-synuclein aggregation. Measuring FRET signals in the *unc*-54::SC+SV (I) strain could serve as a surrogate indicator of α-synuclein aggregation since FRET is only possible when CFP and YFP moieties are in very close proximity. Using a standard microplate fluorometer the FRET signal was measured in the *unc*-54::SC+SV (I) worms by exciting at a wavelength of 430nm for CFP and measuring emissions at a wavelength of 530nm for YFP. Low FRET signals were observed in the negative control strains (C, V and C+V) and even in the wild type N2 worms, none of which express α-synuclein. By contrast, the positive control expressing both CFP and YFP tags as a fusion protein under the *unc*-54

promoter, showed very high FRET signals due to the molecular proximity of these fluorophores at all times. As expected, the *unc*-54::SC+SV (I) strain showed intermediate FRET signals, because the fluorophores CFP and YFP are brought together only during α-synuclein aggregation. Confocal images of this strain showed the presence of FRET as compared with the control *unc*-54::V (I) strain (Figure 5.5). The relative strength of the FRET signal in these *unc*-54::SC+SV (I) worms should therefore reflect the extent of α-synuclein aggregation.

Previous studies have used FRET as a technique to find protein-protein interaction between synphilin-1 and α−synuclein in human neuroglioma cells (Kawamata et al. 2001). Mutant forms of α-synuclein that are associated with inherited (familial) forms of PD are the A30P and A53T variants. It was found that the C-terminus of synphilin-1 forms stable aggregates with the C-terminus of wild-type α−synuclein, whereas the N-termini of these proteins do not interact strongly (Kawamata et al. 2001). As a result, a high FRET signal was observed with the C-terminus aggregates and much less with the N-terminal aggregates. In addition, in experiments involving mutant forms of α-synuclein, lower FRET signals were observed between the C-terminus of synphilin-1 and C-terminus of A53T α−synuclein. This suggests that the A53T mutation may interfere

in the formation of aggregates with synphilin-1. However, no change in FRET signal was observed between the C-terminus of synphilin-1 and C-terminus of A30P α−synuclein, suggesting no interaction between these two proteins (Kawamata et al. 2001).

Brignull et al. (2006) used *C. elegans* as a model to study polyglutamine expansions and their role in Huntington's disease, by creating transgenic animals showing pan-neuronal (*aex*-3 driven) expression of different lengths of polyglutamine expansions (containing 0, 19, 29, 40, 67, 86 glutamine residues) fused to CFP and/or YFP. *C. elegans* expressing shorter polyQs (e.g. Q19::CFP/YFP) did not produce any FRET signal whereas animals expressing longer polyQs (e.g. Q86::CFP /YFP) produced high FRET signals. FRET data showed insoluble polyglutamine aggregates throughout the nervous system of *C.elegans*, which was also confirmed using confocal images (Brignull et al. 2006). However, none of the above mentioned studies have quantitatively measured the FRET signal. This may be due to the lack of stably integrated forms of the tagged fusion proteins. In our studies, the generation of stably integrated *unc*-54::SC+SV (I) double transgenic strains enables us to measure quantitative FRET signals as an indicator of α−synuclein aggregation .

6.5 Influence of ageing on protein aggregation

During ageing, several physiological parameters such as gene expression, chaperone levels and protein degradation are disturbed (Cuervo and Dice 2000). In addition, ageing also renders the organism more susceptible to oxidative stress, with consequent effects on cellular components such as protein oxidation and nitration leading to protein degradation (Squier 2001). Hence, in neurodegenerative diseases, these changes might lead to or exacerbate protein aggregation during ageing (Balch et al. 2008).

The study of Morley et al (2002) described above (section 6.4) demonstrated that protein aggregates accumulate during ageing. In our experiments, there was a 3-fold increase in FRET signal in *unc*-54::SC+SV (I) worms during early adult life as compared to L4 larvae, whereas in the control NL5901 strain there was only a slight increase in YFP fluorescence. Since this latter takes account of any changes in *unc*-54 expression, we conclude that most of the FRET signal (Figure 5.8) observed during aging in *unc*-54::SC+SV (I) worms is due to α-synuclein aggregation. Confocal images of this strain showed larger and brighter aggregates after several days of adulthood (Figure 5.9). This is in agreement with previous studies and confirms that the ageing process accelerates protein aggregation.

6.6 Effect of RNAi against Hip-1 in *unc*-54:: SC+SV (I) strain

The heat shock protein (Hsp70) is one of the important protein chaperones that play a vital role in PD and protein trafficking generally. This is mainly because of its anti-aggregation functions which help to inhibit protein misfolding (Gragerov et al. 1992). This is supported by experimental evidence; for instance, over-expression of Hsp70 in *Drosophila* was found to prevent α-synuclein aggregation (Auluck et al. 2002), and a similar effect was also observed in neuroglioma cells (Klucken et al. 2004). In support of this evidence, the expression levels of Hsp70 were found to be highly disturbed (up-regulated) in the substantia nigra of Parkinson's patients (Hauser et al. 2005). Hsp70 inhibits protein misfolding by binding to hydrophobic regions and to positively charged amino acids of alpha synuclein (Rudiger et al. 1997a; Rudiger et al. 1997b). If the Hsp70 is ATP-bound then it has a low affinity for α-synuclein. This prevents α-synuclein aggregation and there is no toxic fibril formation. On the other hand, if the Hsp70 is ADP-bound then it has a high affinity for α-synuclein. Hence Hsp70 and α-synuclein co-aggregate resulting in α-synuclein aggregation and toxic fibril formation (Mayer and Bukau 2005; Roodveldt et al. 2009).

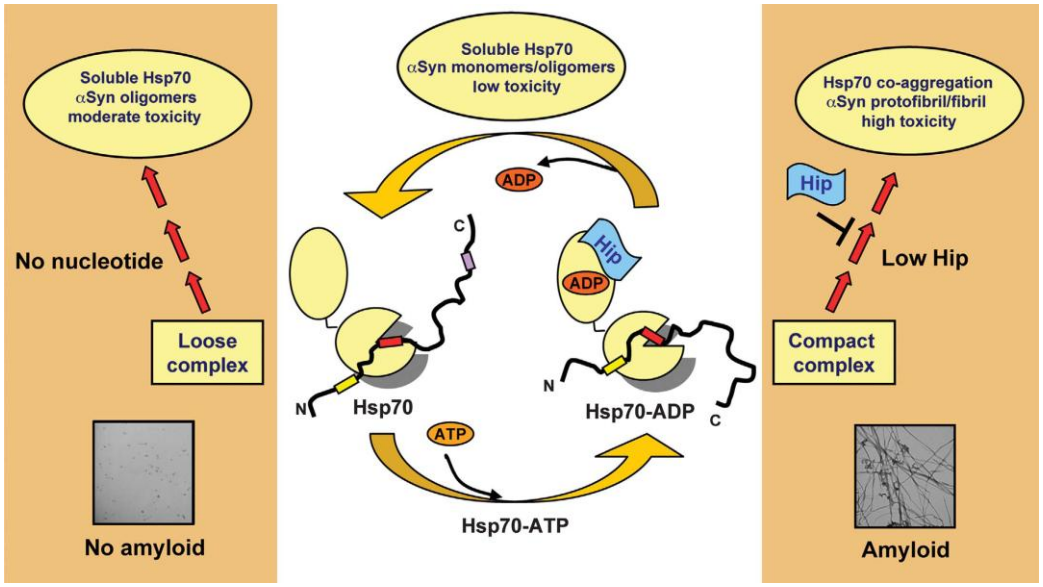

Figure 6.2: **Mechanism of Hsp70/Hip chaperone function in protein aggregation.** (adapted from Roodveldt et al. 2009)
The chaperone protein Hsp70 binds to hydrophobic patches and highly positively charged amino acids on alpha synuclein, producing a loose complex. In this complex, Hsp70 is in an ATP bound state and has a low affinity for binding to alpha synuclein. This prevents alpha synuclein aggregation and toxic fibril formation, resulting in moderate toxicity (left). Hsp70 in the ADP bound state has a higher affinity for alpha synuclein. This reduces the concentration of Hsp70 in solution and, as a consequence, Hsp70 and alpha synuclein co-aggregate enabling alpha synuclein to form toxic amyloid fibrils. To prevent this, Hip, a co-chaperone protein, binds to an ATPase domain on Hsp70 and prolongs the complex between Hsp70 and alpha synuclein, preventing co-aggregation (right). However, Parkinson's patients have reduced Hip and Hsp70 concentration so the Hsp70/alpha synuclein complex is not stabilized, leading to complex co-aggregation and toxic amyloid fibril formation.

The co-chaperone Hip also plays an important role in PD. The pro-amyloid activity of the Hsp70/ α-synuclein complex can be prevented *in vitro* and *in vivo* by the co-chaperone Hip. This is due to the fact that Hip binds to the ATPase domain of Hsp70 and thereby increases the half life of Hsp70/ α-synuclein complex, thus preventing co-aggregation (Hohfeld et al. 1995; Roodveldt et al. 2009). To validate the role of Hip, RNA interference was used to knock down the functions of both the

chaperone Hsp70 and co-chaperone Hip in a *C.elegans* model expressing an SV fusion protein (strain OW40; Roodveldt et al. 2009). Knock down of the chaperone Hsp70 led to a slight increase in the number of protein aggregates, whereas the number of aggregates was significantly increased when the co-chaperone Hip was knocked down (Roodveldt et al. 2009). While Hsp70 may be redundant, Hip function acts upstream and is central to the Hsp70/Hip complex activity. These results provide evidence that there is some kind of interaction between Hsp70 and Hip which is vital for coordinating protein homeostasis.

Our RNAi results for RNAi against the co-chaperone Hip-1 show a similar result, with an increase in the number of α-synuclein aggregates. This was observed as a high FRET signal in the *unc*-54::SC+SV (I) strain, and was also confirmed by confocal microscopy. The effect of RNAi against Hip-1 from L1 onwards was minimal in F1 worms but much greater in their F1 progeny (RNAi over 2 generations), as was also found by Roodveldt et al. (2009). One key advantage of the *unc*-54::SC+SV (I) strain for studying PD is the ease of identifying molecular players involved in the aggregation pathway as measured by the FRET signal. For example, a previous RNAi screening study has identified some common genes involved in polyQ and α-synuclein aggregation (Nollen et al. 2004; van Ham

et al. 2008). Our transgenic PD worm model could be used to test the involvement of these and other candidate genes, where increased FRET signals will indicate the formation of α-synuclein aggregates when gene function is compromised.

6.7 External stressors and Parkinson's disease

6.7.1 Rotenone toxicity and PD

Intravenous exposure to rotenone (a mitochondrial complex I inhibitor) has been shown to cause PD-like symptoms, along with the depletion of dopaminergic neurons. In PD patients, the activity of mitochondrial complex I is suppressed, leading to dopaminergic neuronal cell death. Interestingly, rotenone causes the formation of α-synuclein inclusions as well as subsequent neuronal cell death, a classic feature of PD (Betarbet et al. 2000; Sherer et al. 2003). Betarbet et al. (2000) showed in rats that rotenone exposure had severe effects on mitochondria, which could be related to PD pathogenesis. Since rotenone inhibits mitochondrial complex I, chronic exposure to rotenone may impair the energy production of mitochondria thus reducing the levels of ATP in the cell. As a consequence, the function of ATP-dependant Hsp70 may also be compromised, leading to increased α-synuclein aggregation (figure 6.2). However, there is also a direct effect of rotenone in the absence of other cellular proteins, since rotenone significantly speeds up

the fibrillation of α-synuclein *in vitro* (Uversky et al. 2001; Uversky et al. 2002).

6.7.2 Chlorpyrifos toxicity and PD

Chlorpyrifos is a common organophosphate pesticide used in agriculture as an insecticide. Parkinsonism has been reported in several cases after exposure to organophosphates. This is one line of evidence which suggests that organophosphates may have a role in the pathogenesis of Parkinson's (Bhatt et al. 1999). Organophosphates and other insecticides are thought to be involved in Parkinson's disease based on a case-control study (Hancock et al. 2008). There might be a balance between dopamine and acetylcholine systems in both humans and animal models, but when exposed to organophosphates this balance becomes disturbed potentially leading to Parkinson's disease (Hatcher et al. 2008). Chlorpyrifos is known to have a dose dependent effect on the growth and development of *C.elegans*. Specifically, the early larval stages L2 and L3 were more prone to the effects of chlorpyrifos (Boyd et al. 2009).

Our data shows a 2-fold increase in FRET signal in *unc*-54::SC+SV (I) worms when exposed to the pesticides chlorpyrifos or rotenone. In addition, confocal images of the *unc*-

54::SC+SV (I) strain confirm that the increase in FRET signal was due to the formation of larger and brighter α-synuclein aggregates. When exposed to rotenone, this *unc*-54::SC+SV (I) strain displayed difficulties in egg hatching, growth and development (L1 arrest), whereas chlorpyrifos does not have any such effect. This could imply that rotenone causes a systemic shock to the cell (as a mitochondrial inhibitor) resulting in the impairment of all energy-dependent processes (such as egg hatching, growth and development), whereas the effect of chlorpyrifos (an acetylcholine esterase inhibitor) is mainly limited to the nervous system. Therefore, general functions such as growth and reproduction are not severely compromised by chlorpyrifos, in contrast to rotenone. This may explain why exposure of *unc*-54::SC+SV (I) worms to rotenone not chlorpyrifos caused L1 growth arrest. However, most importantly, both toxins caused α-synuclein aggregation as evidenced by increased FRET signal and confocal microscopy.

The *unc*-54::SC+SV (I) strain should allow us to investigate the role of these and many other potential environmental risk factors for PD, both singly and combined, as promoters of α-synuclein aggregation in larval and young adult worms. Moreover, this strain might be of great use for high-throughput screening of candidate drugs aimed at

identifying agents that could dissociate α-synuclein aggregates or prevent their formation *in vivo* (Kritzer et al. 2009).

6.8 Oxidative stress in Parkinson's disease

In Parkinson's disease, the dopaminergic neurons of the substantial nigra in the brain undergo neurodegenration due to oxidative stress (Dexter et al. 1989). It has been confirmed that there are elevated levels of protein nitration in Lewy bodies (Good et al. 1998). The α-synuclein protein present in the Lewy bodies undergoes nitration of the tyrosine residues (Giasson et al. 2000). The earliest known characteristic of Parkinson's disease is a reduced level of the anti-oxidant glutathione (GSH) in dopaminergic neurons of the substantia nigra (Yong et al. 1986). Moreover, concentrations of iron (a catalyst for oxidative reactions) were found to be elevated in the substantia nigra (Sofic et al. 1991).

Increased protein misfolding may also be associated with the increased oxidative stress characteristic of PD, leading to α-synuclein aggregates accumulates in the substantia nigra, a key feature of neurodegenration in PD. In addition, a reduced level of Hsp induction may also contribute to the increased levels of oxidatively damaged proteins, because increased Hsp70 and Hsp40 expression is known to protect against protein misfolding

(Takeuchi et al. 2002). Oxidative stress not only causes damage to intracellular components but can also trigger programmed cell death. Moreover, reduced levels of glutathione can also induce programmed cell death, which is supported by the fact that glutathione supplements are known to prevent dopamine-dependent neurotoxicity (Stokes et al. 2000).

The mitochondrial complex I inhibitors *N*-methyl-4-phenyl-1,2,3,6-tetrahydropyridine (MPTP) and rotenone cause a reduction of mitochondrial function leading to an increase in oxidative stress in PD (Hensley et al. 1998; German et al. 2000). Exposure of rodents to rotenone also results in α-synuclein aggregates which accumulate in the brain in the form of Lewy bodies (Andersen 2004). These facts imply a link in the sequence of events that causes both oxidative stress and α-synuclein aggregation following rotenone exposure (Sullivan et al. 2004).

Our results show an increase in FRET signal (indicating α-synuclein aggregation) following exposure to both rotenone and chlorpyrifos. It is possible that these chemicals cause oxidative stress as a result of mitochondrial dysfunction, leading to protein misfolding in our experimental model. However,

further assays to measure mitochondrial activity and ROS production are needed in order to confirm this hypothesis.

Therefore we performed the H_2-DCF-DA assay (measurement of ROS production) on the *unc*-54::SC+SV (I) transgenic strain following exposure to rotenone and chlorpyrifos. Remarkably, we only observed a slight increase in DCF fluorescence upon exposure to rotenone, but a 5 fold increase upon exposure to chlorpyrifos. However, using another transgenic strain, NL5901 (which expresses an *unc*-54::α-synuclein:YFP fusion gene; van Ham et al. 2008), there was a significant increase in the production of DCF upon exposure to both pesticides. Therefore, these results support the hypothesis of oxidative damage facilitating protein aggregation in PD. Both NL5901 and our *unc*-54::SC+SV (I) strains might be helpful for examining oxidative stress after exposure to heavy metals and/or pesticides.

The presence of non-soluble cellular inclusions containing aggregated α-synuclein is the neuropathological hallmark of human Parkinson's patients (Spillantini et al. 1997), whereas in a *C.elegans* model expressing α-synuclein only in the dopaminergic neurons, aggregated cytoplasmic inclusions were very rarely found (Lakso et al. 2003). In our *unc*-54::SC+SV

strain and other transgenic worm models for PD (Brignull et al. 2006; van Ham et al. 2008) confocal fluorescent imaging confirms the presence of multiple fluorescent aggregates in the expected tissues where the fusion transgenes are expressed (throughout the body wall muscle or nervous system). However, it remains to be confirmed whether these are fibrillar amyloid aggregates, and *in vitro* experiments using an SV fusion protein suggest that such amyloid fibrils form only very slowly over ~8 days (van Ham et al. 2010). Nevertheless, behavioral, biochemical and other changes in these transgenic synuclein-expressing worm models (Lakso et al. 2003; Vartiainen et al. 2006) have all been attributed to synuclein overexpression. The same is likely to be true for our transgenic strains expressing α-synuclein fusion genes studied here.

Future work

1. Can the SC+SV fusion proteins form fibrillar aggregates in vitro and/or in vivo?
2. Genome wide (van Ham et al. 2008) or targeted (Hamamichi et al 2003) RNA interference screening for genetic modifiers of aggregation (either increasing or decreasing the FRET signal).
3. Screening candidate metals, pesticides and other environmental agents across a wide range of doses for significant effects on α-synuclein aggregation. Preliminary data (Fineberg, Nagarajan & de Pomerai, unpublished) suggest that low doses of mercury are particularly potent at inducing aggregation (increased FRET) in *unc*-54::SC+SV (I) worms.
4. Screening mixtures of such agents using chequerboard assays across a wide concentration range for each agent, looking for additive, antagonistic or (most seriously) synergistic effects on aggregation.
5. Combining RNAi against genetic modifiers of aggregation with exposure to known environmental risk factors (above) to determine whether the latter cause greater aggregation in genetically compromised animals.

6. Screening candidate drugs (in older SC+SV worms) aimed at preventing the formation or encouraging the dissociation of α-synuclein aggregates.
7. Investigation of apoptosis using immunohistochemistry in these fusion strains.
8. RNA interference to achieve both a single knock out of Hsp70 and a double knockout of Hsp70 and/ Hip-1, in terms of α-synuclein aggregation.

Appendix 1

Time (min)	rads	No of P0's for gamma radiation	% of sterility P0	No of F1's Selfed	% of sterility F1
2	1626	35	0%	222	19%
4	3252	46	15%	250	25%
4.5	3659	40	40%	300	43%
6	4878	30	43%	200	49%
7	5691	30	43%	100	48%
9	7317	30	50%	50	38%

Table 1.1 : % sterility in line 1:unc-54::SV (NI) worms

Time (min)	rads	No of P0's for gamma radiation	% of sterility P0	No of F1's Selfed	% of sterility F1
6	4878	30	0%	200	0%
10	8130	30	7%	180	31%
30	24390	30	26%	50	88%

Table 1.2 : % sterility in unc-54::V (I) worms

Time (min)	rads	No of P0's for gamma radiation	% of sterility P0	No of F1's Selfed	% of sterility F1
6	4878	20	0%	200	0%
10	8130	20	3%	200	7%
20	16260	20	10%	180	25%
30	24390	20	35%	50	96%

Table 1.3 : % sterility in N2 worms

Time (min)	rads	No of P0's for gamma radiation	% sterility P0	No of F1's Selfed	% sterility F1
5	4065	20	0%	200	10%
10	8130	30	10%	250	42%
20	16260	20	20%	100	66%
25	20325	20	27%	50	100%
30	24390	20	32%	18	100%

Table 1.4 : % sterility in line 2:unc-54::SV (NI) worms

Time (min)	rads	No of P0's for gamma radiation	% of sterility P0	No of F1's Selfed	% of sterility F1
5	4065	20	0%	200	19%
10	8130	30	4%	200	48%
20	16260	20	12%	200	72%
30	2439	20	28%	100	100%

Table 1.5 : % sterility in line 3:unc-54::SV (NI) worms

Time (min)	rads	No of P0's for gamma radiation	% of sterility P0	No of F1's Selfed	% of sterility F1
5	4065	20	4%	200	26%
10	8130	20	12%	200	40%
20	16260	20	22%	100	82%
30	24390	20	36%	50	100%

Table 1.6 : % sterility in unc-54::S+V (I) worms

Time (min)	rads	No of P0's for gamma radiation	% of sterility P0	No of F1's Selfed	% of sterility F1
5	4065	30	0%	200	5%
10	8130	30	5%	200	23%
20	16260	30	10%	100	73%
30	24390	30	20%	50	100%

Table 1.7 : % sterility in unc-54::SC+SV (I) worms

NO OF WORMS	BROOD SIZE				
	DAY 1	DAY 2	DAY 3	DAY 4	TOTAL
1	142	63	82	9	**296**
2	127	77	68	5	**277**
3	168	55	61	33	**317**
4	71	63	68	7	**209**
5	152	89	57	24	**322**

Table 1.8: Brood size analysis of N2 strain at 15ºC

NO OF WORMS	BROOD SIZE										
	DAY 1		DAY 2		DAY 3		DAY 4		TOTAL		
	F	NF	F	NF	F	NF	F	NF	F	NF	T
1	33	121	27	67	3	9	2	5	63	197	**267**
2	47	88	29	45	6	29	12	5	82	162	**261**
3	31	57	69	103	23	21	9	14	123	181	**327**
4	96	87	41	24	15	26	11	20	152	137	**320**
5	82	142	22	32	13	22	3	7	117	196	**323**
6	28	127	33	61	5	68	9	3	66	256	**334**
7	19	101	38	66	20	39	6	4	77	206	**293**

F- Fluorescent, NF-Non-Fluorescent

Table 1.9: Brood size analysis of non-integrated line2: *unc*-54:: SV (NI) Fusion worms at 15ºC

NO OF WORMS	BROOD SIZE										
	DAY 1		DAY 2		DAY 3		DAY 4		TOTAL		
	F	NF	F	NF	F	NF	F	NF	F	NF	T
1	97	52	82	48	37	16	0	3	216	116	**335**
2	101	56	86	30	20	5	4	1	207	91	**303**
3	66	25	107	39	19	11	7	3	192	75	**277**
4	46	15	62	57	7	2	2	0	115	74	**191**
5	59	43	77	62	33	31	11	5	169	136	**321**
6	87	66	33	30	32	08	15	3	152	104	**274**
7	82	39	71	41	30	25	19	6	183	105	**313**

F- Fluorescent, NF-Non-Fluorescent

Table 1.10: Brood size analysis of non-integrated *unc*-54:: C (NI) Fusion worms at 15ºC

NO OF WORMS	BROOD SIZE				
	DAY 1	**DAY 2**	**DAY 3**	**DAY 4**	**TOTAL**
1	133	82	69	15	**299**
2	123	65	78	9	**275**
3	154	81	42	5	**282**
4	88	75	72	43	**278**
5	165	91	65	3	**324**

Table 1.11: Brood size analysis of *unc*-54:: S+V (I) strain at 15ºC

NO OF WORMS	BROOD SIZE				
	DAY 1	**DAY 2**	**DAY 3**	**DAY 4**	**TOTAL**
1	85	101	93	24	**303**
2	121	78	87	13	**299**
3	111	81	79	6	**277**
4	156	99	66	4	**325**
5	141	77	71	11	**300**

Table 1.12: Brood size analysis of *unc*-54:: SC+SV (I) strain at 15ºC

NO OF WORMS	BROOD SIZE				
	DAY 1	**DAY 2**	**DAY 3**	**DAY 4**	**TOTAL**
1	107	91	89	20	**307**
2	133	106	67	8	**314**
3	95	94	99	2	**290**
4	127	92	77	1	**297**
5	88	110	79	11	**288**

Table 1.13: Brood size analysis of *unc*-54:: C+V (I) strain at 15ºC

NO OF WORMS	BROOD SIZE				
	DAY 1	**DAY 2**	**DAY 3**	**DAY 4**	**TOTAL**
1	77	80	92	32	**281**
2	98	132	64	5	**299**
3	123	91	69	13	**296**
4	101	95	85	21	**302**
5	119	73	61	9	**262**

Table 1.14: Brood size analysis of *unc*-54:: V (I) strain at 15ºC

NO OF WORMS	BROOD SIZE				
	DAY 1	**DAY 2**	**DAY 3**	**DAY 4**	**TOTAL**
1	125	51	90	42	**308**
2	100	97	88	8	**293**
3	143	119	39	16	**317**
4	79	81	87	3	**250**
5	93	83	77	9	**262**

Table 1.15: Brood size analysis of *unc*-54:: CV (I) strain at 15º C.

Appendix 2

2.1 Suppliers

2.1.1 Transgenic organisms

The non-integrated transgenic lines of *C.elegans* were created in David Bell's laboratory at the University of Nottingham, U.K. The fusion constructs were prepared by Jody Winter and David Bell and the microinjection was performed by Ademola Adenle and Declan Brady.

2.1.2 Chemicals

All chemicals were obtained from Sigma Chemicals Ltd., Poole, U.K.

2.2 Laboratory Equipments

- 9cm Petri dishes – Bibby Sterilin Ltd., Staffordshire, U.K.
- Transfer pipettes – Samco Scientific Corporation, San Fernando, U.S.A.
- 50 ml Falcon tubes – Cellstar, Greiner bio-one, Germany.
- Magnetic stirrer – Hanna Instruments, Inc.
- p1000/p20 pipettes – Gilson Pipetman®, France.
- Pipette tips – Sarstedt, Germany.

- 24-well exposure plates – Corning Cell- Wells, Corning Incorporated, U.S.A.
- Light microscope – Leitz Wetzlar, Germany.
- 3.5cm Petri dishes – Nalge Nunc International, Denmark.
- 14cm Petri dishes – Fisher Scientific, U.K.
- 6-well cluster plates - Corning Cell- Wells, Corning Incorporated, U.S.A.
- Fluoremeter – Wallac Victor 1420 Multilabel Counter. PerkinElmer™ Life Sciences, Berkshire, U.K.
- Fluorescence microscope – Olympus Model SZX12
- Greyscale digital camera (mounted on fluorescence microscope) – Model CFW – 1310M, Scion Corporation, Maryland, U.S.A.
- CCD camera software package – Scion Visicapture™
- Gamma cell unit with a ^{137}Caesium source – NORDION international INC.
- Leica TCS SP2 Confocal Laser Scanning Microscope (CLSM).

References

Albert, P. S. and D. L. Riddle (1988). "Mutants of Caenorhabditis-Elegans That Form Dauer-Like Larvae." Developmental Biology **126**(2): 270-293.

Albertson, D. G. and J. N. Thomson (1976). "Pharynx of Caenorhabditis Elegans." Philosophical Transactions of the Royal Society of London Series B-Biological Sciences **275**(938): 299-&.

Allsop, D., J. Mayes, S. Moore, A. Masad and B. J. Tabner (2008). "Metal-dependent generation of reactive oxygen species from amyloid proteins implicated in neurodegenerative disease." Biochemical Society Transactions **36**: 1293-1298.

Altschuler, E. (1999). "Aluminum-containing antacids as a cause of idiopathic Parkinson's disease." Medical Hypotheses **53**(1): 22-23.

Ambros, V. (2000). "Control of developmental timing in Caenorhabditis elegans." Current Opinion in Genetics & Development **10**(4): 428-433.

Andersen, J. K. (2004). "Oxidative stress in neurodegeneration: cause or consequence?" Nature Medicine **10**(7): S18-S25.

Angier, N. (1995). “The beauty of the beastly: new views on the nature of life”. Boston, MA: Houghton Mifflin.

Antony, T., W. Hoyer, D. Cherny, G. Heim, T. M. Jovin and V. Subramaniam (2003). "Cellular polyamines promote the aggregation of alpha-synuclein." Journal of Biological Chemistry **278**(5): 3235-3240.

Auluck, P. K. and N. M. Bonini (2002). "Pharmacological prevention of Parkinson disease in Drosophila." Nature Medicine **8**(11): 1185-1186.

Auluck, P. K., H. Y. E. Chan, J. Q. Trojanowski, V. M. Y. Lee and N. M. Bonini (2002). "Chaperone suppression of alpha-synuclein toxicity in a Drosophila model for Parkinson's disease." Science **295**(5556): 865-868.

Auman, J. T., F. J. Seidler and T. A. Slotkin (2000). "Neonatal chlorpyrifos exposure targets multiple proteins governing the hepatic adenylyl cyclase signaling cascade: implications for neurotoxicity." Developmental Brain Research **121**(1): 19-27.

Balch, W. E., R. I. Morimoto, A. Dillin and J. W. Kelly (2008). "Adapting proteostasis for disease intervention." Science **319**(5865): 916-919.

Baumeister, R. and L. M. Ge (2002). "The worm in us - Caenorhabditis elegans as a model of human disease." Trends in Biotechnology **20**(4): 147-148.

Bender. A., K. J Krishnan, C. M Morris, G. A Taylor, A. K Reeve, R. H Perry, E. Jaros, J. S Hersheson, J. Betts, T. Klopstock,

R. W Taylor and D. M Turnbull (2006). "High levels of mitochondrial DNA deletions in substantia nigra neurons in aging and Parkinson disease." Nature Genetics 38: 515 – 517.

Bernards, A. and I. K. Hariharan (2001). "Of flies and men - studying human disease in Drosophila." Current Opinion in Genetics & Development **11**(3): 274-278.

Berry, C., C. La Vecchia and P. Nicotera (2010). "Paraquat and Parkinson's disease." Cell Death and Differentiation **17**(7): 1115-1125.

Betarbet, R., T. B. Sherer, G. MacKenzie, M. Garcia-Osuna, A. V. Panov and J. T. Greenamyre (2000). "Chronic systemic pesticide exposure reproduces features of Parkinson's disease." Nature Neuroscience **3**(12): 1301-1306.

Bharathi, P. Nagabhushan and K. S. J. Rao (2008). "Mathematical approach to understand the kinetics of alpha-synuclein aggregation: Relevance to Parkinson's disease." Computers in Biology and Medicine **38**(10): 1084-1093.

Bhatt, M. H., M. A. Elias and A. K. Mankodi (1999). "Acute and reversible parkinsonism due to organophosphate pesticide intoxication - Five cases." Neurology **52**(7): 1467-1471.

Bolanowski, M. A., R. L. Russell and L. A. Jacobon (1981). "Quantitative Measures of Aging in the Nematode

Caenorhabditis-Elegans .1. Population and Longitudinal-Studies of 2 Behavioral Parameters." Mechanisms of Ageing and Development **15**(3): 279-295.

Bonifati, V., P. Rizzu, M. J. van Baren, O. Schaap, G. J. Breedveld, E. Krieger, M. C. J. Dekker, F. Squitieri, P. Ibanez, M. Joosse, J. W. van Dongen, N. Vanacore, J. C. van Swieten, A. Brice, G. Meco, C. M. van Duijn, B. A. Oostra and P. Heutink (2003). "Mutations in the DJ-1 gene associated with autosomal recessive early-onset parkinsonism." Science **299**(5604): 256-259.

Boyd, W. A., M. V. Smith, G. E. Kissling, J. R. Rice, D. W. Snyder, C. J. Portier and J. H. Freedman (2009). "Application of a Mathematical Model to Describe the Effects of Chlorpyrifos on Caenorhabditis elegans Development." Plos One **4**(9): -.

Brenner, S. (1974). "Genetics of Caenorhabditis-Elegans." Genetics **77**(1): 71-94.

Brignull, H. R., J. F. Morley, S. M. Garcia and R. I. Morimoto (2006). "Modeling polyglutamine pathogenesis in C-elegans." Amyloid, Prions, and Other Protein Aggregates, Pt B **412**: 256-282.

Canet-Aviles, R. M., M. A. Wilson, D. W. Miller, R. Ahmad, C. McLendon, S. Bandyopadhyay, M. J. Baptista, D. Ringe, G. A. Petsko and M. R. Cookson (2004). "The Parkinson's

disease protein DJ-1 is neuroprotective due to cysteine-sulfinic acid-driven mitochondrial localization." Proceedings of the National Academy of Sciences of the United States of America **101**(24): 9103-9108.

Carrell, R. W. and D. A. Lomas (1997). "Conformational disease." Lancet **350**(9071): 134-138.

Cassada, R. C. and R. L. Russell (1975). "Dauerlarva, a Post-Embryonic Developmental Variant of Nematode Caenorhabditis-Elegans." Developmental Biology **46**(2): 326-342.

Chalfie, M., Y. Tu, G. Euskirchen, W. W. Ward and D. C. Prasher (1994). "Green Fluorescent Protein as a Marker for Gene-Expression." Science **263**(5148): 802-805.

Chen, Z., J. C. Jiang, Z. G. Lin, W. R. Lee, M. E. Baker and S. H. Chang (1993). "Site-Specific Mutagenesis of Drosophila Alcohol-Dehydrogenase - Evidence for Involvement of Tyrosine-152 and Lysine-156 in Catalysis." Biochemistry **32**(13): 3342-3346.

Choi, W., S. Zibaee, R. Jakes, L. C. Serpell, B. Davletov, R. A. Crowther and M. Goedert (2004). "Mutation E46K increases phospholipid binding and assembly into filaments of human alpha-synuclein." Febs Letters **576**(3): 363-368.

Chow, D. K., C. F. Glenn, J. L. Johnston, I. G. Goldberg and C. A. Wolkow (2006). "Sarcopenia in the Caenorhabditis elegans

pharynx correlates with muscle contraction rate over lifespan." Experimental Gerontology **41**(3): 252-260.

Coghill, E. L., A. Hugill, N. Parkinson, C. Davison, P. Glenister, S. Clements, J. Hunter, R. D. Cox and S. D. M. Brown (2002). "A gene-driven approach to the identification of ENU mutants in the mouse." Nature Genetics **30**(3): 255-256.

Consortium, C. e. S. (1998). "Genome sequence of the nematode C-elegans: A platform for investigating biology." Science **282**(5396): 2012-2018.

Coulom, H. and S. Birman (2004). "Chronic exposure to rotenone models sporadic Parkinson's disease in Drosophila melanogaster." Journal of Neuroscience **24**(48): 10993-10998.

Crumpton, T. L., F. J. Seidler and T. A. Slotkin (2000). "Is oxidative stress involved in the developmental neurotoxicity of chlorpyrifos?" Developmental Brain Research **121**(2): 189-195.

Cuervo, A. M. and J. F. Dice (2000). "Age-related decline in chaperone-mediated autophagy." Journal of Biological Chemistry **275**(40): 31505-31513.

Dauer, W. and S. Przedborski (2003). "Parkinson's disease: Mechanisms and models." Neuron **39**(6): 889-909.

Davis, R. J. (2000). "Signal transduction by the JNK group of MAP kinases." Cell **103**(2): 239-252.

Dawson, T. M. and V. L. Dawson (2003). "Molecular pathways of neurodegeneration in Parkinson's disease." Science **302**(5646): 819-822.

Dexter, D. T., C. J. Carter, F. R. Wells, F. Javoyagid, Y. Agid, A. Lees, P. Jenner and C. D. Marsden (1989). "Basal Lipid-Peroxidation in Substantia Nigra Is Increased in Parkinsons-Disease." Journal of Neurochemistry **52**(2): 381-389.

Diamond, S. G., C. H. Markham, M. M. Hoehn, F. H. Mcdowell and M. D. Muenter (1990). "An Examination of Male-Female Differences in Progression and Mortality of Parkinsons-Disease." Neurology **40**(5): 763-766.

Diane, L and G. Iva (1995). "facilitation of lin-12-mediated signalling by sel-12, a *caenorhabditis elegans* S182 Alzheimer's disease gene." Nature **377**: 351-354.

Ding, Q. X., J. J. Lewis, K. M. Strum, E. Dimayuga, A. J. Bruce-Keller, J. C. Dunn and J. N. Keller (2002). "Polyglutamine expansion, protein aggregation, proteasome activity, and neural survival." Journal of Biological Chemistry **277**(16): 13935-13942.

Dobson, C. M. (2003). "Protein folding and misfolding." Nature **426**(6968): 884-890.

Donald, D. L. (Ed.). (1997). "*C. elegans* II. New York, NY: Cold Spring Harbor Laboratory Press".

Drago, D., S. Bolognin and P. Zatta (2008). "Role of Metal Ions in the A beta Oligomerization in Alzheimer's Disease and in Other Neurological Disorders." Current Alzheimer Research **5**(6): 500-507.

Duyao, M., C. Ambrose, R. Myers, A. Novelletto, F. Persichetti, M. Frontali, S. Folstein, C. Ross, M. Franz, M. Abbott, J. Gray, P. Conneally, A. Young, J. Penney, Z. Hollingsworth, I. Shoulson, A. Lazzarini, A. Falek, W. Koroshetz, D. Sax, E. Bird, J. Vonsattel, E. Bonilla, J. Alvir, J. B. Conde, J. H. Cha, L. Dure, F. Gomez, M. Ramos, J. Sanchezramos, S. Snodgrass, M. Deyoung, N. Wexler, C. Moscowitz, G. Penchaszadeh, H. Macfarlane, M. Anderson, B. Jenkins, J. Srinidhi, G. Barnes, J. Gusella and M. Macdonald (1993). "Trinucleotide Repeat Length Instability and Age-of-Onset in Huntingtons-Disease." Nature Genetics **4**(4): 387-392.

Eaton, D. L., R. B. Daroff, H. Autrup, J. Bridges, P. Buffler, L. G. Costa, J. Coyle, G. McKhann, W. C. Mobley, L. Nadel, D. Neubert, R. Schulte-Hermann and P. S. Spencer (2008). "Review of the toxicology of chlorpyrifos with an emphasis on human exposure and neurodevelopment." Critical Reviews in Toxicology **38**: 1-125.

Ebadi, M., S. K. Srinivasan and M. D. Baxi (1996). "Oxidative stress and antioxidant therapy in Parkinson's disease." Progress in Neurobiology **48**(1): 1-19.

Elbashir, S. M., J. Harborth, W. Lendeckel, A. Yalcin, K. Weber and T. Tuschl (2001). "Duplexes of 21-nucleotide RNAs mediate RNA interference in cultured mammalian cells." Nature **411**(6836): 494-498.

Epstein, H. F., R. H. Waterston and S. Brenner (1974). "Mutant Affecting Heavy-Chain of Myosin in Caenorhabditis-Elegans." Journal of Molecular Biology **90**(2): 291-&.

Feany, M. B. and W. W. Bender (2000). "A Drosophila model of Parkinson's disease." Nature **404**(6776): 394-398.

Fernagut, P. O., C. B. Hutson, S. M. Fleming, N. A. Tetreaut, J. Salcedo, E. Masliah and M. F. Chesselet (2007). "Behavioral and histopathological consequences of paraquat intoxication in mice: Effects of alpha-synuclein over-expression." Synapse **61**(12): 991-1001.

Fire, A. (1986). "Integrative Transformation of Caenorhabditis-Elegans." Embo Journal **5**(10): 2673-2680.

Fire, A., S. Q. Xu, M. K. Montgomery, S. A. Kostas, S. E. Driver and C. C. Mello (1998). "Potent and specific genetic interference by double-stranded RNA in Caenorhabditis elegans." Nature **391**(6669): 806-811.

Gallo, M., A. K. Mah, R. C. Johnsen, A. M. Rose and D. L. Baillie (2006). "Caenorhabditis elegans dpy-14: an essential collagen gene with unique expression profile and physiological roles in early development." Molecular Genetics and Genomics **275**(6): 527-539.

Garigan, D., A. L. Hsu, A. G. Fraser, R. S. Kamath, J. Ahringer and C. Kenyon (2002). "Genetic analysis of tissue aging in Caenorhabditis elegans: A role for heat-shock factor and bacterial proliferation." Genetics **161**(3): 1101-1112.

Gerber, I. B and I. A. Dubery (2003). "Fluorescence microplate assay for the detection of oxidative burst products in tobacco cell suspensions using 2',7'-dichlorofluorescein" Methods in Cell Science **25**: 115–122.

German, D. C., C. L. Liang, K. F. Manaye, K. Lane and P. K. Sonsalla (2000). "Pharmacological inactivation of the vesicular monoamine transporter can enhance 1-methyl-4-phenyl-1,2,3,6-tetrahydropyridine-induced neurodegeneration of midbrain dopaminergic neurons, but not locus coeruleus noradrenergic neurons." Neuroscience **101**(4): 1063-1069.

Giasson, B. I., J. E. Duda, I. V. J. Murray, Q. P. Chen, J. M. Souza, H. I. Hurtig, H. Ischiropoulos, J. Q. Trojanowski and V. M. Y. Lee (2000). "Oxidative damage linked to

neurodegeneration by selective alpha-synuclein nitration in synucleinopathy lesions." Science **290**(5493): 985-989.

Goers, J., V. N. Uversky and A. L. Fink (2003). "Polycation-induced oligomerization and accelerated fibrillation of human alpha-synuclein in vitro." Protein Science **12**(4): 702-707.

Good, P. F., A. Hsu, P. Werner, D. P. Perl and C. W. Olanow (1998). "Protein nitration in Parkinson's disease." Journal of Neuropathology and Experimental Neurology **57**(4): 338-342.

Gordon, J. W. and F. H. Ruddle (1981). "Integration and Stable Germ Line Transmission of Genes Injected into Mouse Pronuclei." Science **214**(4526): 1244-1246.

Gorell, J. M., C. C. Johnson, B. A. Rybicki, E. L. Peterson, G. X. Kortsha, G. G. Brown and R. J. Richardson (1999). "Occupational exposure to manganese, copper, lead, iron, mercury and zinc and the risk of Parkinson's disease." Neurotoxicology **20**(2-3): 239-247.

Gossler, A., T. Doetschman, R. Korn, E. Serfling and R. Kemler (1986). "Transgenesis by Means of Blastocyst-Derived Embryonic Stem-Cell Lines." Proceedings of the National Academy of Sciences of the United States of America **83**(23): 9065-9069.

Gotz, J., F. Chen, R. Barmettler and R. M. Nitsch (2001). "Tau filament formation in transgenic mice expressing P301L tau." Journal of Biological Chemistry **276**(1): 529-534.

Gragerov, A., E. Nudler, N. Komissarova, G. A. Gaitanaris, M. E. Gottesman and V. Nikiforov (1992). "Cooperation of Groel/Groes and Dnak/Dnaj Heat-Shock Proteins in Preventing Protein Misfolding in Escherichia-Coli." Proceedings of the National Academy of Sciences of the United States of America **89**(21): 10341-10344.

Greenbaum, E. A., C. L. Graves, A. J. Mishizen-Eberz, M. A. Lupoli, D. R. Lynch, S. W. Englander, P. H. Axelsen and B. I. Giasson (2005). "The E46K mutation in alpha-synuclein increases amyloid fibril formation." Journal of Biological Chemistry **280**(9): 7800-7807.

Greene, J. C., A. J. Whitworth, I. Kuo, L. A. Andrews, M. B. Feany and L. J. Pallanck (2003). "Mitochondrial pathology and apoptotic muscle degeneration in Drosophila parkin mutants." Proceedings of the National Academy of Sciences of the United States of America **100**(7): 4078-4083.

Grishok, A., H. Tabara and C. C. Mello (2000). "Genetic requirements for inheritance of RNAi in C-elegans." Science **287**(5462): 2494-2497.

Guarente, L. and C. Kenyon (2000). "Genetic pathways that regulate ageing in model organisms." Nature **408**(6809): 255-262.

Guo, S. and K. J. Kemphues (1995). "Par-1, a Gene Required for Establishing Polarity in C-Elegans Embryos, Encodes a Putative Ser/Thr Kinase That Is Asymmetrically Distributed." Cell **81**(4): 611-620.

Hancock, D. B., E. R. Martin, G. M. Mayhew, J. M. Stajich, R. Jewett, M. A. Stacy, B. L. Scott, J. M. Vance and W. K. Scott (2008). "Pesticide exposure and risk of Parkinson's disease: A family-based case-control study." Bmc Neurology **8**: -.

Hardy, J., K. Duff, K. G. Hardy, J. Perez-Tur and M. Hutton (1998). "Genetic dissection of Alzheimer's disease and related dementias: Amyloid and its relationship to tau." Nature Neuroscience **1**(5): 355-358.

Hatcher, J. M., K. D. Pennell and G. W. Miller (2008). "Parkinson's disease and pesticides: a toxicological perspective." Trends in Pharmacological Sciences **29**(6): 322-329.

Haun, C., J. Alexander, D. Y. Stainier and P. G. Okkema (1998). "Rescue of Caenorhabditis elegans pharyngeal development by a vertebrate heart specification gene."

Proceedings of the National Academy of Sciences of the United States of America **95**(9): 5072-5075.

Hauser, M. A., Y. J. Li, H. Xu, M. A. Noureddine, Y. S. Shao, S. R. Gullans, C. R. Scherzer, R. V. Jensen, A. C. McLaurin, J. R. Gibson, B. L. Scott, R. M. Jewett, J. E. Stenger, D. E. Schmechel, C. M. Hulette and J. M. Vance (2005). "Expression profiling of substantia nigra in Parkinson disease, progressive supranuclear palsy, and frontotemporal dementia with parkinsonism." Archives of Neurology **62**(6): 917-921.

Hensley, K., Q. N. Pye, M. L. Maidt, C. A. Stewart, K. A. Robinson, F. Jaffrey and R. A. Floyd (1998). "Interaction of alpha-phenyl-N-tert-butyl nitrone and alternative electron acceptors with complex I indicates a substrate reduction site upstream from the rotenone binding site." Journal of Neurochemistry **71**(6): 2549-2557.

Herman, R. K. (1978). "Crossover Suppressors and Balanced Recessive Lethals in Caenorhabditis-Elegans." Genetics **88**(1): 49-65.

Herndon, L. A., P. J. Schmeissner, J. M. Dudaronek, P. A. Brown, K. M. Listner, Y. Sakano, M. C. Paupard, D. H. Hall and M. Driscoll (2002). "Stochastic and genetic factors influence tissue-specific decline in ageing C-elegans." Nature **419**(6909): 808-814.

Hetman, M. and Z. G. Xia (2000). "Signaling pathways mediating anti-apoptotic action of neurotrophins." Acta Neurobiologiae Experimentalis **60**(4): 531-545.

Higuchi, M., T. Ishihara, B. Zhang, M. Hong, A. Andreadis, J. Q. Trojanowski and V. M. Y. Lee (2002). "Transgenic mouse model of tauopathies with glial pathology and nervous system degeneration." Neuron **35**(3): 433-446.

Hirsh, D., D. Oppenheim and M. Klass (1976). "Development of Reproductive-System of Caenorhabditis-Elegans." Developmental Biology **49**(1): 200-219.

Hodgkin, J., H. R. Horvitz and S. Brenner (1979). "Nondisjunction Mutants of the Nematode Caenorhabditis-Elegans." Genetics **91**(1): 67-94.

Hohfeld, J., Y. Minami and F. U. Hartl (1995). "Hip, a Novel Cochaperone Involved in the Eukaryotic Hsc70/Hsp40 Reaction Cycle." Cell **83**(4): 589-598.

Honda, Y. and S. Honda (2002). "Life span extensions associated with upregulation of gene expression of antioxidant enzymes in Caenorhabditis elegans, studies of mutation in the age-1, PI3 kinase homologue and short-term exposure to hyperoxia." Journal of the American Aging Association **25**(1): 21-28.

Horvitz, H. R. (1997). "A nematode as a model organism: the genetics of programmed death" [Film]. Cogito Learning Media, Inc. Available: http://www.cogitomedia.com [1999, Jul 20].

Hosono, R., S. Nishimoto and S. Kuno (1989). "Alterations of Life-Span in the Nematode Caenorhabditis-Elegans under Monoxenic Culture Conditions." Experimental Gerontology **24**(3): 251-264.

Huang, C., C. J. Xiong and K. Kornfeld (2004). "Measurements of age-related changes of physiological processes that predict lifespan of Caenorhabditis elegans." Proceedings of the National Academy of Sciences of the United States of America **101**(21): 8084-8089.

Iijima, K., H. P. Liu, A. S. Chiang, S. A. Hearn, M. Konsolaki and Y. Zhong (2004). "Dissecting the pathological effects of human A beta 40 and A beta 42 in Drosophila: A potential model for Alzheimer's disease." Proceedings of the National Academy of Sciences of the United States of America **101**(17): 6623-6628.

Ishiguro, H., K. Yasuda, N. Ishii, K. Ihara, T. Ohkubo, M. Hiyoshi, K. Ono, N. Senoo-Matsuda, O. Shinohara, F. Yosshii, M. Murakami, P. S. Hartman and M. Tsuda (2001). "Enhancement of oxidative damage to cultured cells and

Caenorhabditis elegans by mitochondrial electron transport inhibitors." Iubmb Life **51**(4): 263-268.

Izant, J. G. and H. Weintraub (1984). "Inhibition of Thymidine Kinase Gene-Expression by Anti-Sense Rna - a Molecular Approach to Genetic-Analysis." Cell **36**(4): 1007-1015.

Jackson, G. R., I. Salecker, X. Z. Dong, X. Yao, N. Arnheim, P. W. Faber, M. E. MacDonald and S. L. Zipursky (1998). "Polyglutamine-expanded human huntingtin transgenes induce degeneration of Drosophila photoreceptor neurons." Neuron **21**(3): 633-642.

Jaenisch, R. (1976). "Germ Line Integration and Mendelian Transmission of Exogenous Moloney Leukemia-Virus." Proceedings of the National Academy of Sciences of the United States of America **73**(4): 1260-1264.

Jenner, P. (1998). "Oxidative mechanisms in nigral cell death in Parkinson's disease." Movement Disorders **13**: 24-34.

Jensen, P. H., K. Islam, J. Kenney, M. S. Nielsen, J. Power and W. P. Gai (2000). "Microtubule-associated protein 1B is a component of cortical Lewy bodies and binds alpha-synuclein filaments." Journal of Biological Chemistry **275**(28): 21500-21507.

Jeske, D. R., H. K. Xu, T. Blessinger, P. Jensen and J. Trumble (2009). "Testing for the Equality of EC50 Values in the Presence of Unequal Slopes With Application to Toxicity of

Selenium Types." Journal of Agricultural Biological and Environmental Statistics **14**(4): 469-483.

Johnstone, D. B., A. G. Wei, A. Butler, L. Salkoff and J. H. Thomas (1997). "Behavioral defects in C-elegans egl-36 mutants result from potassium channels shifted in voltage-dependence of activation." Neuron **19**(1): 151-164.

Kamath, R. S. and J. Ahringer (2003). "Genorne-wide RNAi screening in Caenorhabditis elegans." Methods **30**(4): 313-321.

Kamath, R. S., A. G. Fraser, Y. Dong, G. Poulin, R. Durbin, M. Gotta, A. Kanapin, N. Le Bot, S. Moreno, M. Sohrmann, D. P. Welchman, P. Zipperlen and J. Ahringer (2003). "Systematic functional analysis of the Caenorhabditis elegans genome using RNAi." Nature **421**(6920): 231-237.

Kamel, H. K. (2003). "Sarcopenia and aging." Nutrition Reviews **61**(5): 157-167.

Kanthasamy, A. G., M. Kitazawa, A. Kanthasamy and V. Anantharam (2005). "Dieldrin-induced neurotoxicity: Relevance to Parkinson's disease pathogenesis." Neurotoxicology **26**(4): 701-719.

Karanth, S. and C. Pope (2000). "Carboxylesterase and A-esterase activities during maturation and aging: Relationship to the toxicity of chlorpyrifos and parathion in rats." Toxicological Sciences **58**(2): 282-289.

Karpuj, M. V., H. Garren, H. Slunt, D. L. Price, J. Gusella, M. W. Becher and L. Steinman (1999). "Transglutaminase aggregates huntingtin into nonamyloidogenic polymers, and its enzymatic activity increases in Huntington's disease brain nuclei." Proceedings of the National Academy of Sciences of the United States of America **96**(13): 7388-7393.

Kawamata, H., P. J. McLean, N. Sharma and B. T. Hyman (2001). "Interaction of alpha-synuclein and synphilin-1: effect of Parkinson's disease-associated mutations." Journal of Neurochemistry **77**(3): 929-934.

Kayed, R., E. Head, J. L. Thompson, T. M. McIntire, S. C. Milton, C. W. Cotman and C. G. Glabe (2003). "Common structure of soluble amyloid oligomers implies common mechanism of pathogenesis." Science **300**(5618): 486-489.

Kenyon, C. J. (2010). "The genetics of ageing." Nature **464**(7288): 504-512.

Keston, A. S. and R. Brandt (1965). "Fluorometric Analysis of Ultramicro Quantities of Hydrogen Peroxide." Analytical Biochemistry **11**(1): 1-&.

Khurana, R., C. Coleman, C. Ionescu-Zanetti, S. A. Carter, V. Krishna, R. K. Grover, R. Roy and S. Singh (2005). "Mechanism of thioflavin T binding to amyloid fibrils." Journal of Structural Biology **151**(3): 229-238.

Kitada, T., S. Asakawa, N. Hattori, H. Matsumine, Y. Yamamura, S. Minoshima, M. Yokochi, Y. Mizuno and N. Shimizu (1998). "Mutations in the parkin gene cause autosomal recessive juvenile parkinsonism." Nature **392**(6676): 605-608.

Klass, M. and D. Hirsh (1976). "Non-Aging Developmental Variant of Caenorhabditis-Elegans." Nature **260**(5551): 523-525.

Klass, M. R. (1977). "Aging in Nematode Caenorhabditis-Elegans - Major Biological and Environmental-Factors Influencing Life-Span." Mechanisms of Ageing and Development **6**(6): 413-429.

Klawans, H. L., R. W. Stein, C. M. Tanner and C. G. Goetz (1982). "A Pure Parkinsonian Syndrome Following Acute Carbon-Monoxide Intoxication." Archives of Neurology **39**(5): 302-304.

Klucken, J., Y. Shin, E. Masliah, B. T. Hyman and P. J. McLean (2004). "Hsp70 reduces alpha-synuclein aggregation and toxicity." Journal of Biological Chemistry **279**(24): 25497-25502.

Kopito, R. R. and D. Ron (2000). "Conformational disease." Nature Cell Biology **2**(11): E207-E209.

Kraytsberg. Y, E. Kudryavtseva, A. C McKee, C. Geula, N. W Kowall and K. Khrapko (2006). "Mitochondrial DNA

deletions are abundant and cause functional impairment in aged human substantia nigra neurons." Nature Genetics 38: 518 – 520.

Kritzer, J. A., S. Hamamichi, J. M. McCaffery, S. Santagata, T. A. Naumann, K. A. Caldwell, G. A. Caldwell and S. Lindquist (2009). "Rapid selection of cyclic peptides that reduce alpha-synuclein toxicity in yeast and animal models." Nature Chemical Biology **5**(9): 655-663.

Kruger, R., W. Kuhn, T. Muller, D. Woitalla, M. Graeber, S. Kosel, H. Przuntek, J. T. Epplen, L. Schols and O. Riess (1998). "Ala30Pro mutation in the gene encoding alpha-synuclein in Parkinson's disease." Nature Genetics **18**(2): 106-108.

Kuwahara, T., A. Koyama, K. Gengyo-Ando, M. Masuda, H. Kowa, M. Tsunoda, S. Mitani and T. Iwatsubo (2006). "Familial Parkinson mutant alpha-synuclein causes dopamine neuron dysfunction in transgenic Caenorhabditis elegans." Journal of Biological Chemistry **281**(1): 334-340.

Lai, C. H., C. Y. Chou, L. Y. Ch'ang, C. S. Liu and W. C. Lin (2000). "Identification of novel human genes evolutionarily conserved in Caenorhabditis elegans by comparative proteomics." Genome Research **10**(5): 703-713.

Lakowski, B. and S. Hekimi (1998). "The genetics of caloric restriction in Caenorhabditis elegans." Proceedings of the National Academy of Sciences of the United States of America **95**(22): 13091-13096.

Lakso, M., S. Vartiainen, A. M. Moilanen, J. Sirvio, J. H. Thomas, R. Nass, R. D. Blakely and G. Wong (2003). "Dopaminergic neuronal loss and motor deficits in Caenorhabditis elegans overexpressing human alpha-synuclein." Journal of Neurochemistry **86**(1): 165-172.

Lang, A. E. and A. M. Lozano (1998). "Parkinson's disease - Second of two parts." New England Journal of Medicine **339**(16): 1130-1143.

Langston, J. W. and P. A. Ballard (1983). "Parkinsons-Disease in a Chemist Working with 1-Methyl-4-Phenyl-1,2,5,6-Tetrahydropyridine." New England Journal of Medicine **309**(5): 310-310.

Lee, M. K., W. Stirling, Y. Q. Xu, X. Y. Xu, D. Qui, A. S. Mandir, T. M. Dawson, N. G. Copeland, N. A. Jenkins and D. L. Price (2002). "Human alpha-synuclein-harboring familial Parkinson's disease-linked Ala-53 -> Thr mutation causes neurodegenerative disease with alpha-synuclein aggregation in transgenic mice." Proceedings of the National Academy of Sciences of the United States of America **99**(13): 8968-8973.

Lehner, B., Fraser, A.G., Sanderson,C.M (2004). "How to use RNA interference: Briefings in functional" genomics and proteomics, **3**: 68–83.

Lennon, S. V., S. J. Martin and T. G. Cotter (1991). "Dose-Dependent Induction of Apoptosis in Human Tumor-Cell Lines by Widely Diverging Stimuli." Cell Proliferation **24**(2): 203-214.

Leung, M. C. K., P. L. Williams, A. Benedetto, C. Au, K. J. Helmcke, M. Aschner and J. N. Meyer (2008). "Caenorhabditis elegans: An emerging model in biomedical and environmental toxicology." Toxicological Sciences **106**(1): 5-28.

Lewis, J. (2000). "Neurofibrillary tangles, amyotrophy and progressive motor disturbance in mice expressing mutant (P301L) tau protein (vol 25, pg 402, 2000)." Nature Genetics **26**(1): 127-127.

Li, J., V. N. Uversky and A. L. Fink (2001). "Effect of familial Parkinson's disease point mutations A30P and A53T on the structural properties, aggregation, and fibrillation of human alpha-synuclein." Biochemistry **40**(38): 11604-11613.

Link, C. D. (1995). "Expression of Human Beta-Amyloid Peptide in Transgenic Caenorhabditis-Elegans." Proceedings of the

National Academy of Sciences of the United States of America **92**(20): 9368-9372.

Link, C. D., C. J. Johnson, V. Fonte, M. C. Paupard, D. H. Hall, S. Styren, C. A. Mathis and W. E. Klunk (2001). "Visualization of fibrillar amyloid deposits in living, transgenic Caenorhabditis elegans animals using the sensitive amyloid dye, X-34." Neurobiology of Aging **22**(2): 217-226.

Maeda, I., Y. Kohara, M. Yamamoto and A. Sugimoto (2001). "Large-scale analysis of gene function in Caenorhabditis elegans by high-throughput RNAi." Current Biology **11**(3): 171-176.

Mangiarini, L., K. Sathasivam, M. Seller, B. Cozens, A. Harper, C. Hetherington, M. Lawton, Y. Trottier, H. Lehrach, S. W. Davies and G. P. Bates (1996). "Exon 1 of the HD gene with an expanded CAG repeat is sufficient to cause a progressive neurological phenotype in transgenic mice." Cell **87**(3): 493-506.

Manning-Bog, A. B., A. L. McCormack, J. Li, V. N. Uversky, A. L. Fink and D. A. Di Monte (2002). "The herbicide paraquat causes up-regulation and aggregation of alpha-synuclein in mice - Paraquat and alpha-synuclein." Journal of Biological Chemistry **277**(3): 1641-1644.

Maupas E (1900). "Modes et formes de reproduction des nematodes." Arch Zool Exp Gen **8**:463-624.

Marsh, J. L. and L. M. Thompson (2004). "Can flies help humans treat neurodegenerative diseases?" Bioessays **26**(5): 485-496.

Marttila, R. J. and U. K. Rinne (1991). "Progression and Survival in Parkinsons-Disease." Acta Neurologica Scandinavica **84**: 24-28.

Martyn, C. and C. Gale (2003). "Tobacco, coffee, and Parkinson's disease - Caffeine and nicotine may improve the health of dopaminergic systems." British Medical Journal **326**(7389): 561-562.

Mayer, M. P. and B. Bukau (2005). "Hsp70 chaperones: Cellular functions and molecular mechanism." Cellular and Molecular Life Sciences **62**(6): 670-684.

McCormack, A. L., M. Thiruchelvam, A. B. Manning-Bog, C. Thiffault, J. W. Langston, D. A. Cory-Slechta and D. A. Di Monte (2002). "Environmental risk factors and Parkinson's disease: Selective degeneration of nigral dopaminergic neurons caused by the herbicide paraquat." Neurobiology of Disease **10**(2): 119-127.

McLean, P. J., H. Kawamata and B. T. Hyman (2001). "alpha-synuclein-enhanced green fluorescent protein fusion

proteins form proteasome sensitive inclusions in primary neurons." Neuroscience **104**(3): 901-912.

Mello, C. and A. Fire (1995). "DNA transformation." Methods in Cell Biology, Vol 48 **48**: 451-482.

Mello, C. C., J. M. Kramer, D. Stinchcomb and V. Ambros (1991). "Efficient Gene-Transfer in C-Elegans - Extrachromosomal Maintenance and Integration of Transforming Sequences." Embo Journal **10**(12): 3959-3970.

Meneely, P. M. and R. K. Herman (1979). "Lethals, Steriles and Deficiencies in a Region of the X-Chromosome of Caenorhabditis-Elegans." Genetics **92**(1): 99-115.

Miyawaki, A. (2003). "Visualization of the spatial and temporal dynamics of intracellular signaling." Developmental Cell **4**(3): 295-305.

Miyawaki, A. and R. Y. Tsien (2000). "Monitoring protein conformations and interactions by fluorescence resonance energy transfer between mutants of green fluorescent protein." Applications of Chimeric Genes and Hybrid Proteins Pt B **327**: 472-500.

Montgomery, M. K., S. Q. Xu and A. Fire (1998). "RNA as a target of double-stranded RNA-mediated genetic interference in Caenorhabditis elegans." Proceedings of the National Academy of Sciences of the United States of America **95**(26): 15502-15507.

Morley, J. F., H. R. Brignull, J. J. Weyers and R. I. Morimoto (2002). "The threshold for polyglutamine-expansion protein aggregation and cellular toxicity is dynamic and influenced by aging in Caenorhabditis elegans." Proceedings of the National Academy of Sciences of the United States of America **99**(16): 10417-10422.

Mouradian, M. M. (2002). "Recent advances in the genetics and pathogenesis of Parkinson disease." Neurology **58**(2): 179-185.

Munoz, E., R. Oliva, V. Obach, M. J. Marti, P. Pastor, F. Ballesta and E. Tolosa (1997). "Identification of Spanish familial Parkinson's disease and screening for the Ala53Thr mutation of the alpha-synuclein gene in early onset patients." Neuroscience Letters **235**(1-2): 57-60.

Mutwakil, M. H. A. Z., T. J. G. Steele, K. C. Lowe and D. I. dePomerai (1997). "Surfactant stimulation of growth in the nematode Caenorhabditis elegans." Enzyme and Microbial Technology **20**(6): 462-470.

Narendra, D., A. Tanaka, D. F. Suen and R. J. Youle (2008). "Parkin is recruited selectively to impaired mitochondria and promotes their autophagy." Journal of Cell Biology **183**(5): 795-803.

Narendra, D. P., S. M. Jin, A. Tanaka, D. F. Suen, C. A. Gautier, J. Shen, M. R. Cookson and R. J. Youle (2010). "PINK1 Is

Selectively Stabilized on Impaired Mitochondria to Activate Parkin." Plos Biology **8**(1): -.

Nollen, E. A. A., S. M. Garcia, G. van Haaften, S. Kim, A. Chavez, R. I. Morimoto and R. H. A. Plasterk (2004). "Genome-wide RNA interference screen identifies previously undescribed regulators of polyglutamine aggregation." Proceedings of the National Academy of Sciences of the United States of America **101**(17): 6403-6408.

Oddo, S., A. Caccamo, J. D. Shepherd, M. P. Murphy, T. E. Golde, R. Kayed, R. Metherate, M. P. Mattson, Y. Akbari and F. M. LaFerla (2003). "Triple-transgenic model of Alzheimer's disease with plaques and tangles: Intracellular A beta and synaptic dysfunction." Neuron **39**(3): 409-421.

Ozgocmen, S., H. Ozyurt, S. Sogut and O. Akyol (2006). "Current concepts in the pathophysiology of fibromyalgia: the potential role of oxidative stress and nitric oxide." Rheumatology International **26**(7): 585-597.

Pandey, N., R. E. Schmidt and J. E. Galvin (2006). "The alpha-synuclein mutation E46K promotes aggregation in cultured cells." Experimental Neurology **197**(2): 515-520.

Parkinson, J. (1922). "An essay on the shaking palsy." Archives of Neurology and Psychiatry **7**(6): 683-710.

Polymeropoulos, M. H., C. Lavedan, E. Leroy, S. E. Ide, A. Dehejia, A. Dutra, B. Pike, H. Root, J. Rubenstein, R. Boyer, E. S. Stenroos, S. Chandrasekharappa, A. Athanassiadou, T. Papapetropoulos, W. G. Johnson, A. M. Lazzarini, R. C. Duvoisin, G. DiIorio, L. I. Golbe and R. L. Nussbaum (1997). "Mutation in the alpha-synuclein gene identified in families with Parkinson's disease." Science **276**(5321): 2045-2047.

Reinhart, B. J. and G. Ruvkun (2001). "Isoform-specific mutations in the Caenorhabditis elegans heterochronic gene lin-14 affect stage-specific patterning." Genetics **157**(1): 199-209.

Richardson, H. and S. Kumar (2002). "Death to flies: Drosophila as a model system to study programmed cell death." Journal of Immunological Methods **265**(1-2): 21-38.

Rocheleau, C. E., W. D. Downs, R. L. Lin, C. Wittmann, Y. X. Bei, Y. H. Cha, M. Ali, J. R. Priess and C. C. Mello (1997). "Wnt signaling and an APC-related gene specify endoderm in early C-elegans embryos." Cell **90**(4): 707-716.

Roodveldt, C., C. W. Bertoncini, A. Andersson, A. T. van der Goot, S. T. Hsu, R. Fernandez-Montesinos, J. de Jong, T. J. van Ham, E. A. Nollen, D. Pozo, J. Christodoulou and C. M. Dobson (2009). "Chaperone proteostasis in Parkinson's

disease: stabilization of the Hsp70/alpha-synuclein complex by Hip." Embo Journal **28**(23): 3758-3770.

Rosenbluth, R. E., C. Cuddeford and D. L. Baillie (1983). "Mutagenesis in Caenorhabditis-Elegans .1. A Rapid Eukaryotic Mutagen Test System Using the Reciprocal Translocation, Eti(Iii-V)." Mutation Research **110**(1): 39-48.

Rosenbluth, R. E., C. Cuddeford and D. L. Baillie (1985). "Mutagenesis in Caenorhabditis-Elegans .2. A Spectrum of Mutational Events Induced with 1500-R of Gamma-Radiation." Genetics **109**(3): 493-511.

Rosenkranz, A. R., S. Schmaldienst, K. M. Stuhlmeier, W. J. Chen, W. Knapp and G. J. Zlabinger (1992). "A Microplate Assay for the Detection of Oxidative Products Using 2',7'-Dichlorofluorescin-Diacetate." Journal of Immunological Methods **156**(1): 39-45.

Ross, C. A. (2002). "Polyglutamine pathogenesis: Emergence of unifying mechanisms for Huntington's disease and related disorders." Neuron **35**(5): 819-822.

Ross, G. W., R. D. Abbott, H. Petrovitch, D. M. Morens, A. Grandinetti, K. H. Tung, C. M. Tanner, K. H. Masaki, P. L. Blanchette, J. D. Curb, J. S. Popper and L. R. White (2000). "Association of coffee and caffeine intake with the

risk of Parkinson disease." Jama-Journal of the American Medical Association **283**(20): 2674-2679.

Ross, G. W. and H. Petrovitch (2001). "Current evidence for neuroprotective effects of nicotine and caffeine against Parkinson's disease." Drugs & Aging **18**(11): 797-806.

Rubinsztein, D. C., J. Leggo, R. Coles, E. Almqvist, V. Biancalana, J. J. Cassiman, K. Chotai, M. Connarty, D. Craufurd, A. Curtis, D. Curtis, M. J. Davidson, A. M. Differ, C. Dode, A. Dodge, M. Frontali, N. G. Ranen, O. C. Stine, M. Sherr, M. H. Abbott, M. L. Franz, C. A. Graham, P. S. Harper, J. C. Hedreen, A. Jackson, J. C. Kaplan, M. Losekoot, J. C. MacMillan, P. Morrison, Y. Trottier, A. Novelletto, S. A. Simpson, J. Theilmann, J. L. Whittaker, S. E. Folstein, C. A. Ross and M. R. Hayden (1996). "Phenotypic characterization of individuals with 30-40 CAG repeats in the Huntington disease (HD) gene reveals HD cases with 36 repeats and apparently normal elderly individuals with 36-39 repeats." American Journal of Human Genetics **59**(1): 16-22.

Rudiger, S., A. Buchberger and B. Bukau (1997a). "Interaction of Hsp70 chaperones with substrates." Nature Structural Biology **4**(5): 342-349.

Rudiger, S., L. Germeroth, J. SchneiderMergener and B. Bukau (1997b). "Substrate specificity of the DnaK chaperone

determined by screening cellulose-bound peptide libraries." Embo Journal **16**(7): 1501-1507.

Ryu, J., K. Girigoswami, C. Ha, S. H. Ku and C. B. Park (2008). "Influence of multiple metal ions on beta-amyloid aggregation and dissociation on a solid surface." Biochemistry **47**(19): 5328-5335.

Sathasivam, K., I. Amaechi, L. Mangiarini and G. Bates (1997). "Identification of an HD patient with a (CAG)(180) repeat expansion and the propagation of highly expanded CAG repeats in lambda phage." Human Genetics **99**(5): 692-695.

Satyal, S. H., E. Schmidt, K. Kitagawa, N. Sondheimer, S. Lindquist, J. M. Kramer and R. I. Morimoto (2000). "Polyglutamine aggregates alter protein folding homeostasis in Caenorhabditis elegans." Proceedings of the National Academy of Sciences of the United States of America **97**(11): 5750-5755.

Schuler, F. and J. E. Casida (2001). "Functional coupling of PSST and ND1 subunits in NADH : ubiquinone oxidoreductase established by photoaffinity labeling." Biochimica Et Biophysica Acta-Bioenergetics **1506**(1): 79-87.

Selkoe, D. J. (2001). "Presenilin, Notch, and the genesis and treatment of Alzheimer's disease." Proceedings of the

National Academy of Sciences of the United States of America **98**(20): 11039-11041.

Seydoux, G. and A. Fire (1994). "Soma-Germline Asymmetry in the Distributions of Embryonic Rnas in Caenorhabditis-Elegans." Development **120**(10): 2823-2834.

Sharon, R., I. Bar-Joseph, G. E. Mirick, C. N. Serhan and D. J. Selkoe (2003). "Altered fatty acid composition of dopaminergic neurons expressing alpha-synuclein and human brains with alpha-synucleinopathies." Journal of Biological Chemistry **278**(50): 49874-49881.

Sherer, T. B., J. H. Kim, R. Betarbet and J. T. Greenamyre (2003). "Subcutaneous rotenone exposure causes highly selective dopaminergic degeneration and alpha-synuclein aggregation." Experimental Neurology **179**(1): 9-16.

Sherman, J. D. (1996). "Chlorpyrifos (Dursban) - Associated birth defects: Report of four cases." Archives of Environmental Health **51**(1): 5-8.

Shimura, H., M. C. Schlossmacher, N. Hattori, M. P. Frosch, A. Trockenbacher, R. Schneider, Y. Mizuno, K. S. Kosik and D. J. Selkoe (2001). "Ubiquitination of a new form of alpha-synuclein by parkin from human brain: Implications for Parkinson's disease." Science **293**(5528): 263-269.

Silvestri, L., V. Caputo, E. Bellacchio, L. Atorino, B. Dallapiccola, E. M. Valente and G. Casari (2005). "Mitochondrial import

and enzymatic activity of PINK1 mutants associated to recessive parkinsonism." Human Molecular Genetics **14**(22): 3477-3492.

Skinner, P. J., B. T. Koshy, C. J. Cummings, I. A. Klement, K. Helin, A. Servadio, H. Y. Zoghbi and H. T. Orr (1997). "Ataxin-1 with an expanded glutamine tract alters nuclear matrix-associated structures." Nature **389**(6654): 971-974.

Slotkin, T. A. (2004). "Cholinergic systems in brain development and disruption by neurotoxicants: nicotine, environmental tobacco smoke, organophosphates." Toxicology and Applied Pharmacology **198**(2): 132-151.

Smegal, D. C. (2000) "Human Health Risk Assessment Chlorpyrifos"; U.S. Environmental Protection Agency, Office of Prevention, Pesticides and Toxic Substances, Office of Pesticide Programs, Health Effects Division, U.S. Government Printing Office: Washington, DC, 2000; pp 1-131.

Sofic, E., W. Paulus, K. Jellinger, P. Riederer and M. B. H. Youdim (1991). "Selective Increase of Iron in Substantia-Nigra Zona Compacta of Parkinsonian Brains." Journal of Neurochemistry **56**(3): 978-982.

Sommer, B., S. Barbieri, K. Hofele, K. H. Wiederhold, A. Probst, C. Mistl, S. Danner, S. Kauffmann, W. Spooren, M. Tolnay,

G. Bilbe, H. van der Putten, S. Kafmann, P. Caromi and M. A. Ruegg (2000). "Mouse models of alpha-synucleinopathy and Lewy pathology." Experimental Gerontology **35**(9-10): 1389-1403.

Spillantini, M. G., M. L. Schmidt, V. M. Y. Lee, J. Q. Trojanowski, R. Jakes and M. Goedert (1997). "alpha-synuclein in Lewy bodies." Nature **388**(6645): 839-840.

Squier, T. C. (2001). "Oxidative stress and protein aggregation during biological aging." Experimental Gerontology **36**(9): 1539-1550.

Stokes, A. H., D. Y. Lewis, L. H. Lash, W. G. Jerome, K. W. Grant, M. Aschner and K. E. Vrana (2000). "Dopamine toxicity in neuroblastoma cells: role of glutathione depletion by L-BSO and apoptosis." Brain Research **858**(1): 1-8.

Sugimoto, A. (2004). "High-throughput RNAi in Caenorhabditis elegans: genome-wide screens and functional genomics." Differentiation **72**(2-3): 81-91.

Sullivan, P. G., N. B. Dragicevic, J. H. Deng, Y. D. Bai, E. Dimayuga, Q. X. Ding, Q. H. Chen, A. J. Bruce-Keller and J. N. Keller (2004). "Proteasome inhibition alters neural mitochondrial homeostasis and mitochondria turnover." Journal of Biological Chemistry **279**(20): 20699-20707.

Sulston, J. E. and H. R. Horvitz (1977). "Post-Embryonic Cell Lineages of Nematode, Caenorhabditis-Elegans." Developmental Biology **56**(1): 110-156.

Sulston, J. E., E. Schierenberg, J. G. White and J. N. Thomson (1983). "The Embryonic-Cell Lineage of the Nematode Caenorhabditis-Elegans." Developmental Biology **100**(1): 64-119.

Sun, F., V. Anantharam, C. Latchoumycandane, A. Kanthasamy and A. G. Kanthasamy (2005). "Dieldrin induces ubiquitin-proteasome dysfunction in alpha-synuclein overexpressing dopaminergic neuronal cells and enhances susceptibility to apoptotic cell death." Journal of Pharmacology and Experimental Therapeutics **315**(1): 69-79.

Tabara, H., A. Grishok and C. C. Mello (1998). "RNAi in C-elegans: Soaking in the genome sequence." Science **282**(5388): 430-431.

Tabara, H., M. Sarkissian, W. G. Kelly, J. Fleenor, A. Grishok, L. Timmons, A. Fire and C. C. Mello (1999). "The rde-1 gene, RNA interference, and transposon silencing in C-elegans." Cell **99**(2): 123-132.

Takeshi, I (2004). "The γ-secretase complex: machinery for intramembrane proteolysis." Current Opinion in Neurobiology **14**:379–383.

Takeuchi, H., Y. Kobayashi, T. Yoshihara, J. Niwa, M. Doyu, K. Ohtsuka and G. Sobue (2002). "Hsp70 and Hsp40 improve neurite outgrowth and suppress intracytoplasmic aggregate formation in cultured neuronal cells expressing mutant SOD1." Brain Research **949**(1-2): 11-22.

Talpade, D. J., J. G. Greene, D. S. Higgins and J. T. Greenamyre (2000). "In vivo labeling of mitochondrial complex I (NADH : ubiquinone oxidoreductase) in rat brain using [H-3]dihydrorotenone." Journal of Neurochemistry **75**(6): 2611-2621.

Tanner, C. M. (1989). "The Role of Environmental Toxins in the Etiology of Parkinsons-Disease." Trends in Neurosciences **12**(2): 49-54.

Temussi, P. A., L. Masino and A. Pastore (2003). "From Alzheimer to Huntington: why is a structural understanding so difficult?" Embo Journal **22**(3): 355-361.

Thompson, A. J. and C. J. Barrow (2002). "Protein conformational misfolding and amyloid formation: Characteristics of a new class of disorders that include Alzheimer's and prion diseases." Current Medicinal Chemistry **9**(19): 1751-1762.

Tofaris, G. K. and M. G. Spillantini (2005). "Alpha-Synuclein dysfunction in Lewy body diseases." Movement Disorders **20**: S37-S44.

Tuschl, T., P. D. Zamore, R. Lehmann, D. P. Bartel and P. A. Sharp (1999). "Targeted mRNA degradation by double-stranded RNA in vitro." Genes & Development **13**(24): 3191-3197.

Uitti, R. J., B. J. Snow, H. Shinotoh, F. J. G. Vingerhoets, M. Hayward, S. Hashimoto, J. Richmond, S. P. Markey, C. J. Markey and D. B. Calne (1994). "Parkinsonism Induced by Solvent Abuse." Annals of Neurology **35**(5): 616-619.

Uversky, V. N. (2004). "Neurotoxicant-induced animal models of Parkinson's disease: understanding the role of rotenone, maneb and paraquat in neurodegeneration." Cell and Tissue Research **318**(1): 225-241.

Uversky, V. N., J. Li, K. Bower and A. L. Fink (2002). "Synergistic effects of pesticides and metals on the fibrillation of alpha-synuclein: Implications for Parkinson's disease." Neurotoxicology **23**(4-5): 527-536.

Uversky, V. N., J. Li and A. L. Fink (2001). "Metal-triggered structural transformations, aggregation, and fibrillation of human alpha-synuclein - A possible molecular link between Parkinson's disease and heavy metal exposure." Journal of Biological Chemistry **276**(47): 44284-44296.

Uversky, V. N., J. Li and A. L. Fink (2001). "Pesticides directly accelerate the rate of alpha-synuclein fibril formation: a

possible factor in Parkinson's disease." Febs Letters **500**(3): 105-108.

van der Putten, H., K. H. Wiederhold, A. Probst, S. Barbieri, C. Mistl, S. Danner, S. Kauffmann, K. Hofele, W. P. J. M. Spooren, M. A. Ruegg, S. Lin, P. Caroni, B. Sommer, M. Tolnay and G. Bilbe (2000). "Neuropathology in mice expressing human alpha-synuclein." Journal of Neuroscience **20**(16): 6021-6029.

van Ham, T., K. Thijssen, R. Breitling, R. Hofstra, R. Plasterk and E. Nollen (2008). "Identification of modifiers of alpha-synuclein inclusion in a C. elegans model by genome-wide RNAi." Parkinsonism & Related Disorders **13**: S125-S125.

van Ham, T. J., A. Esposito, J. R. Kumita, S. T. D. Hsu, G. S. K. Schierle, C. F. Kaminsk, C. M. Dobson, E. A. A. Nollen and C. W. Bertoncini (2010). "Towards Multiparametric Fluorescent Imaging of Amyloid Formation: Studies of a YFP Model of alpha-Synuclein Aggregation." Journal of Molecular Biology **395**(3): 627-642.

Vartiainen, S., V. Aarnio, M. Lakso and G. Wong (2006). "Increased lifespan in transgenic Caenorhabditis elegans overexpressing human alpha-synuclein." Experimental Gerontology **41**(9): 871-876.

Ved, R., S. Saha, B. Westlund, C. Perier, L. Burnam, A. Sluder, M. Hoener, C. M. P. Rodrigues, A. Alfonso, C. Steer, L. Liu,

S. Przedborski and B. Wolozin (2005). "Similar patterns of mitochondrial vulnerability and rescue induced by genetic modification of alpha-synuclein, parkin, and DJ-1 in Caenorhabditis elegans." Journal of Biological Chemistry **280**(52): 42655-42668.

Walker, G., K. Houthoofd, J. R. Vanfleteren and D. Gems (2005). "Dietary restriction in C. elegans: From rate-of-living effects to nutrient sensing pathways." Mechanisms of Ageing and Development **126**(9): 929-937.

Warrick, J. M., H. L. Paulson, G. L. Gray-Board, Q. T. Bui, K. H. Fischbeck, R. N. Pittman and N. M. Bonini (1998). "Expanded polyglutamine protein forms nuclear inclusions and causes neural degeneration in Drosophila." Cell **93**(6): 939-949.

Williams, P. L. and D. B. Dusenbery (1990). "Aquatic Toxicity Testing Using the Nematode, Caenorhabditis-Elegans." Environmental Toxicology and Chemistry **9**(10): 1285-1290.

Wolozin, B., S. Saha, M. Guillily, A. Ferree and M. Riley (2008). "Investigating convergent actions of genes linked to familial Parkinson's disease." Neurodegenerative Diseases **5**(3-4): 182-185.

Wood, W. B. (Ed.). (1988). "The nematode *Caenorhabditis elegans*. New York, NY: Cold Spring Harbor Laboratory Press".

Wu, J. G. and D. A. Laird (2004). "Interactions of chlorpyrifos with colloidal materials in aqueous systems." Journal of Environmental Quality **33**(5): 1765-1770.

Xia, Z. G., M. Dickens, J. Raingeaud, R. J. Davis and M. E. Greenberg (1995). "Opposing Effects of Erk and Jnk-P38 Map Kinases on Apoptosis." Science **270**(5240): 1326-1331.

Yang, W., J. R. Dunlap, R. B. Andrews and R. Wetzel (2002). "Aggregated polyglutamine peptides delivered to nuclei are toxic to mammalian cells." Human Molecular Genetics **11**(23): 2905-2917.

Yong, V. W., T. L. Perry and A. A. Krisman (1986). "Depletion of Glutathione in Brain-Stem of Mice Caused by N-Methyl-4-Phenyl-1,2,3,6-Tetrahydropyridine Is Prevented by Antioxidant Pretreatment." Neuroscience Letters **63**(1): 56-60.

Zan, Y. H., J. D. Haag, K. S. Chen, L. A. Shepel, D. Wigington, Y. R. Wang, R. Hu, C. C. Lopez-Guajardo, H. L. Brose, K. I. Porter, R. A. Leonard, A. A. Hitt, S. L. Schommer, A. F. Elegbede and M. N. Gould (2003). "Production of knockout

rats using ENU mutagenesis and a yeast-based screening assay." Nature Biotechnology **21**(6): 645-651.

Zarranz, J. J., J. Alegre, J. C. Gomez-Esteban, E. Lezcano, R. Ros, I. Ampuero, L. Vidal, J. Hoenicka, O. Rodriguez, B. Atares, V. Llorens, E. G. Tortosa, T. del Ser, D. G. Munoz and J. G. de Yebenes (2004). "The new mutation, E46K, of alpha-synuclein causes Parkinson and Lewy body dementia." Annals of Neurology **55**(2): 164-173.

Zeitlin, S., J. P. Liu, D. L. Chapman, V. E. Papaioannou and A. Efstratiadis (1995). "Increased Apoptosis and Early Embryonic Lethality in Mice Nullizygous for the Huntingtons-Disease Gene Homolog." Nature Genetics **11**(2): 155-163.

Zhang, J., R. E. Campbell, A. Y. Ting and R. Y. Tsien (2002). "Creating new fluorescent probes for cell biology." Nature Reviews Molecular Cell Biology **3**(12): 906-918.

Zhang, S. F., C. Ma and M. Chalfie (2004). "Combinatorial marking of cells and organelles with reconstituted fluorescent proteins." Cell **119**(1): 137-+.

Ziviani, E., R. N. Tao and A. J. Whitworth (2010). "Drosophila Parkin requires PINK1 for mitochondrial translocation and ubiquitinates Mitofusin." Proceedings of the National Academy of Sciences of the United States of America **107**(11): 5018-5023.

Zoghbi, H. Y. and H. T. Orr (2000). "Glutamine repeats and neurodegeneration." Annual Review of Neuroscience **23**: 217-247.

Zuhlke, C., O. Riess, K. Schroder, I. Siedlaczck, J. T. Epplen, W. Engel and U. Thies (1993). "Expansion of the (Cag)(N) Repeat Causing Huntingtons-Disease in 352 Patients of German Origin." Human Molecular Genetics **2**(9): 1467-1469.